FUNCTIONAL ROLES OF CONSERVED ACTIVE SITE AMINO ACIDS IN THE DESULFONATION REACTION CATALYZED BY THE ALKANESULFONATE MONOOXYGENASE FROM ESCHERICHIA COLI

Except where reference is made to the work of others, the work described in this dissertation is my own or was done in collaboration with my advisory committee. This dissertation does not include proprietary or classified information.

_____

Russell Carpenter

Certificate of approval:

_____	_____
Douglas C. Goodwin Associate Professor Chemistry and Biochemistry	Holly R. Ellis, Chair Associate Professor Chemistry and Biochemistry
_____	_____
Evert C. Duin Assistant Professor Chemistry and Biochemistry	Smita Mohanty Associate Professor Chemistry and Biochemistry

_____

George Flowers
Dean
Graduate School

FUNCTIONAL ROLES OF CONSERVED ACTIVE SITE AMINO ACIDS IN THE DESULFONATION REACTION CATALYZED BY THE ALKANESULFONATE MONOOXYGENASE FROM ESCHERICHIA COLI

Russell Carpenter

A Dissertation

Submitted to

the Graduate Faculty of

Auburn University

in Partial Fulfillments of the

Requirements for the

Degree of

Doctor of Philosophy

Auburn, AL
December 19, 2008

FUNCTIONAL ROLES OF CONSERVED ACTIVE SITE AMINO ACIDS IN THE DESULFONATION REACTION CATALYZED BY THE ALKANESULFONATE MONOOXYGENASE FROM ESCHERICHIA COLI

Russell Carpenter

Permission is granted to Auburn University to make copies of this dissertation at its discretion, upon request of individuals or institutions at their expense.
The author reserves all publication rights.

_____
Signature of Author

_____
Date of Graduation

VITA

Russell Carpenter, son of Ken and Karen Carpenter, was born November 2, 1979, in Auburn, Alabama. He graduated with a Bachelor of Science degree in Chemistry in 2002 from Georgia Southern University in Statesboro, GA. In the fall of 2003 he entered the Graduate School in the Department of Chemistry and Biochemistry where he joined the laboratory of Dr. Holly R. Ellis and is currently pursuing a Ph.D. degree.

DISSERTATION ABSTRACT

FUNCTIONAL ROLES OF CONSERVED ACTIVE SITE AMINO ACIDS IN THE DESULFONATION REACTION CATALYZED BY THE ALKANESULFONATE MONOOXYGENASE FROM ESCHERICHIA COLI

Russell Carpenter

Doctor of Philosophy, December 19, 2008

(B. S., Georgia Southern University, 2002)

187 Typed Pages

Directed by: Holly R. Ellis

The flavin-dependent alkanesulfonate monooxygenase (SsuD) catalyzes the oxidation of 1-substituted alkanesulfonates producing sulfite and a corresponding aldehyde in the presence of O_2 and $FMNH_2$. The reduced flavin is supplied by the NAD(P)H-dependent FMN reductase, SsuE. The goal of these studies was to investigate the roles of conserved amino acids located in or around the postulated active site of SsuD through various kinetic and substrate binding experiments. A conserved cysteine residue located at position 54 in SsuD is proposed to stabilize the C4a-(hydro)peroxyflavin intermediate formed during the desulfonation reaction. This conserved residue was replaced with either serine or alanine (C54S and C54A). The catalytic efficiencies

(k_{cat}/K_m) obtained for C54S and C54A with octanesulfonate were 3-fold greater and 6-fold lower than wild-type SsuD, respectively. Results from fluorescence titration experiments with octanesulfonate suggest that the Cys54 residue is not involved in $FMNH_2$ binding; however, the binding of octanesulfonate substrate was affected by substitution with Ser or Ala. Stopped-flow kinetic analysis gave evidence that the polar nature of the amino acid residue at position 54 was key to a high accumulation of the C4a-(hydro)peroxyflavin intermediate. These results suggest that the cysteine residue located at position 54 in SsuD is involved in the stabilization of the C4a-(hydro)peroxyflavin intermediate formed during the desulfonation reaction catalyzed by SsuD.

When SsuD was first purified an aberrant mutation of Arg297 to Cys abolished all activity. It was postulated that this arginine residue was located on a flexible loop and mutation to cysteine would cause a disulfide bond to form with Cys54. This flexible loop containing the conserved Arg297 residue is proposed to close over the active site to protect intermediates during catalysis. This conserved residue was replaced with either lysine or alanine (R297K and R297A). The R297K SsuD variant exhibited a 30-fold decrease in the k_{cat}/K_m value compared to wild-type. In contrast, the R297A SsuD variant had no detectible activity, even at higher enzyme concentrations. Fluorescence titrations with $FMNH_2$ showed a minor 3-fold increase in the dissociation constant (K_d) of $FMNH_2$ for both SsuD variants; however, octanesulfonate was unable bind. Stopped-flow kinetic experiments show the formation of the C4a-(hydro)peroxyflavin intermediate with both R297K and R297A SsuD variants. Rapid-reaction kinetic traces of the R297 SsuD

variants in the presence of SsuE showed an altered step in flavin oxidation compared to wild-type. Proteolytic digestions suggest that the Arg297 located on the postulated mobile loop is important for protecting the SsuD enzyme from proteolysis. These studies give evidence for the stabilization of the C4a-(hydro)peroxyflavin intermediate by Cys54 and the protection of substrates and/or intermediates during the desulfonation reaction by Arg297.

ACKNOWLEDGEMENTS

First and foremost I would like to express my appreciation and thanks to my advisor, Dr. Holly R. Ellis, for her guidance and encouragement throughout my studies here at Auburn University. My dissertation would not be possible without her advice and undying devotion to this research. Secondly, I would like to thank my other committee members Dr. Douglas C. Goodwin, Dr. Evert C. Duin, and Dr. Smita Mohanty for their helpful discussions and constructive suggestions to my dissertation. I would also like to express my thanks to Dr. Goodwin for the use of his stopped-flow instrument and Dr. Duin for the use of his anaerobic glove box. I would also like to thank my former and current lab mates Dr. Benlian Gao, Dr. Kholis Abdurachim, Dr. Xuanzhi Zhan, Mary Millwood, Mick Robbins, and Jingyuan "Bear" Xiong for their meaningful discussions and help during my studies. I would also like to extend my thanks to the many friends I have made during this stage of my life. I want to especially express my gratitude to my parents Ken and Karen Carpenter and my brothers Philip and Jeffrey for always supporting me throughout my life. And last, but certainly not least, I would like to thank the Department of Chemistry and Biochemistry and the National Science Foundation for their monetary support.

Style manual used: Biochemistry

Computer software used: Microsoft Word, Microsoft Excel, ChemDraw, KaleidaGraph

TABLE OF CONTENTS

LIST OF TABLES xiv

LIST OF SCHEMES xv

LIST OF FIGURES xvii

CHAPTER ONE: LITERATURE REVIEW 1

1.1 Sulfur assimilation in bacterial organisms 1

1.2 Sulfate starvation induced gene expression 2

1.3 Regulation of sulfur assimilation in *E. coli* 6

1.4 Sulfonate-sulfur uptake in *E. coli* 10

1.5 Gene cluster arrangement 13

1.6 Properties of flavin 13

1.7 Activation of Molecular Oxygen by Free Flavin 20

1.8 Flavoproteins 21

1.8.1 Flavin oxidases 21

1.8.2 Flavin dehydrogenases 24

1.8.3 Flavin reductases 25

1.8.4 Flavin oxygenases 26

1.9 Mechanism of flavin oxygenases 27

1.9.1 Hydroperoxyflavin intermediates as electrophiles 31

1.9.2 Peroxyflavin intermediates as nucleophiles 35
1.10 Two-component alkanesulfonate monooxygenase system from *E. coli* 37
1.11 Comparison of SsuD with related TIM-barrel enzymes 43
1.11.1 Bacterial luciferase from *Vibrio harveyi* (LuxA) 44
1.11.2 Long-chain alkane monooxygenase (LadA) 52
1.11.3 Alkanesulfonate monooxygenase (SsuD) 55
1.12 Flexible loop 61
1.13 Summary 66
CHAPTER TWO: Catalytic Role of a Conserved Cysteine Residue in the Desulfonation Reaction by the Alkanesulfonate Monooxygenase Enzyme 68
2.1 INTRODUCTION 68
2.2 MATERIALS AND METHODS 73
2.2.1 Materials 73
2.2.2 Site-Directed Mutagenesis 73
2.2.3 Expression and purification of variant and wild-type SsuD 74
2.2.4 Far-UV circular dichroism 74
2.2.5 Cysteine Accessibility Assays 75
2.2.6 Steady-state kinetic studies 75
2.2.7 Flavin binding studies 76
2.2.8 Octanesulfonate binding 77
2.2.9 Rapid reaction kinetic experiments 78
2.3 RESULTS 80

2.3.1 Structural properties of the SsuD variants 80
2.3.2 Steady-state kinetic parameters for octanesulfonate.....81
2.3.3 Substrate binding to the C54 SsuD variants 85
2.3.4 Kinetic studies of flavin oxidation by the SsuD variants.....86
2.3.5 Kinetic studies of flavin oxidation by SsuD variants in the presence of octanesulfonate 91
2.4 DISCUSSION.....94
CHAPTER THREE: Functional Role of the Active Site Arg297 Residue Located in a Postulated Mobile Loop of SsuD 104
3.1 INTRODUCTION 104
3.2 MATERIALS AND METHODS.....108
3.2.1 Materials 108
3.2.2 Site-Directed Mutagenesis 108
3.2.3 Expression and purification of wild type and variant SsuD 109
3.2.4 Far-UV circular dichroism.....109
3.2.5 SsuD steady-state kinetic measurements 110
3.2.6 Flavin binding studies.....110
3.2.7 Octanesulfonate binding 112
3.2.8 Rapid-reaction kinetics of FMNH2 oxidation 112
3.2.9 Rapid-reaction kinetics of flavin oxidation in the presence of SsuE....113
3.2.10 Proteolytic susceptibility of the variants and wild-type SsuD.....114
3.3 RESULTS 116

3.3.1 Far-UV circular dichroism 116
3.3.2 SsuD steady-state kinetic measurements 116
3.3.3 Substrate binding to the R297 SsuD variants 118
3.3.4 Rapid-reaction kinetics of flavin oxidation 123
3.3.5 Kinetic studies of flavin oxidation by SsuD variants in the presence of octanesulfonate substrate 126
3.3.6 Rapid reaction kinetics of FMNH2 oxidation in the presence of SsuE 129
3.3.7 Proteolytic susceptibility of SsuD and variants 132
3.4 DISCUSSION 137
CHAPTER FOUR: SUMMARY 147
4.1 Flavin binding and transfer in the alkanesulfonate monooxygenase system 148
4.2 Catalytic mechanism of the alkanesulfonate monooxygenase 149
4.3 Putative active site of SsuD and the catalytic role of Cys54 150
4.4 Functional role of Arg297 located on a flexible loop in SsuD 152
REFERENCES 155

LIST OF TABLES

Table 1.1 Substrate ranges for SsuD and TauD 12

Table 2.1 Dissociation Constants and Steady-state Kinetic Parameters for C54S, C54A, and wild-type SsuD 84

Table 2.2 Single-turnover kinetic rate constants for the oxidation of $FMNH_2$ for WT, C54S, and C54A SsuD in the absence of octanesulfonate 91

Table 3.1 % Secondary Structural Elements of R297K, R297A, and wild-type SsuD 116

Table 3.2 Dissociation constants and steady-state kinetic parameters for R297K, R297A, and wild-type SsuD 121

Table 3.3 Single turnover kinetic rate constants for WT, R297K, and R297A SsuD in the absence of octanesulfonate. 124

Table 3.4 Single turnover kinetic rate constants for R297K and R297 A SsuD in the presence of octanesulfonate 128

LIST OF SCHEMES

Scheme 1.1 The mechanism of desulfonation by taurine dioxygenase (TauD).....7

Scheme 1.2 Activation of molecular oxygen by flavins 21

Scheme 1.3 General mechanism for flavin-containing monooxygenases 28

Scheme 1.4 Reactions of reduced flavin with oxygen 29

Scheme 1.5 Reaction mechanism of p-hydroxybenzoate hydroxylase.....32

Scheme 1.6 Catalytic mechanism of p-hydroxyphenylacetate 3-hydroxylase using hydroperoxyflavin as an electrophile 34

Scheme 1.7 Reaction mechanism of cyclohexanone monooxygenase using a peroxyflavin intermediate as a nucleophile.....36

Scheme 1.8 Intermediates involved in the reaction catalyzed by bacterial luciferase....38

Scheme 1.9 Overall reaction mechanism of the two-component alkanesulfonate monooxygenase system.....39

Scheme 1.10 Proposed mechanism of the desulfonation reaction catalyzed by SsuD 41

Scheme 1.11 Order of substrate binding for SsuD.....42

Scheme 1.12 Overall reaction catalyzed by LadA 52

Scheme 2.1 Overall mechanism of the alkanesulfonate monooxygenase system 69

Scheme 2.2 Proposed mechanism of the desulfonation reaction catalyzed by SsuD 99

Scheme 3.1 Proposed mechanism of the desulfonation reaction catalyzed by SsuD ...142

LIST OF FIGURES

Figure 1.1 Cysteine biosynthesis for sulfate and alkanesulfonates in *E. coli* 3

Figure 1.2 Diagram of *ssu* and *tau* gene clusters responsible for synthesis of proteins involved in the uptake and utilization of alkanesulfonates and taurine in *E. coli* 5

Figure 1.3 Gene expression regulation of sulfur assimilation in *E. coli* 8

Figure 1.4 Uptake and desulfonation of alkanesulfonates and taurine in *E. coli* 11

Figure 1.5 Genetic organization of related *ssu* and *msu* operons from different bacterial organisms 14

Figure 1.6 Structures of riboflavin, FMN, lumiflavin, and FAD 16

Figure 1.7 Flavin isoalloxazine ring numbering system 18

Figure 1.8 Oxidation states of flavin mononucleotide (FMN) 19

Figure 1.9 Flavin spectra in three different oxidation states 22

Figure 1.10 Topology diagram showing the α and β subunits of luciferase 46

Figure 1.11 Model of the luciferase:flavin complex 48

Figure 1.12 Three-dimensional crystal structure of the active site of luciferase 49

Figure 1.13 Topology diagram showing the LadA monomer 54

Figure 1.14 Topology diagram showing each SsuD monomer 57

Figure 1.15 Tetrameric structure of SsuD 58
Figure 1.16 Putative active site of the alkanesulfonate monooxygenase, SsuD 62
Figure 2.1 Far-UV CD spectra of C54S, C54A, and wild-type SsuD 82
Figure 2.2 Steady-state kinetic analyses of C54S and C54A SsuD 83
Figure 2.3 Fluorimetric titration of C54S SsuD/$FMNH_2$ complex with octanesulfonate 87
Figure 2.4 Kinetics traces of flavin oxidation by C54S and C54A SsuD in the absence of octanesulfonate substrate 90
Figure 2.5 Kinetics of flavin oxidation by C54S and C54A SsuD in the presence of variable amounts of octanesulfonate 92
Figure 3.1 Far-UV CD spectra of R297K, R297A, and wild-type SsuD 117
Figure 3.2 Steady-state kinetic analysis of R297K SsuD 119
Figure 3.3 Fluorimetric titration of R297K SsuD with $FMNH_2$ 122
Figure 3.4 Kinetics of flavin oxidation by R297K and R297A SsuD in the absence of octanesulfonate substrate 125
Figure 3.5 Kinetics of flavin oxidation by R297K SsuD in the presence of variable amounts of octanesulfonate 127
Figure 3.6 Kinetics of flavin oxidation by R297A SsuD in the presence of variable amounts of octanesulfonate 130
Figure 3.7 Kinetic traces following FMN reduction and $FMNH_2$ oxidation in the presence of SsuE 131

Figure 3.8 Effect of substrates on the time course of proteolysis of wild-type and R297K SsuD by low levels of trypsin 135

Figure 3.9 Effect of substrates on the time course of proteolysis of wild-type and R297A SsuD by low levels of trypsin 136

CHAPTER ONE

LITERATURE REVIEW

1.1 Sulfur assimilation in bacterial organisms

Sulfur is a critical element for the optimal growth of organisms. All bacteria have inorganic sulfur requirements for the production of sulfur-containing compounds. Bacteria will primarily use inorganic sulfate for the assimilation of sulfur through the cysteine biosynthetic pathway (*1*). The assimilation of sulfur in bacterial systems can be obtained from a wide range of sources including cysteine, methionine, inorganic sulfur, and organosulfur compounds such as taurine and alkanesulfonates (Figure 1.1) (*2*). Although cysteine and sulfate are the primary sources of sulfur in bacterial organisms, *Escherichia coli* prefers to use cysteine as its sulfur source, as the presence of cysteine in the environment represses enzymes involved in sulfur assimilation from sulfate (*2*). Many bacterial species can use these alternative aliphatic sulfonates as a source of sulfur for cysteine and methionine biosynthesis, as well as iron-sulfur cluster formation and other cofactors involved in enzymatic catalysis. The uptake of inorganic sulfate from the environment to the cell is accomplished by a series of proteins that transport sulfate, reduce it to sulfite and sulfide, and then use it to synthesize cysteine through the cysteine

biosynthetic pathway (Figure 1.1) (*2*). In the absence of inorganic sulfate and cysteine some bacterial organisms will synthesize a specific set of enzymes that can utilize organosulfur compounds for the synthesis of essential sulfur containing compounds. A wide range of sulfur containing compounds can enter the cell through various pathways, but they are all converted to sulfide before incorporation into cysteine.

1.2 Sulfate starvation induced gene expression

The sulfur content in aerobic environments mainly consists of sulfonates and sulfate esters. Conversely, inorganic sulfur is poorly represented in aerobic soil, comprising less than 5% of the total sulfur content. Therefore bacteria in these environments must have an alternative process for obtaining this essential element to meet their sulfur requirements (*3*). Sulfate or cysteine starvation induces a set of proteins that are involved in the uptake and utilization of alkanesulfonates and taurine (*1, 2, 4*). In minimal media deprived of sulfate, *E. coli* will increase the synthesis of sulfate starvation induced (ssi) proteins. Several of these enzymes are involved in obtaining sulfur from various alternative sulfur compounds (*5*). Two separate methods have been employed to identify the genes and proteins involved in sulfonate-sulfur utilization (*1, 4*). By comparing cells grown in the presence or absence of sulfate or cysteine and using two-dimensional gel electrophoresis, several proteins (Ssi1-8) were identified which are upregulated when *E. coli* is grown when sulfur sources other than sulfate or cysteine are present in the media. These proteins included a sulfate-binding protein (Sbp), cysteine binding protein (FliY), *O*-acetyl serine lyase (CysK), and the antioxidant

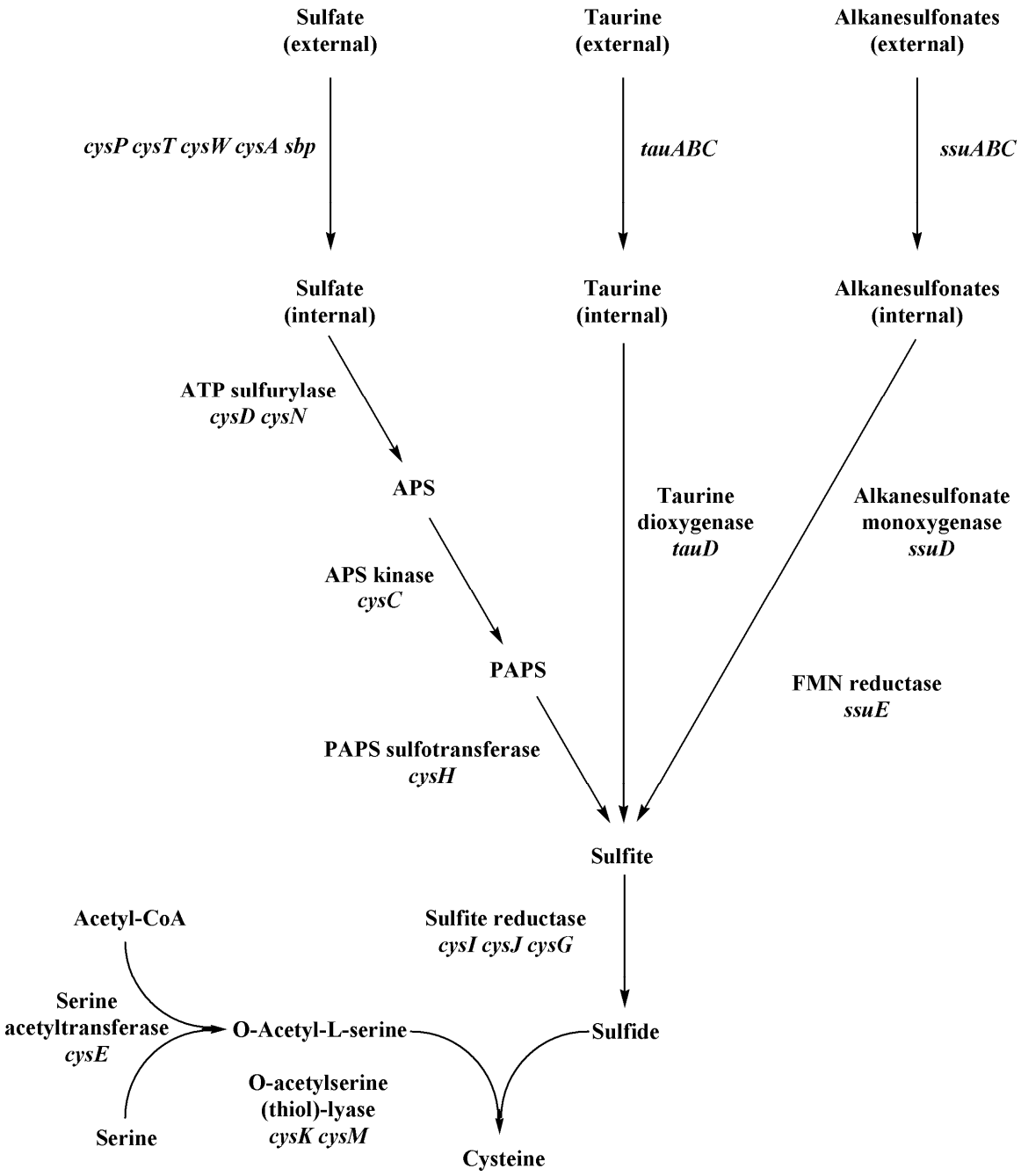

Figure 1.1. Cysteine biosynthesis for sulfate and alkanesulfonates in *E. coli* (Adapted from (*2*)).

alkylhydroperoxide reductase C22 (AhpC), with the first three being involved in sulfate metabolism and the latter serving as an antioxidant. CysK is also known as cysteine synthase, and catalyzes the formation of cysteine from free or bound sulfide and O-acetyl-L-serine (*6*). This step represents a turning point for the incorporation of sulfur into cysteine in microorganisms (*6*). Both the substrate (O-acetyl-L-serine) and the product (cysteine) of this reaction have been postulated to be involved in the regulation of sulfur uptake and assimilation in plants as well as bacterial organisms (*7*). Cysteine-mediated reduction of peroxide substrates is accomplished by the alkylhydroperoxide reductase C22 (AhpC), which produces a cysteinesulfenic acid (Cys-SOH) within the enzyme, and catalyzes the detoxification of organic peroxides (ROOH) to their corresponding alcohols (*8, 9*).

The operon containing the genes designating the Ssi4 and Ssi6 proteins was mapped to the chromosome of *E. coli* by hybridization analysis using probes derived from remaining unknown Ssi proteins (*2, 4*). The function of the Ssi proteins translated by this operon could be inferred from their sequence similarities to proteins of known function. Five open reading frames were present on the operon which was designated *ssuEADCB* for **s**ulfonate-**s**ulfur **u**tilization enzymes (Figure 1.2). Mutagenesis studies were used to determine the function of these encoded proteins. The *ssuA*, *B*, and *C* genes encode an ABC-type transport system for uptake of alkanesulfonates into the cell, while genes designated *ssuD* and *E* encode the Ssi6 and Ssi4 proteins, respectively, that are involved in the desulfonation of alkanesulfonates. Another group of Ssi proteins was shown to be expressed by the *tauABCD* gene cluster (Figure 1.2) (*1*). This gene cluster

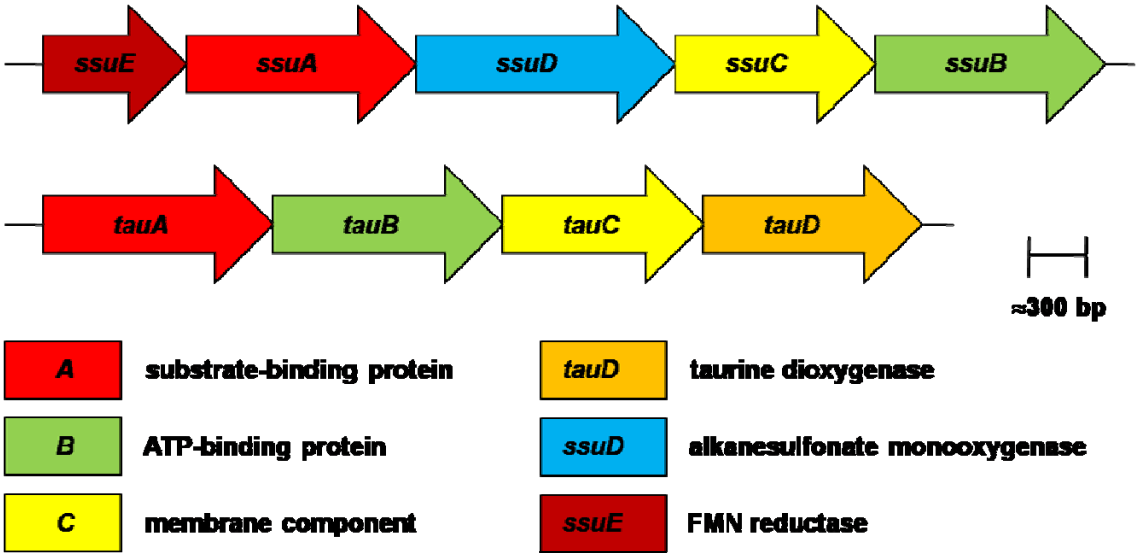

Figure 1.2. *ssu* and *tau* gene clusters responsible for synthesis of proteins involved in the uptake and utilization of alkanesulfonates and taurine in *E. coli* (Adapted from (*2*)).

encoded an ABC-type transporter system (TauABC) and a taurine oxygenase enzyme (TauD). TauD is an α-ketoglutarate dependent, non-heme Fe(II) containing enzyme that converts taurine to aminoacetaldehyde with the liberation of sulfite (*10*). This conversion is absolutely dependent on the presence of iron (II), molecular oxygen, and α-ketoglutarate. Equimolar amounts of sulfite and succinate are formed in the reaction, indicating that the desulfonation reaction and α-ketoglutarate decarboxylation are strictly coupled. The kinetic mechanism of TauD has been proposed from stopped-flow kinetic analyses (Scheme 1.1) (*11*). Stopped-flow kinetic analysis indicates that the α-ketoglutarate coenzyme binds first to create a six-coordinate Fe(II) complex. The subsequent binding of taurine causes the release of a water ligand to form a pentacoordinate Fe(II) complex. The geometry of this five-coordinate Fe(II) complex allows O_2 to access the iron center. The α-ketoglutarate coenzyme is subsequently cleaved to produce succinate and CO_2, forming an Fe(IV)=O intermediate, from which oxygen is inserted into taurine to produce aminoacetaldehyde and sulfite.

1.3 Regulation of sulfur assimilation in E. coli

The expression of the genes that encode proteins in the sulfate reduction pathway have been shown to be under the control of the CysB protein, a LysR-type transcriptional regulator (*12*). Recent findings suggest that the function of CysB may not only regulate the assimilatory sulfate reduction pathway, but also regulate sulfur assimilation at a global level (Figure 1.3) (*2*). The CysB protein and the coinducer *N*-acetylserine, formed non-enzymatically from *O*-acetylserine, are required for the complete expression of the

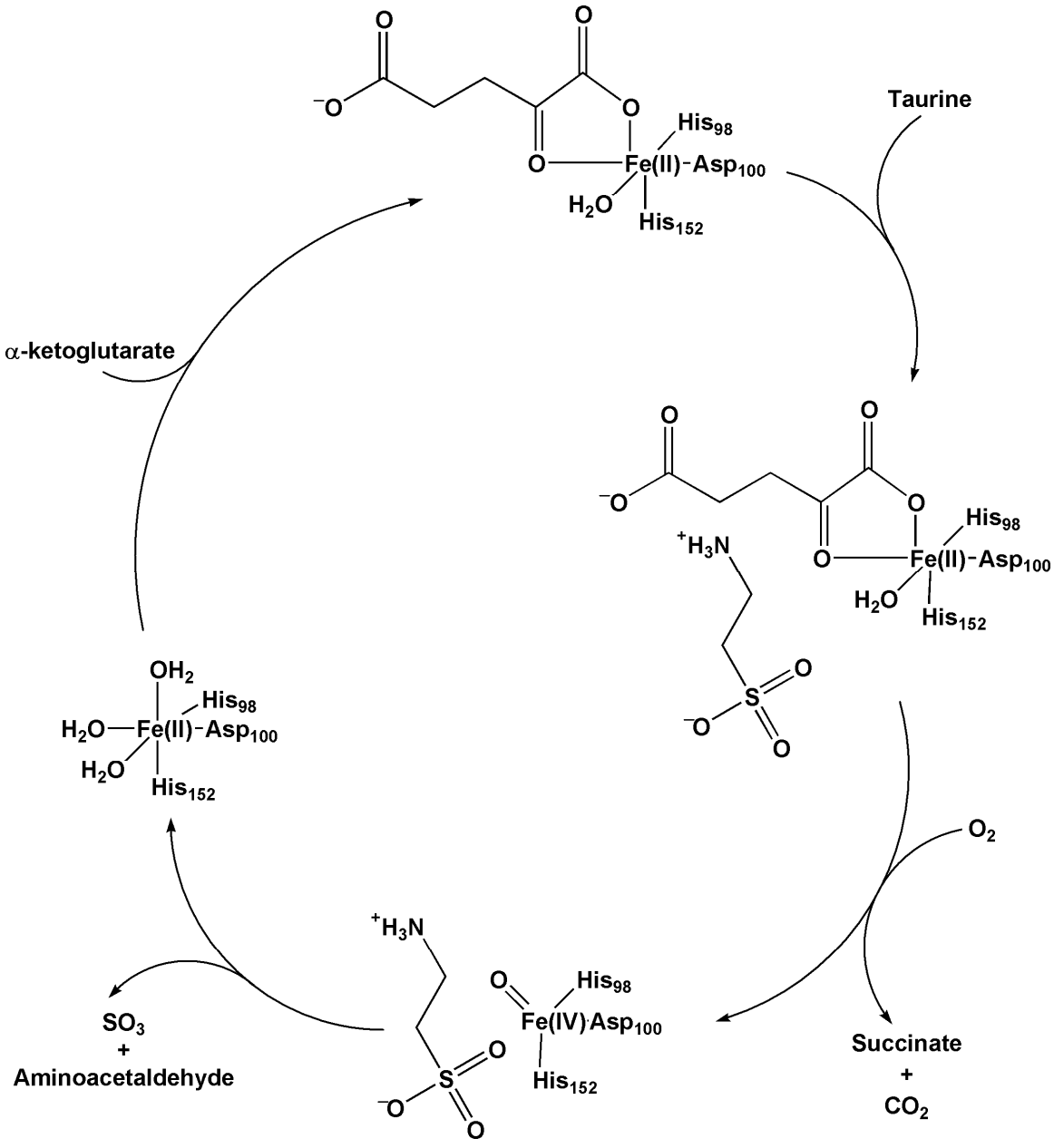

Scheme 1.1. The mechanism of desulfonation by taurine dioxygenase (TauD) (Adapted from (*12*).

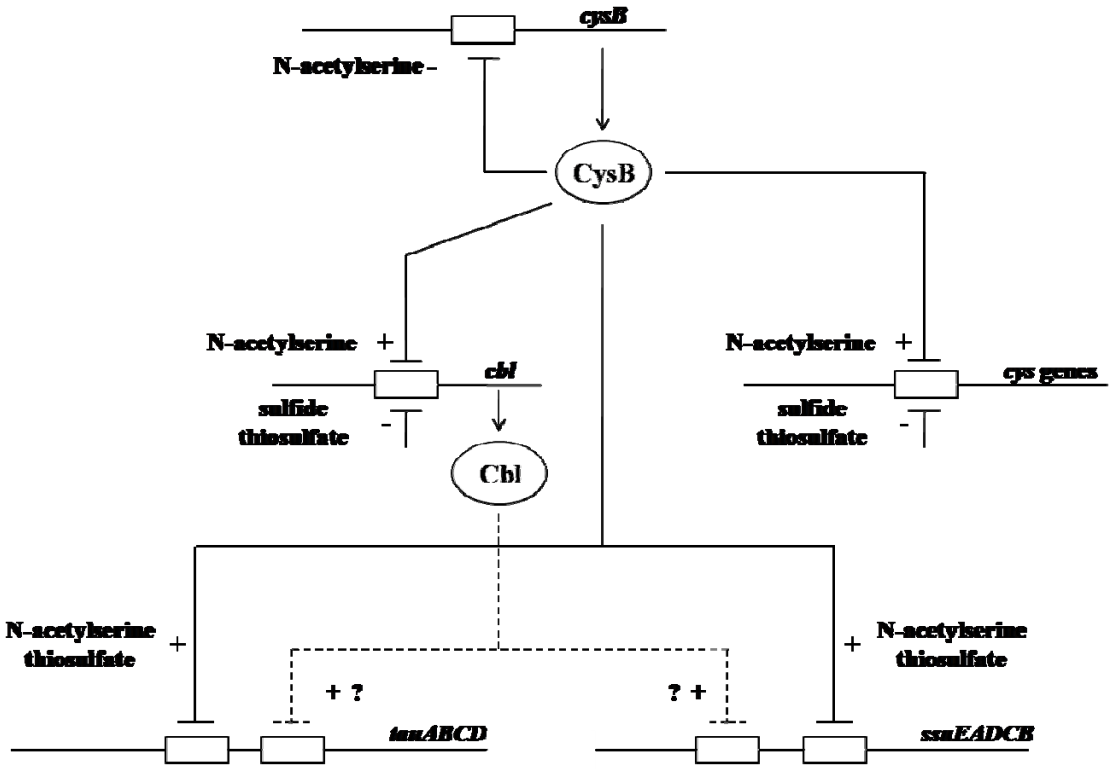

Figure 1.3. Gene expression regulation of sulfur assimilation in *E. coli* (Adapted from (*2*)).

cys genes. The synthesis of *O*-acetylserine is catalyzed by serine acetyltransferase which is regulated through feedback inhibition by cysteine (Figure 1.1). Therefore, expression of the *cys* genes is indirectly controlled by the intracellular concentration of cysteine. Sulfate has also been shown to have no direct effect on expression; however, when sulfate is converted to sulfide and cysteine there is a two-fold reduction in the expression of the *cys* genes.

Conversely, the expression of the *ssu* and *tau* genes is repressed when *E. coli* is grown in the presence of sulfate. The expression of the *ssu* and *tau* genes requires a second regulatory protein, Cbl, which has about 41% amino acid sequence homology with CysB (*13*). The expression of the *cbl* gene is also under the control of CysB, which indirectly regulates the expression of the *ssu* and *tau* genes (*13*). DNA binding experiments have shown that Cbl binds upstream of the -35 region of the *ssu* promoter (*5*). Removal of the binding site for Cbl abolishes expression, which gives evidence that the Cbl protein acts as a transcriptional activator for *ssu* gene expression. To complicate the situation even further, the *ssu* promoter region contains binding sites for CysB and an integration host factor (*5*). It is unclear of their significance because deletion of these binding sites does not have a significant effect on the expression of the *ssu* gene. In contrast, the *tau* operon requires both CysB and Cbl to bind in concert to the DNA for expression (*14*). The observation of multiple complexes of the *tau* promoter fragment with CysB, but only a single complex formed with Cbl, suggest the presence of more than one binding site for CysB but only one unique binding site for Cbl (*14*).

1.4 Sulfonate-sulfur uptake in E. coli

In *E. coli*, the primary source of sulfur is in the form of sulfate. Various enzymes will reduce sulfate to sulfide before incorporation into cysteine and other sulfur-containing biomolecules. However, when sulfate is limiting in the environment *E. coli* will express two gene clusters, designated *tauABCD* and *ssuEADCB*, for the uptake and utilization of alternative sulfur compounds. Both systems are composed of an ABC-type transporter for the uptake of alkanesulfonates and taurine from the periplasm to the cytoplasm (Figure 1.4) (*2*). The A proteins are designated as periplasmic sulfonate binding proteins, B proteins are ATP-hydrolyzing enzymes, and the C proteins are the intergral membrane components of the substrate transport system. In addition to proteins related to the transport of substrate across the membrane, there are the oxygenase enzymes, TauD and SsuD, which are expressed from these operons. TauD is an α-ketoglutarate-dependent, non-heme Fe(II) containing dioxygenase which catalyzes the liberation of sulfite from taurine. SsuD is a $FMNH_2$-dependent monooxygenase involved in the reduction of linear 1-substituted alkanesulfonates to sulfite and the corresponding aldehyde. The *ssu* operon also contains an NAD(P)H-dependent FMN reductase, SsuE, involved in the reduction of FMN to produce $FMNH_2$ for the alkanesulfonate monooxygenase, SsuD. Deletion of the *tauB*, *C*, or *D* genes resulted in the inability of *E. coli* to utilize taurine as a sulfur source, but aliphatic sulfonates could still be utilized (*1*). Conversely, the deletion of the *ssuEADCB* gene prevented the use of aliphatic sulfonates as sulfur sources, but not the use of taurine (*15*). As mentioned, both systems assist *E. coli* with the acquisition of sulfur from alternative sulfur sources. These two systems are

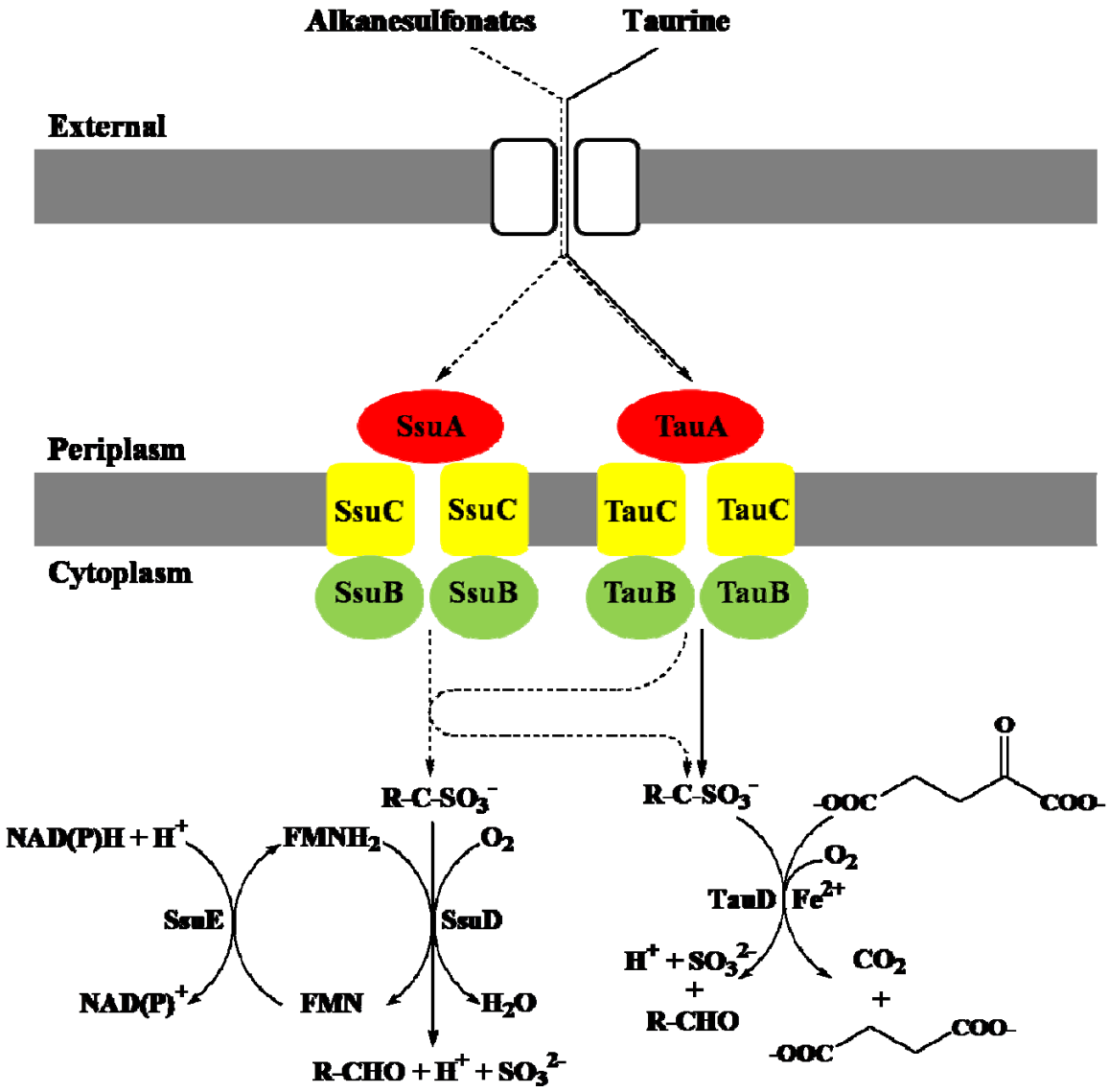

Figure 1.4. Uptake and desulfonation of alkanesulfonates and taurine in *E. coli* (Adapted from (*2*)).

Sulfonated Substrate	Relative Activity	
	SsuD	TauD
	%	
Taurine	0	100
N-Phenyltaurine	65.6	0
4-Phenyl-1-butanesulfonic acid	42.4	2.5
HEPES	10.6	5
MOPS	36.4	34.2
PIPES	29.2	3.1
2-(4-Pyridyl)ethanesulfonic acid	87.4	0.5
1,3-Dioxo-2-isoindolineethanesulfonic acid	100	30.1
Sulfoacetic acid	19.8	—[a]
L-Cysteic acid	0	0
Isethionic acid	14.3	1.2
Methanesulfonic acid	0.7	0
Ethanesulfonic acid	5.2	0.8
Propanesulfonic acid	14	2.3
Butanesulfonic acid	17.8	8.4
Pentanesulfonic acid	40.4	22.5
Hexanesulfonic acid	43.8	11.3
Octanesulfonic acid	46.3	—
Decanesulfonic acid	43.2	—
Dodecanesulfonic acid	20.1	3.3
Tetradecanesulfonic acid	2.9	—

[a]—, not determined

Table 1.1. Substrate ranges for SsuD and TauD (Adapted from (*54*)).

complementary to ensure the survival of the bacterial organism, covering a wide range of aliphatic sulfonates, sulfate esters, and even some sulfonated buffers (Table 1.1). The substrate availability in the environment controls the transport and desulfonation of alkanesulfonates and taurine in bacterial organisms.

1.5 Gene cluster arrangement

The Ssu proteins are expressed under the control of a single promoter on the *ssuEADCB* operon and only exist in bacterial organisms (Figure 1.5) (*3*). The arrangement of the *ssu* gene varies depending on the bacterial organism, but they all contain genes that encode an ABC-type transporter system, along with a monooxygenase, SsuD. There is also a gene that encodes an NAD(P)H-dependent FMN reductase, ssuE, with the exception of *Bacillus subtilis*, which encodes the flavin reductase on a separate operon (*16*). The SsuD enzyme in *Pseudomonas putida* has around 77% amino acid sequence homology with SsuD from *E. coli*, however previous studies show that the *P. putida* S-313 strain was able to desulfonate aromatic sulfonates as well as alkanesulfonates. To accomplish this, an additional enzyme component related to molybdopterin-binding proteins is needed, designated SsuF (*3*). It was determined that the SsuF component was required for the utilization of aromatic and aliphatic sulfate esters as well as aromatic and aliphatic sulfonates (*3*).

1.6 Properties of flavin

Because of their chemical versatility, flavins are involved in a wide variety of reactions. Since they were discovered and characterized in the 1930's, flavins have been

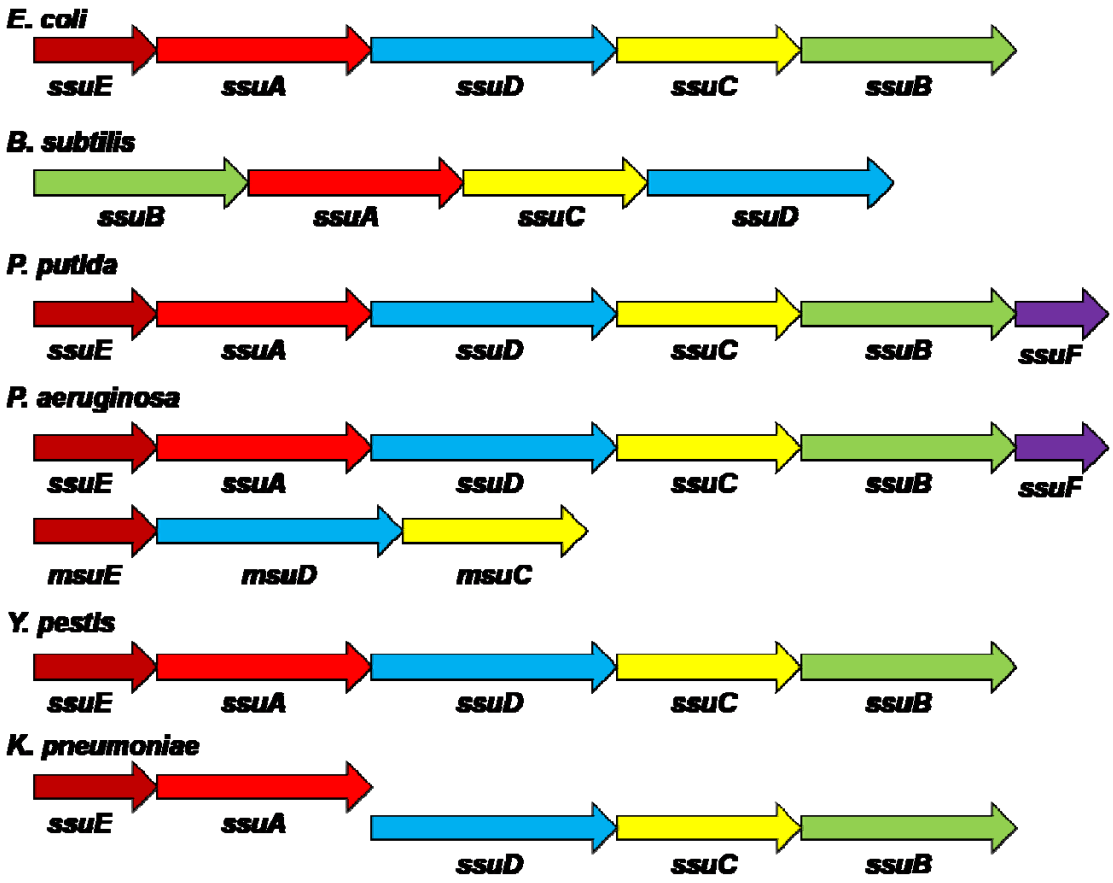

Figure 1.5. Genetic organization of related *ssu* and *msu* operons from different bacterial organisms (Adapted from (*3*)).

shown to play a pivotal role in the electron transport chain, capable of one- and/or two-electron transfer processes, as well as the oxidation of many organic substrates (*17*). Flavins can act as electrophiles and nucleophiles, with intermediates of flavin and substrate being involved in enzyme catalyzed reactions. They have been shown to play an important role in the soil detoxification process, contribute to oxidative stress, as well as the reduction of products generated by oxidative stress, and the production of light in bioluminescent bacteria. The biochemical versatility of flavin can be clearly controlled with the specific interactions associated with the different flavoproteins to which they are bound. Current research aims to determine the nature of these specific interactions and to understand the chemistry of different steps involved in reactions catalyzed by flavoproteins.

Flavin (7,8-dimethylisoalloxazine) is extremely abundant in nature, existing freely in the environment or bound to enzymes (*18*). In general, flavin is a term that generally refers to lumiflavin, riboflavin, flavin mononucleotide (FMN), and flavin adenine dinucleotide (FAD) (Figure 1.6). The functional diversity of the flavin cofactor depends on the covalent linkage of the functional group to the isoalloxazine ring of the flavin. Riboflavin contains a ribityl sugar covalently bound to the isoalloxazine ring at the N-10 position (Riboflavin, Figure 1.6). FMN contains a phosphate group attached to the ribityl sugar moiety by an ester linkage with the terminal hydroxyl group (FMN, Figure 1.6). The isoalloxazine ring of FAD is covalently linked to an adenine dinucleotide group, a product of the condensation of FMN with adenosine monophosphate (*17*). The catalytic

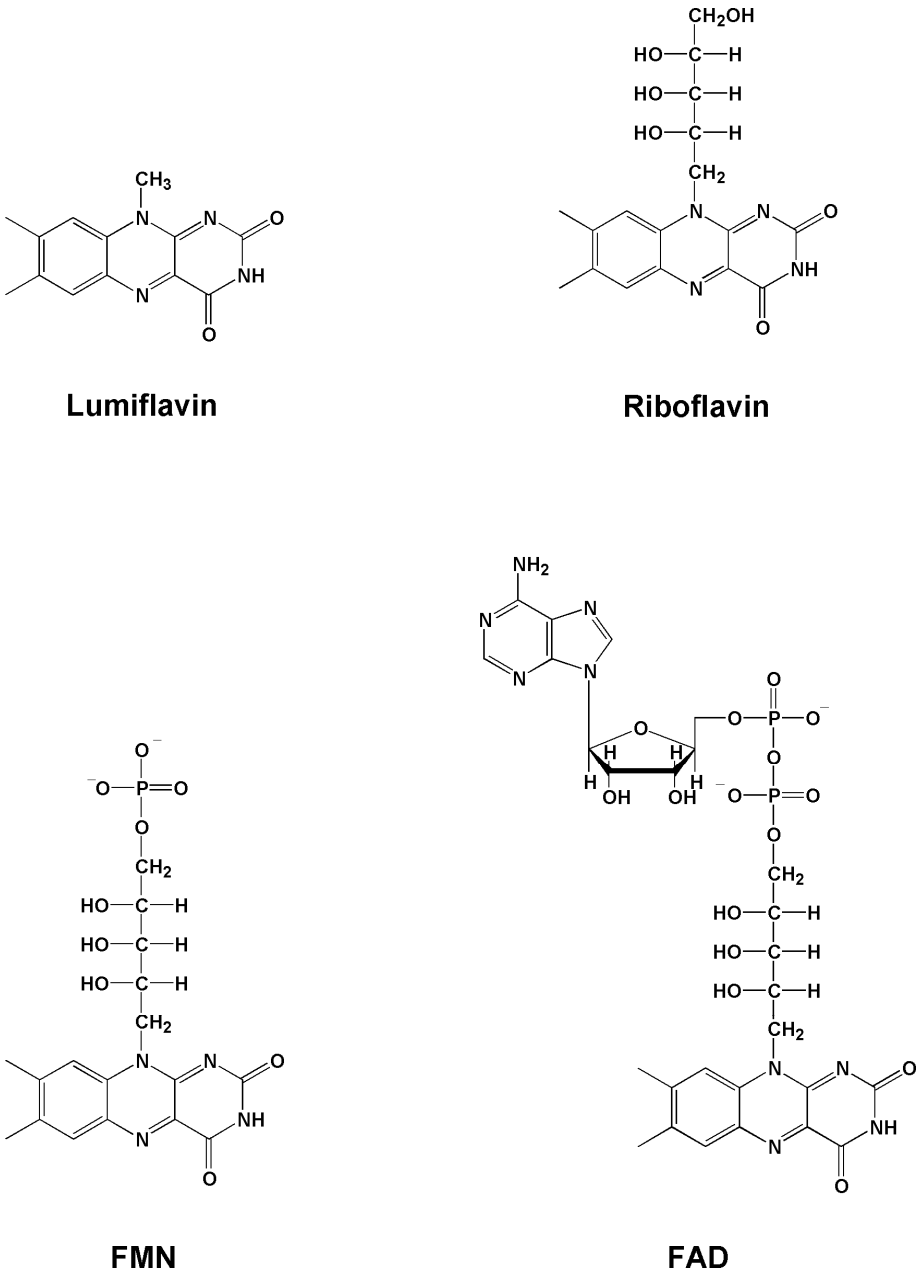

Figure 1.6. Structures of lumiflavin, riboflavin, FMN, and FAD

diversity of the flavin cofactor is associated with specific interactions between the flavin and protein with which it is bound.

Flavin cofactors are associated with protein biomolecules to extend the chemistry available within their active sites (*25*). Flavoproteins exhibit specificity for different forms of flavin depending on the environment and the binding site within the enzyme. In most flavoproteins, the flavin cofactor is tightly, but non-covalently, bound to the enzyme. The covalent flavoproteins, however, can fall into two separate categories depending on where the protein is attached to the flavin moiety. Flavoproteins can contain a covalently bound flavin attached to the protein either though the 8α-methyl group or C6 position of the isoalloxazine ring (Figure 1.7). The first category can be further subdivided depending on the identity of the amino acid with which the flavin moiety is linked. This covalent linkage is bridged by the 8a-methyl group of FMN or FAD linked to a tyrosine, histidine, or cysteine residue (*18*). Proteins covalently attached to the C6 position of the flavin are usually restricted to a linkage between FMN and a cysteine residue (*25*). The numbering of the isoalloxazine ring of FMN is shown in Figure 1.7.

Flavins can adopt three different oxidation states classified as the oxidized (quinone), one electron reduced (semi-quinone), and two electron reduced (hydroquinone) forms (Figure 1.8) (*18, 19*). The existence of a semiquinone form of flavin makes it highly versatile in biocatalysis, being capable of donating or accepting one and/or two electrons. The reduced form of flavin either participates in electron transfer reactions or the activation of molecular oxygen for incorporation into specific

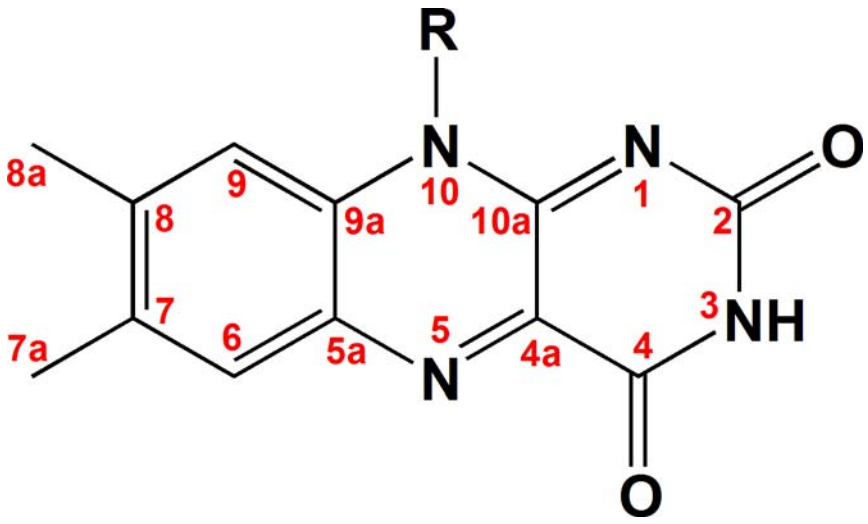

Figure 1.7. Flavin isoalloxazine ring numbering system.

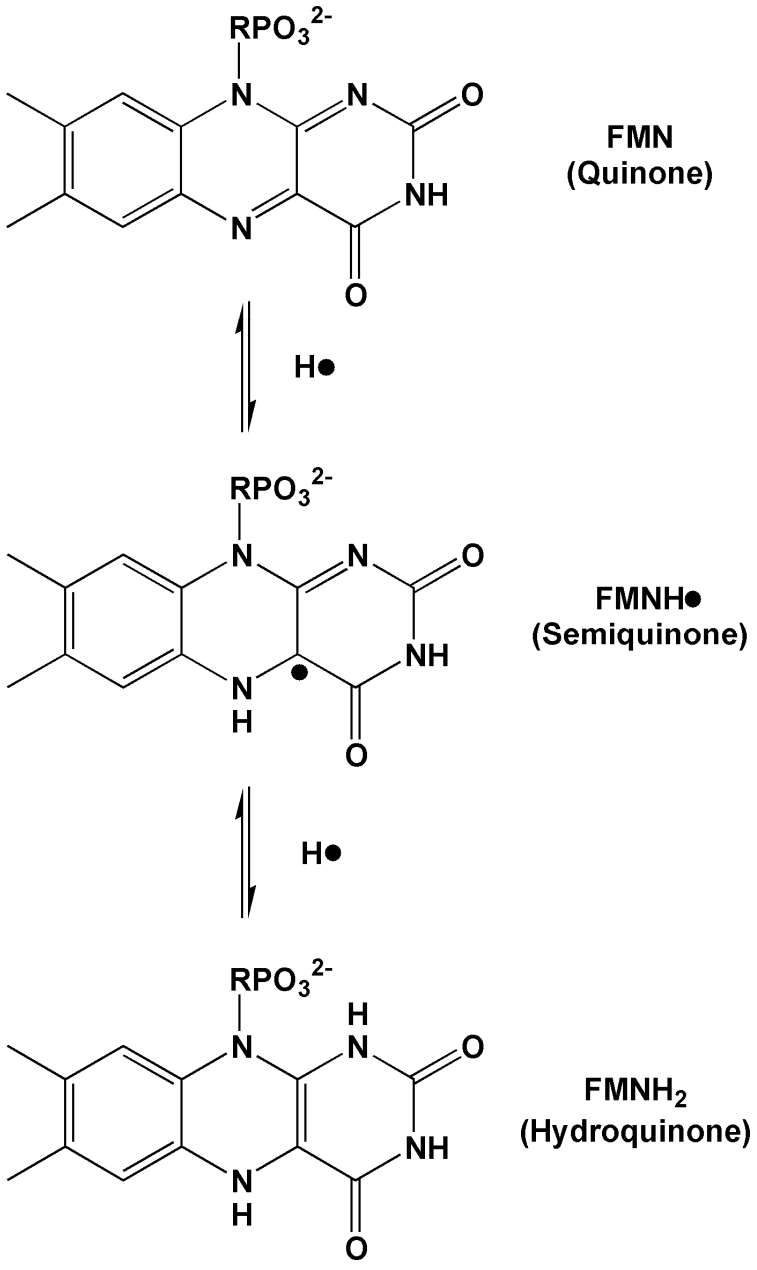

Figure 1.8. Oxidation states of flavin mononucleotide (FMN).

substrates, generating hydroxylated products (oxygenase activity), peroxide H_2O_2 (oxidase activity), or superoxide O_2^- (electron transfer) (*20*).

The ability of flavin to exist in three different oxidation states allows for the characterization of spectral intermediates formed during redox reactions (*23*). The spectra shown in Figure 1.9 represents bound oxidized (spectrum 1), semiquinone (spectrum 2), reduced (spectrum 3), and free oxidized (spectrum 4) forms of flavin. A characteristic absorbance at 450 nm is observed for free or bound flavin, and also has peak fluorescence emission at 520 nm. In contrast, the semiquinone flavin species has an absorbance in the 570 nm region. Reduced flavin has no absorbance in the visible region and is assumed to be non-fluorescent under most experimental conditions, unless it is bound to enzymes.

1.7 Activation of molecular oxygen by free flavin

The reaction of reduced flavins with molecular oxygen is extremely fast and autocatalytic. This is due to the accumulation of the superoxide anion (O_2^-) and flavin radicals (*22*). The analysis of the kinetics of free flavin oxidation required complex formation between flavin and molecular oxygen (*22*). This complex was identified as a C(4a)-flavin hydroperoxide (*23*). The initial reaction of reduced flavin with O_2 proceeds first through the transfer of an electron from a singlet reduced flavin to triplet O_2 to yield a caged radical pair. Spin inversion of this radical pair collapses to form the flavin hydroperoxide (Scheme 1.2). The flavin hydroperoxide then heterolytically dissociates

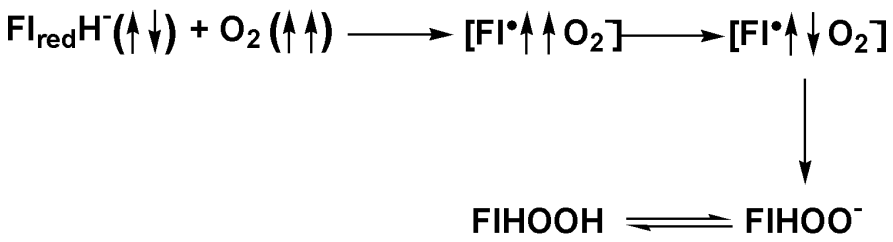

Scheme 1.2. Activation of molecular oxygen by flavins.

to H_2O_2 and oxidized flavin (*23*). Experiments that produced the neutral flavin radical and O_2^- by pulse radiolysis supported this scheme for flavin hydroperoxide formation (*24*). In these experiments a fast exponential decay was observed at 540 nm which can be attributed to the reaction of Fl• with excess O_2^- produced by pulse radiolysis, to produce $FlHOO^-$ which at neutral pH quickly protonates to form FlHOOH (Scheme 1.2).

1.8 Flavoproteins

With individual exceptions, the different groups of flavoproteins are capable of catalyzing a wide variety of enzymatic reactions. The individual classes share many properties that are characteristic of that particular group, but not shared with other groups. These flavoproteins are divided into four different classes based on the type of reaction catalyzed: oxidases, dehydrogenases, reductases, and oxygenases.

1.8.1 Flavin oxidases

Flavin oxidases react with molecular oxygen to oxidize substrates producing large amounts of H_2O_2. Usually, the flavin cofactor of oxidases (E-Fl) accepts two electrons from the substrate (SH_2) (Equation 1). The reduced flavin (E-FlH_2) then forms the

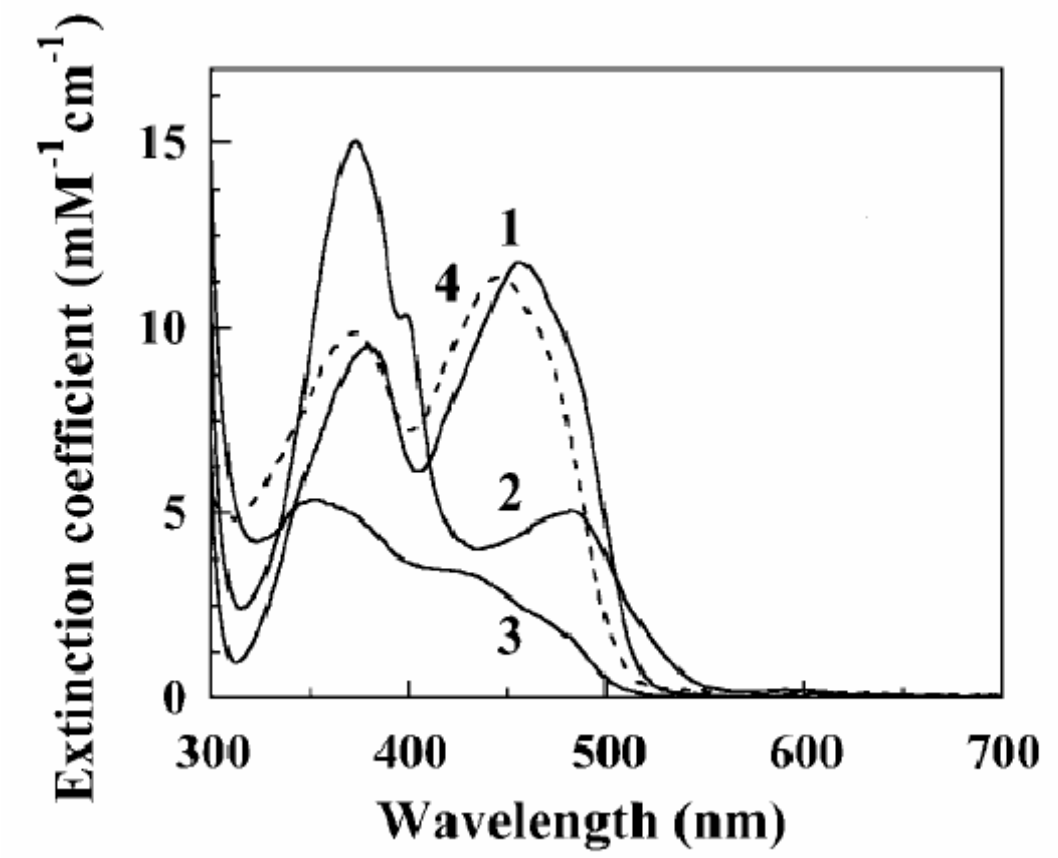

Figure 1.9. Flavin spectra in three different oxidation states (Adapted from (*21*))

(Reprinted with permission).

anionic flavin-bound semiquinone as an intermediate in the one-electron transfer to molecular oxygen with the concomitant formation of H_2O_2 (Equation 2).

$$E\text{-}Fl + SH_2 \leftrightarrow E\text{-}FlH_2 + S \quad \text{(Equation 1)}$$

$$E\text{-}FlH_2 + O_2 \leftrightarrow E\text{-}Fl + H_2O_2 \quad \text{(Equation 2)}$$

A well characterized example of a flavin oxidase is glucose oxidase, an FAD-dependent enzyme found predominantly in fungi, which catalyzes the oxidation of β-D-glucose to D-glucono-1,5-lactone using molecular oxygen as the final electron acceptor forming H_2O_2 (*26*). The most important use of glucose oxidase is in biosensors and diagnostic equipment to determine the amount of glucose in blood samples of diabetics. Another well studied flavin oxidase is the amine oxidizing enzyme glycine oxidase which is involved in the oxidation of glycine with the concomitant formation of H_2O_2. This enzyme was first discovered and classified as a flavoprotein following the complete sequencing of the *Bacillus subtilis* genome (*27*). Glycine oxidase can deaminate a wide range of amino acids to form the corresponding α-keto acid, and is important for the biosynthesis of the thiazole moiety of thiamin (*28*). Flavin amine oxidases catalyze the oxidation of amines *via* an oxidative cleavage of the α-CH bond of the substrate to form an imine product resulting in the reduction of the flavin cofactor (*29*). The imine product is then hydrolyzed to the corresponding aldehyde and ammonia. The cycle is completed by the reaction of reduced flavin with molecular oxygen to form H_2O_2 and oxidized flavin. The amine oxidases are important in a variety of basic biological processes from

lysyl oxidation in the cross-linking of collagen to the metabolism of polyamines and neurotransmitters (*29*).

1.8.2 Flavin dehydrogenases

Flavin dehydrogenases react very slowly with molecular oxygen, transferring a pair of electrons and a proton from the substrate (SH_2) to the bound flavin cofactor (E-Fl) to form the dehydrogenated product (P) (*30*). This can result in the formation of C-C double bonds (succinate dehydrogenase) and the condensation of alcohols to aldehydes (alcohol dehydrogenase) with formation of the reduced flavoprotein ($E\text{-}Fl_2$) (Equation 3).

$$E\text{-}Fl + SH_2 \leftrightarrow E\text{-}FlH_2 + P \qquad \text{(Equation 3)}$$

One example of a well studied flavin dehydrogenase is acyl-CoA dehydrogenase involved in catalyzing the oxidation of fatty acids. This enzyme oxidizes acyl-CoA thioesters to produce the corresponding enoyl-CoA esters, resulting in the reduction of the flavin cofactor, the first step of the β-oxidation of fatty acids (*17*). The reduced flavoprotein is reoxidized by successive one-electron transfers to the electron-transfer flavoprotein (ETF), generating oxidized flavin needed for the next cycle of fatty acid dehydrogenation. Another example is the succinate dehydrogenase enzyme from the citric acid cycle involved in the oxidation of the central single bond in succinate to a *trans* double bond yielding fumarate with the concomitant reduction of the bound FAD cofactor. The electrons from the $FADH_2$ are then transferred directly to Fe-S centers in complex II of the electron transport chain. The oxidized FAD is regenerated to enable succinate dehydrogenase to perform the next round of dehydrogenation reactions.

1.8.3 Flavin reductases

Flavin reductases catalyze the reduction of flavin (E-Fl) through the use of a pyridine nucleotide (NADH or NADPH) to form reduced flavin (FlH_2) and oxidized pyridine nucleotide (NAD^+ or $NADP^+$) (Equation 4). Flavin reductases are able to supply reducing power, in the form of $FMNH_2$, for many diverse enzymatic reactions.

$$E\text{-}Fl + NAD(P)H + H^+ \rightarrow E\text{-}FlH_2 + NAD(P)^+ \quad \text{(Equation 4)}$$

The flavin reductases are classified into three groups based on their substrate specificity for different pyridine nucleotides: FRP, NADPH-preferring flavin reductases; FRD, NADH-preferring flavin reductases; and FRG, the general flavin reductases that can utilize either NADPH or NADH with similar efficiencies. The NADH and NADPH-dependent flavin reductases from *Vibrio harveyi* have been shown to be substrate specific for either NADH or NADPH, but can utilize FMN or FAD (*31-33*). The FRP flavin reductase from *Vibrio harveyi* contains a tightly bound FMN cofactor and utilizes NADPH to reduce the flavin. The $FMNH_2$ substrate required by bacterial luciferase is supplied by FRP. In this reaction, NADPH binds to the enzyme first, resulting in the reduction of the flavin cofactor by NADPH. After the release of $NADP^+$, a second FMN binds to the active site, exchanging the reducing equivalent with the bound $FMNH_2$. The second $FMNH_2$ is released, regenerating the oxidized enzyme (*34*).

The *E. coli* Fre/FRII represents a non-flavoprotein reductase that does not contain a bound flavin cofactor. Fre is able to utilize FMN or FAD as a substrate, but exhibits a stronger affinity for FAD. This enzyme is a component of a multienzymatic system involved in the activation of ribonucleotide reductase, a key enzyme in DNA biosynthesis

(*34*). Fre exhibits a sequential kinetic mechanism with ordered substrate binding of NAD(P)H followed by the binding of flavin, with the reduced flavin product released before NAD^+. Even though Fre does not contain a bound flavin cofactor, Fre may be closely related to a flavoprotein family of which the spinach ferredoxin-$NADP^+$ reductase (FNR) is a structural prototype. Despite very low global sequence similarity, Fre contains an amino acid sequence motif (A_{201}-S-R-T-S-N-G-K_{209}) similar to the FNR family of enzymes. This conserved amino acid sequence is involved in interactions with the NADPH moiety (*35*). The ability to use flavin as a substrate provides versatility in many different biochemical reactions.

1.8.4 Flavin oxygenases

This class of enzymes catalyzes the insertion of oxygen into a broad range of substrates. The flavin cofactor (E-Fl) is first reduced by NAD(P)H (Equation 5), and then the reduced flavin (E-FlH_2) will activate molecular oxygen before reacting with the substrate (Equation 6). The splitting of the oxygen molecule causes one oxygen atom to be inserted into the substrate and the other oxygen atom to be incorporated into water (*37*).

$$E\text{-}Fl + NAD(P)H + H^+ \leftrightarrow E\text{-}FlH_2 + NAD(P)^+ \quad \text{(Equation 5)}$$

$$E\text{-}FlH_2 + S + O_2 \leftrightarrow E\text{-}Fl + SO + H_2O \quad \text{(Equation 6)}$$

A number of microorganisms which can degrade aromatic molecules as a source of carbon contain flavoprotein oxygenases in the degredation pathway. One example of a flavoprotein oxygenase is 4-hydroxybenzoate 3-monooxygenase from *Pseudomonas fluorescens*, which is involved in benzoate degredation *via* hydroxylation and 2,4-

dicholorbenzoate degradation (*38*). This enzyme uses a bound FAD molecule and is part of a class of flavoproteins in which both the reductive and oxidative half-reactions take place on the same enzyme.

1.9 Mechanism of flavin oxygenases

The mechanism by which flavin oxygenases insert a molecular of oxygen into various substrates has been thoroughly studied. The characteristic steps involved in this mechanism are summarized in Scheme 1.3. The enzyme containing bound flavin will form a complex with NAD(P)H resulting in the rapid reduction of the bound flavin cofactor (Scheme 1.3, IV) The reduced flavin-enzyme complex will react with molecular oxygen at the C4a position of the flavin molecule to produce a C4a-(hydro)peroxyflavin intermediate (FlOOH or $FlOO^-$) (Scheme 1.3, V). The enzyme waits, in this highly ractive conformation, for a heteroatom containing substrate. Once the substrate is in place, one of the two oxygen atoms is inserted into the substrate (Scheme 1.3, I), while the other oxygen atom reacts to form H_2O (Scheme 1.3, IV). The release of $NAD(P)^+$ and the binding of NAD(P)H restarts the cycle (Scheme 1.3, III)

The reaction mechanisms of flavin-dependent monooxygenases have been well studied and have been shown to proceed through flavin-oxygen intermediates during catalysis (*42-49*). The generation of a C4a-(hydro)peroxyflavin intermediate has been widely accepted as a common path for the reaction of all flavoprotein monooxygenases with molecular oxygen. There are several pathways associated with the activation of molecular oxygen by flavoproteins (Scheme 1.4) (*17*). Although the intermediates in the reaction may be slightly different, the initial step is the one-electron reduction of

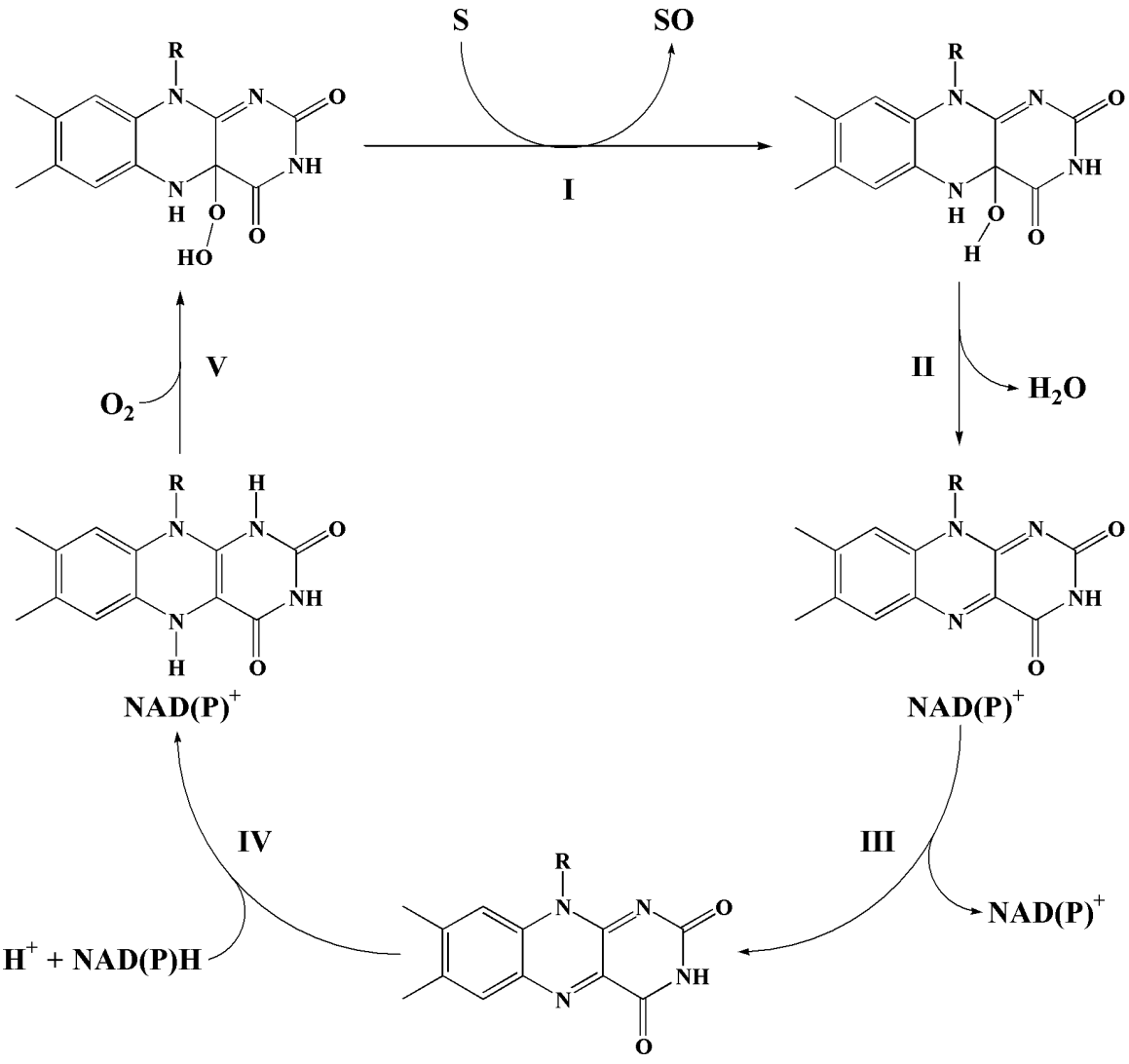

Scheme 1.3 General mechanism for flavin-containing monooxygenases (Adapted from (*17*)).

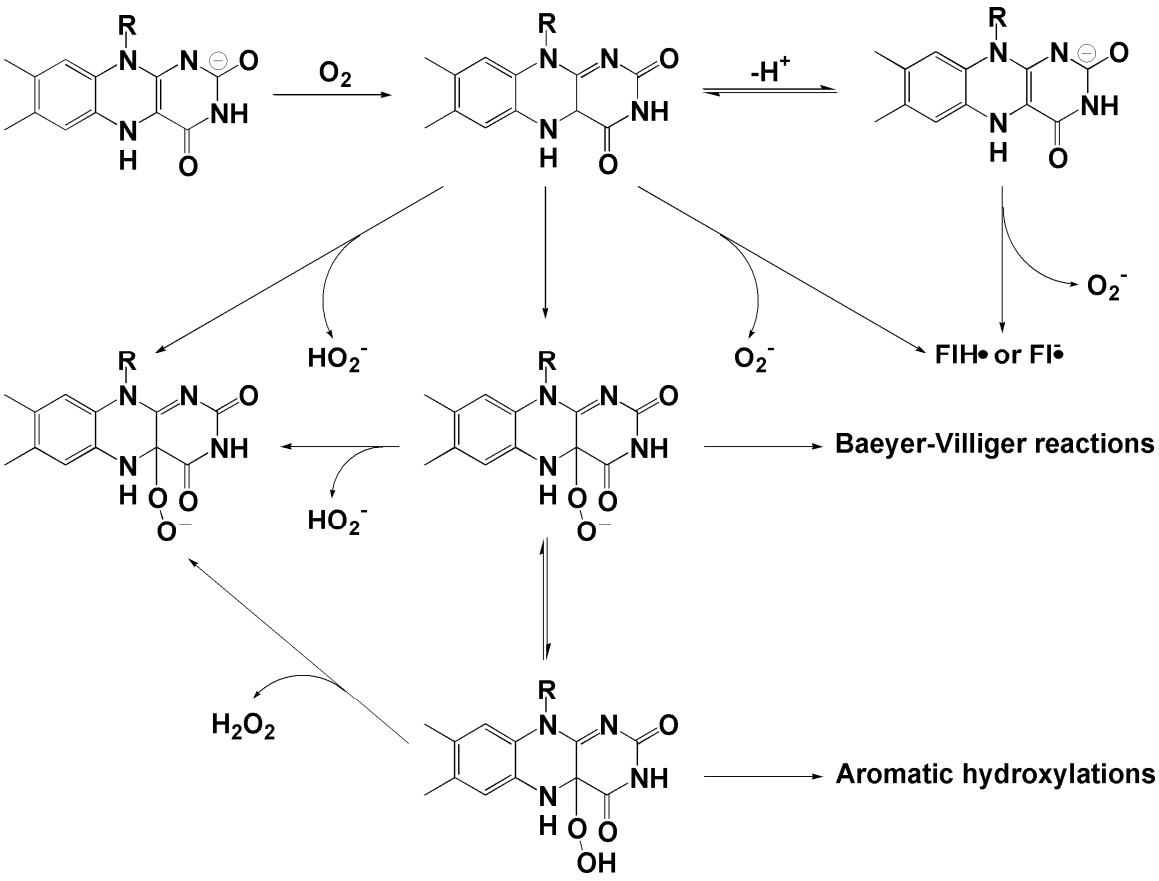

Scheme 1.4. Reactions of reduced flavin with oxygen (Adapted from (*17*)).

molecular oxygen producing a caged radical pair. This radical pair can collapse to form a flavin C4a-hydroperoxide intermediate, shown to be involved in aromatic hydroxylation reactions, or a flavin C4a-peroxide species which performs Baeyer-Villiger rearrangement reactions. The C4a-(hydro)peroxyflavin intermediate is essential in reactions catalyzed by flavoproteins and inserts an oxygen atom directly into the substrate, however it functions in different ways depending on the reaction catalyzed. The C4a-(hydro)peroxyflavin intermediates are capable of oxidizing substrates through either an electrophilic or nucleophilic reaction.

Oxygenase enzymes have been shown to form a peroxyflavin (FMN-OO-) or hydroperoxyflavin (FMN-OOH) intermediate depending on the type of reaction being catalyzed. The bioluminescence reaction catalyzed by bacterial luciferase has been shown to proceed through a C4a-peroxyflavin intermediate, performing a nucleophillic attack on the aldehyde substrate (*17*). The alkanesulfonate monooxygenase, SsuD, is proposed to proceed through a similar peroxyflavin intermediate (*39*). Another well studied flavin monooxygenase that utilizes a C4a-peroxyflavin intermediate is cyclohexanone monooxygenase which is involved in conversion of a cyclic ketone to lactone (*40, 41*). In contrast, p-hydroxybenzoate hydroxylase catalyzes the insertion of an oxygen atom into aromatic compounds *via* a C4a-hydroperoxyflavin intermediate (*17*). This hydroperoxyflavin makes an electrophilic attack on the substrate, incorporating an oxygen atom into the aromatic ring (*40*) (Scheme 1.4). These two contrasting mechanisms involve similar flavin-oxygen intermediates.

1.9.1 Hydroperoxyflavin intermediates as electrophiles

The most extensively studied enzymes in which the C4a-(hydro)peroxyflavin intermediate functions as an electrophile are flavin monooxygenases that catalyze the hydroxylation of aromatic substrates. The first covalent intermediates of flavin and oxygen were first observed experimentally, with this class of enzymes, in the range of 370-400 nm (*40*). The most thoroughly studied members of this group are *p*-hydroxybenzoate hydroxylase (*p*HBH), a single-component monooxygenase, and *p*-hydroxyphenylacetate 3-hydroxylase (*p*HPAH), part of a two-component monooxygenase system, but the reaction proceeds in a similar fashion with all enzymes in this class (*40, 42, 43*). The overall catalytic reaction is described in equation 7,

$$ArX + NAD(P)H + H^+ + O_2 \rightarrow X\text{-}ArOH + NAD(P)^+ + H_2O \qquad \text{(Equation 7)}$$

where X is the activating group in the aromatic substrate, such as –OH, -SH, or NH_2 (*37*). Enzymes in this class have a control mechanism to prevent the wasteful oxidation of NAD(P)H unless substrate is around. The reduction of the enzyme-bound flavin is 100-1000 times faster in the presence of substrates. This is true for the enzyme *p*-hydroxybenzoate hydroxylase, which contains a bound FAD, and interacts with NADPH and *p*-hydroxybenzoate (*p*-HB) in an essentially random order producing $FADH_2$ in the reductive half-reaction (*43*). In the oxidative half-reaction, molecular oxygen is activated by $FADH_2$ to produce a C4a-(hydro)peroxyflavin intermediate that performs an electrophilic attack on the *p*-HB substrate to form 3,4-dihydroxybenzoate (Scheme 1.5). The catalytic mechanism has been investigated in detail, and involves a C4a-hydroperoxyflavin intermediate during its catalytic reaction and employs protein and

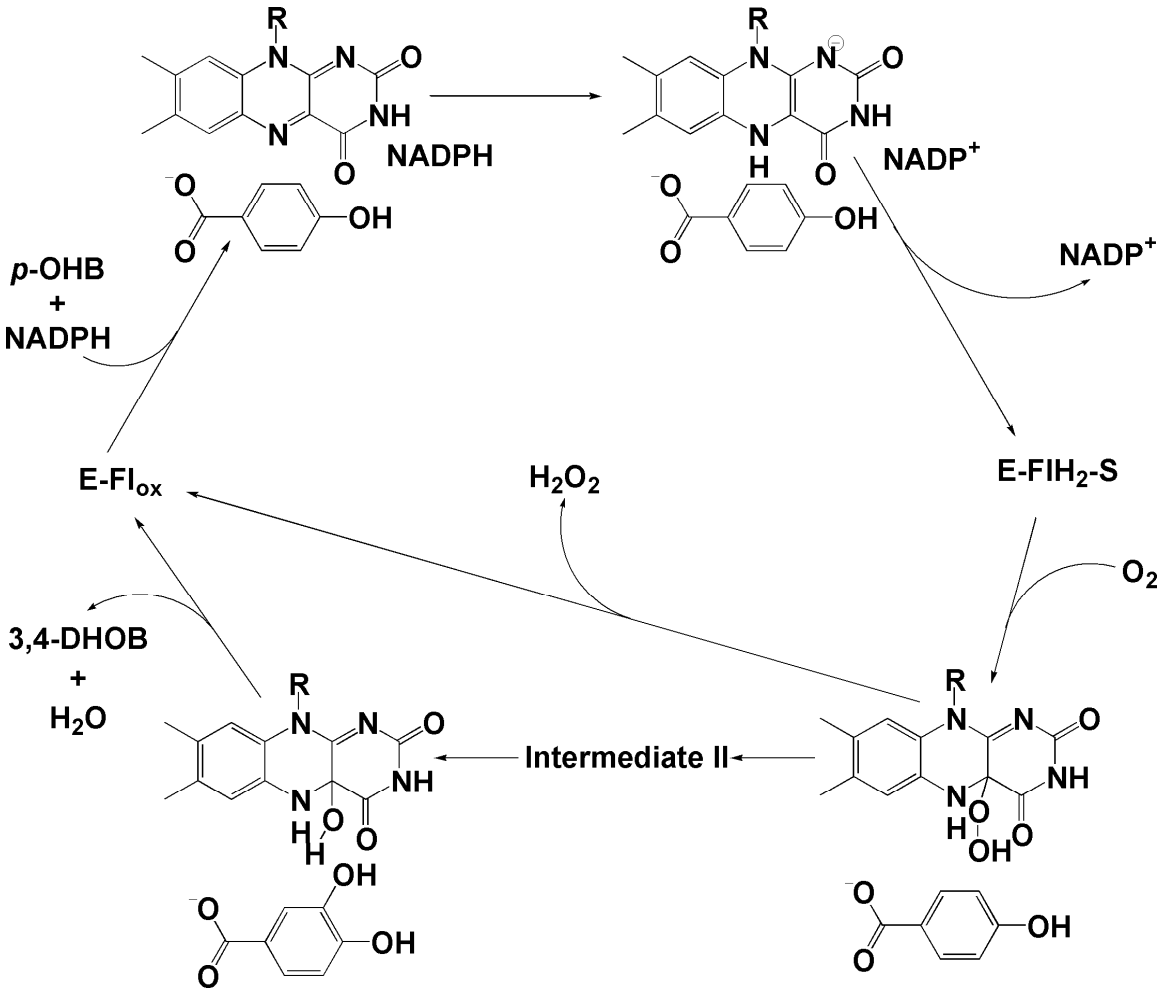

Scheme 1.5. Reaction mechanism of *p*-hydroxybenzoate hydroxylase (Adapted from (*43*)).

flavin dynamics which are essential to catalysis (*42*, *51*). The hydroperoxyflavin intermediate is generated before the substrate is involved in the enzymatic reaction. The hydroxylation of aromatic compounds by single-component flavoproteins hydroxylases, like p-hydroxybenzoate hydroxylase, has been extensively studied for 40 years; however, two-protein or multiprotein monooxygenases have recently been discovered. One enzyme, which is part of a two-component hydroxylase system, that uses a C4a-hydroperoxyflavin as an electrophile is *p*-hydroxyphenylacetate 3-hydroxylase. Although the reaction of pHPAH with O_2 is similar to the reaction of the single component aromatic hydroxylases with the use of a C4a-hydroperoxyflavin intermediate, the overall kinetic mechanism is different (*44*). The first step of the reaction involves the binding of reduced flavin and reaction with molecular oxygen to form a stable *p*HPAH:FMNOOH intermediate complex. Under conditions of catalytic turnover the aromatic substrate then binds to this complex. This is in contrast to the before mentioned single component aromatic hydroxylase, *p*HBH, where the aromatic compound must be bound to the enzyme prior to reduction of the flavin and reaction with molecular oxygen (*43*). The oxidation of *p*-hydroxyphenylacetate (*p*HPA) by electrophilic addition, in which the aromatic substrate performs an electrophilic attack on the flavin intermediate, can only be accomplished by the protonated form of the flavin-oxygen intermediate. As the product of this reaction is released an enzyme bound hydroxyflavin species (FMNOH) is formed, finally decaying to FMN and H_2O (Scheme 1.6) (*44*). This mechanism is also strikingly similar to the mechanisms of bacterial luciferase and cyclohexanone monooxygenase (*41*, *43*).

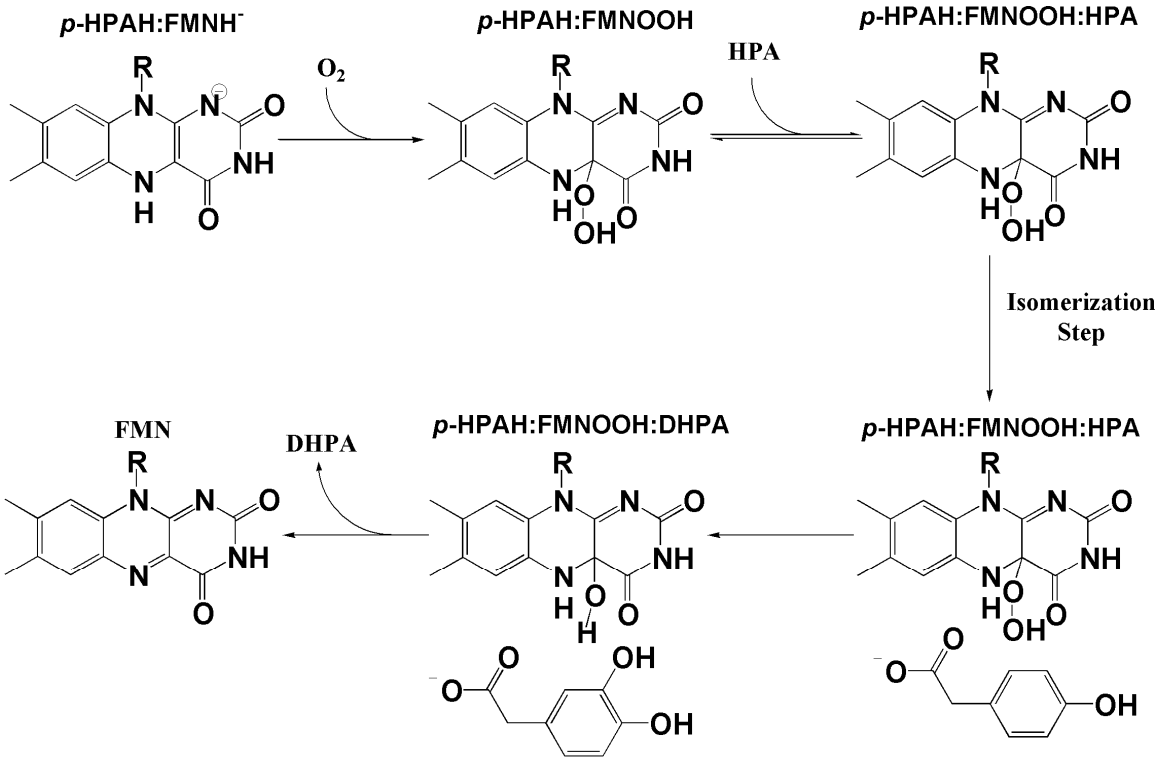

Scheme 1.6. Catalytic mechanism of *p*-hydroxyphenylacetate 3-hydroxylase using hydroperoxyflavin as an electrophile (Adapted from (*44*)).

1.9.2 Peroxyflavin intermediates as nucleophiles

A well characterized example of a flavin containing monooxygenase that uses a peroxyflavin intermediate as a nucleophile is cyclohexanone monooxygenase (*52, 53*). In the presence of cyclohexanone, the C4a-peroxyflavin intermediate is observed and the decay of the hydroperoxide is accelerated along with the insertion of oxygen into the substrate. A Baeyer-Villiger rearrangement is defined as the insertion of an oxygen atom into a substrate resulting from the treatment of a ketone with a peroxy compound. It was also shown by O_2 electrode assays and isotopic labeling studies that NADPH oxidation was fully coupled to substrate oxidation (*52*). The generation of the C4a-peroxyflavin intermediate was observed in the absence of cyclohexanone. Since this intermediate is relatively unstable, the binding of the product $NADP^+$ can drastically improve the stability of $FADOO^-$. Peroxyflavins have been shown to be unstable in aqueous environments, so the binding of $NADP^+$ may protect this intermediate for a longer period of time from subsequent oxidation. The decay of the peroxyflavin intermediate is accelerated in the presence of substrate. The enzymatic reaction is consistent with a nucleophilic attack of the substrate, cyclohexanone, by the peroxyflavin intermediate along with a Baeyer-Villiger rearrangement to form ε-caprolactone (Scheme 1.7) (*52*). Once the product is released an enzyme-bound FADOH is formed, which decays to FAD and H_2O. One oxygen atom is incorporated into the cyclohexanone substrate, while the other is released to form water.

Another flavin-dependent monooxygenase enzyme that involves a peroxyflavin intermediate that acts like a nucleophile is the bioluminescence generating enzyme,

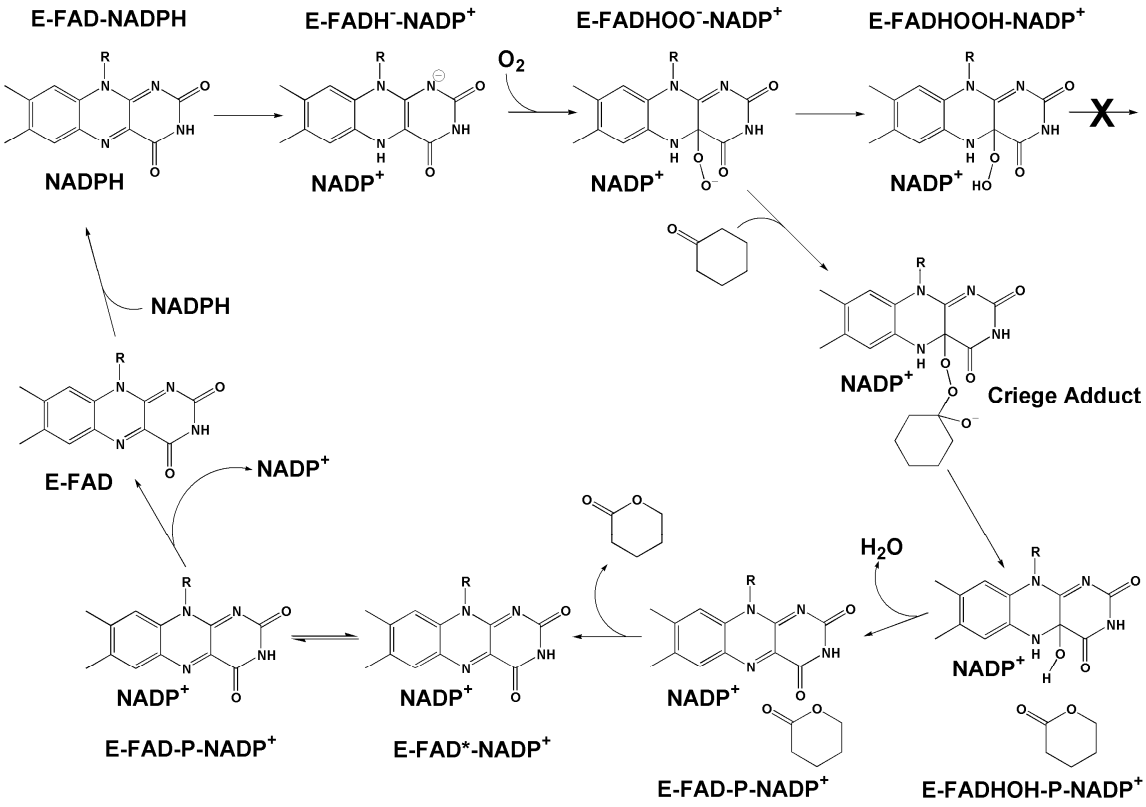

Scheme 1.7. Reaction mechanism of cyclohexanone monooxygenase using a peroxyflavin intermediate as a nucleophile (Adapted from (*52*)).

luciferase. Bacterial luciferase is the most extensively studied flavin-dependent monooxygenase. This enzyme is unusual in that it utilizes $FMNH_2$, supplied by an external NAD(P)H-dependent reductase, as a co-substrate instead of a tightly bound cofactor. The luciferase enzyme is able to form a C4a-peroxyflavin intermediate, and even stabilize it for several hours at 4 °C (*54*). It was first thought that the luciferase-bound FMNOO- intermediate would act as a nucleophile to attack a wide range of aliphatic aldehyde substrates, followed by a Baeyer-Villiger rearrangement to produce the corresponding carboxylic acid and visible light in the blue green region of the spectrum (*55*). However, this mechanism does not account for the observed isotope effects since a large primary effect would be expected for that type of reaction (*86*). Observed isotope effects obtained from a wide variety of reaction conditions have led to the conclusion that the isotope effects arise from a single rate-limiting step. A mechanism has been proposed that agrees with the unusual aldehyde isotope effects and theoretical calculations which involves a dioxirane intermediate (Scheme 1.8) (*86*). The catalytic mechanism of bacterial luciferase will be discussed in greater detail later in this section.

1.10 Two-component flavin-dependent alkanesulfonate monooxygenase system from E. coli

Sulfur starvation is the condition in which the amount of free sulfate or cysteine in the environment is limiting (*56*). Sulfur is usually assimilated *via* the cysteine biosynthetic pathway in *E. coli* and other bacterial organisms (Figure 1.1). However, during times of sulfur starvation bacterial organisms will utilize alternative sulfur sources

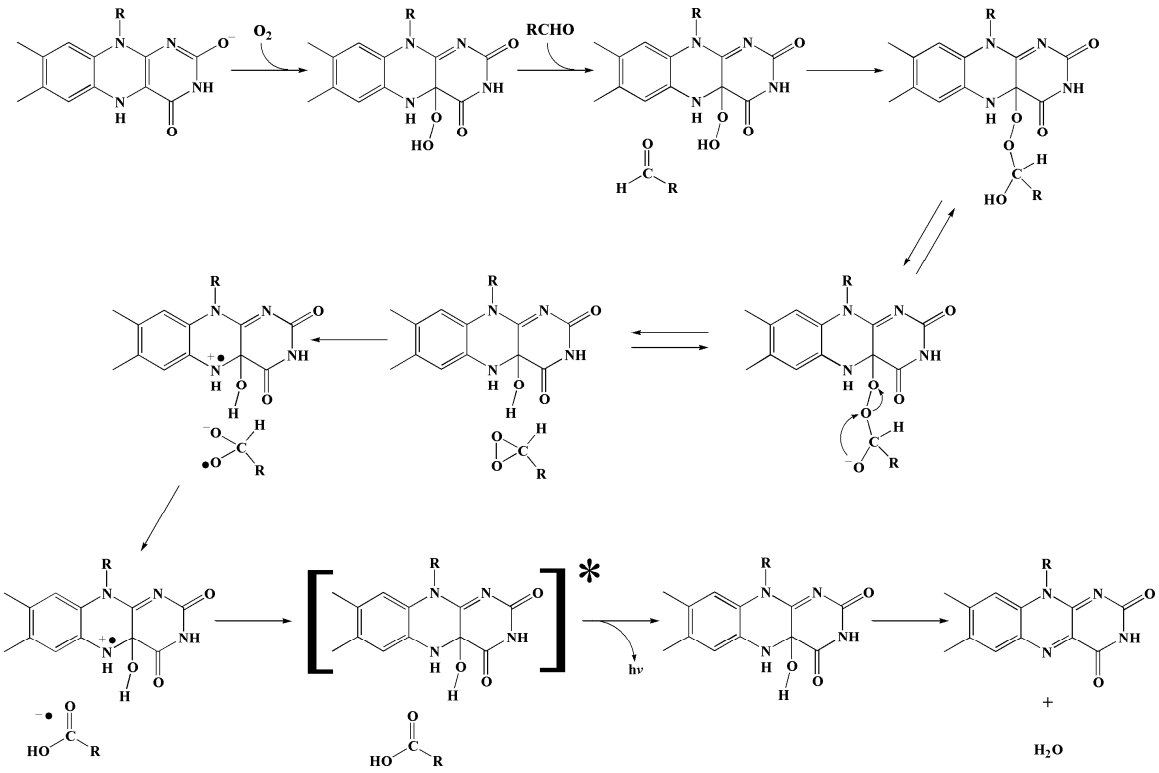

Scheme 1.8. Intermediates involved in the reaction catalyzed by bacterial luciferase (Adapted from (*47*)).

for optimal growth. These include a wide range of organosulfur compounds and sulfonate esters, with alkanesulfonates and taurine being the two most common sources. Specifically, when *E. coli* is starved for sulfur it synthesizes the Ssu proteins for the uptake and utilization of alkanesulfonates.

The alkanesulfonate monooxygenase from *E. coli* consists of two enzymes: an NAD(P)H-dependent FMN reductase (SssuE) and a $FMNH_2$-dependent alkanesulfonate monooxygenase (SsuD). These enzymes are involved in the acquisition of sulfur from alternative sulfur-containing compounds during sulfur starvation. Oxidized FMN is reduced by SsuE then transferred to SsuD where it is used to activate molecular oxygen for the subsequent oxygenolytic cleavage of the C-S bond in 1-substituted alkanesulfonates. The overall reaction mechanism for this two-component flavin-dependent system is shown in Scheme 1.9 (*57*). This enzyme system has also been

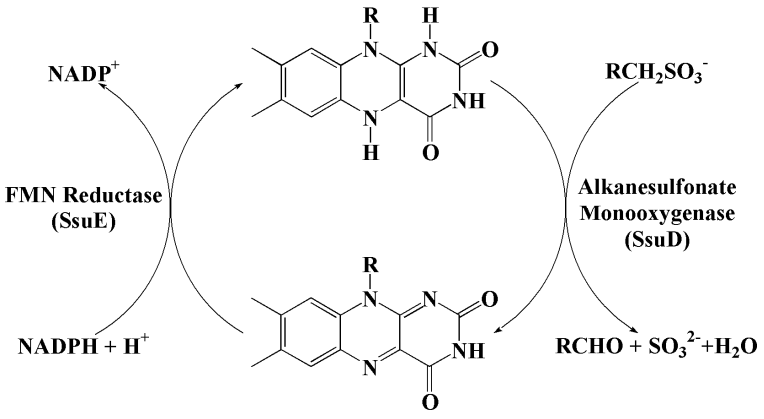

Scheme 1.9. Overall reaction mechanism of the two-component alkanesulfonate monooxygenase system (*56*).

identified in other bacterial organisms in soil including *Bacillus subtilis*, *Pseudomonas aeruginosa*, and *Pseudomonas putida* in addition to several pathogenic bacteria such as *Yersinia pestis*, *Bacillus anthracis*, and, *E. coli* 0157:H7, but has yet to be identified in higher organisms (*2*).

The initial characterization of SsuD was performed to determine binding affinities of substrates, steady-state kinetic parameters, and to characterize any intermediates in the reaction mechanism (*39*). A C4a-(hydro)peroxyflavin intermediate is proposed to be the reactive oxygen species for SsuD and other monooxygenase components belonging to a two-component flavin-dependent system (*39-48, 52, 53*). The flavin-oxygen adduct could act as an electrophile or a nucleophile, depending on the reaction catalyzed (Scheme 1.10) (*39*). A C4a-peroxyflavin is proposed to be an intermediate in the desulfonation reaction of SsuD. This intermediate would perform a nucleophilic attack on the alkanesulfonate substrate, followed by a Baeyer-Villiger rearrangement to produce sufite and the corresponding aldehyde (Scheme 1.10) (*39*). The flavin reductase, SsuE, shows a stronger affinity for the oxidized form of flavin while SsuD shows a higher affinity for the reduced form. These contrasting affinities ensure that once the flavin is reduced by SsuE it will be immediately transferred to SsuD. The activity of SsuD was tested using a coupled assay employing SsuE to provide the $FMNH_2$ for SsuD. The steady-state kinetic parameters were determined for octanesulfonate giving a K_m and k_{cat} of 44.0 ± 8.3 μM

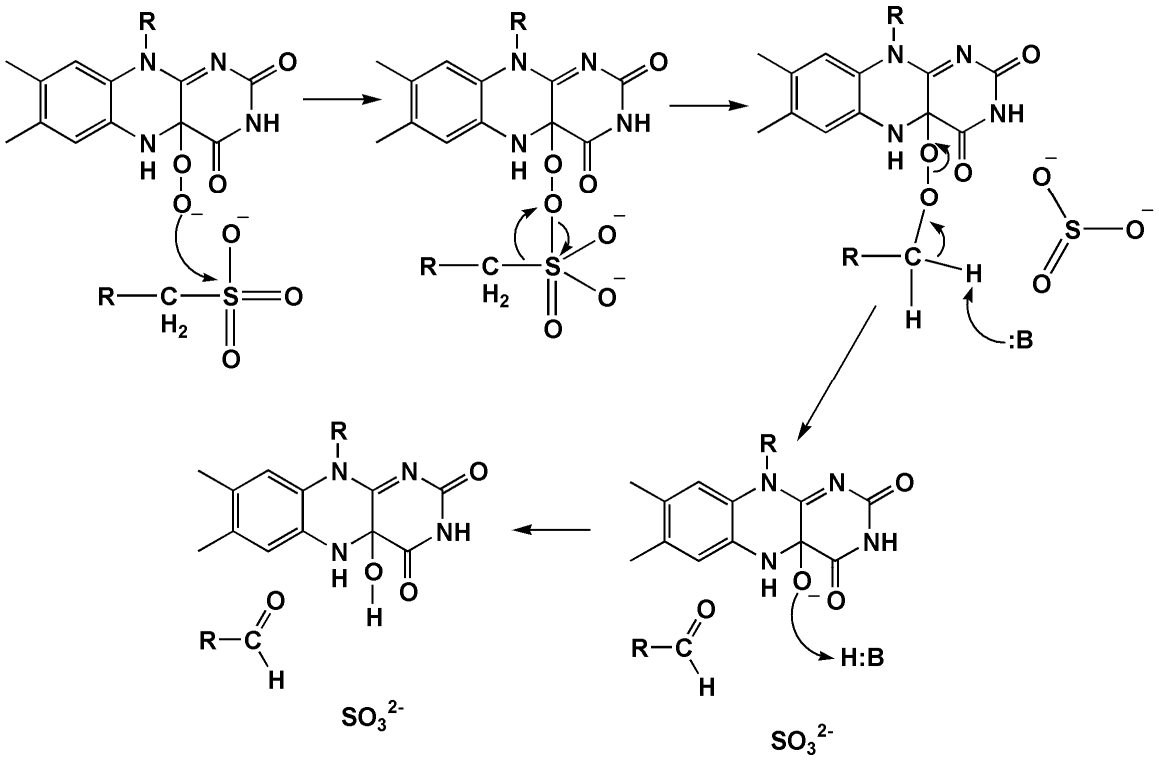

Scheme 1.10. Proposed mechanism of the desulfonation reaction catalyzed by SsuD (Adapted from (*39*)).

and 51.7 ± 2.1 min^{-1}, respectively. A K_d value for octanesulfonte binding to SsuD was 17.5 ± 0.9 μM, and it was determined that $FMNH_2$ must bind first before the octanesulfonate can bind. The formation of a C4a-(hydro)peroxyflavin intermediate was observed in the absence and at low concentrations of octanesulfonate substrate. The mixing order of SsuD and $FMNH_2$ was crucial to the observation of this intermediate because of possible formation of an inactive SsuD:$FMNH_2$ complex when SsuD was pre-mixed with $FMNH_2$ (*39*). From these kinetic and substrate binding studies, a model for substrate binding has been proposed (*39*). After reduced flavin binds, the reaction can follow two different paths: (1) the SsuD-$FMNH_2$-octanesulfonate complex is formed before reacting with O_2, or (2) the SsuD-$FMNH_2$-O_2 complex is formed before reacting with octanesulfonate. Results from the binding and pre-steady-state kinetics studies suggest that octanesulfonate binds before molecular oxygen (*39*). These experiments suggest that O_2 is the last substrate to bind, ensuring that the formation of the C4a-(hydro)peroxyflavin is fully coupled to the desulfonation reaction (Scheme 1.11) (*39*).

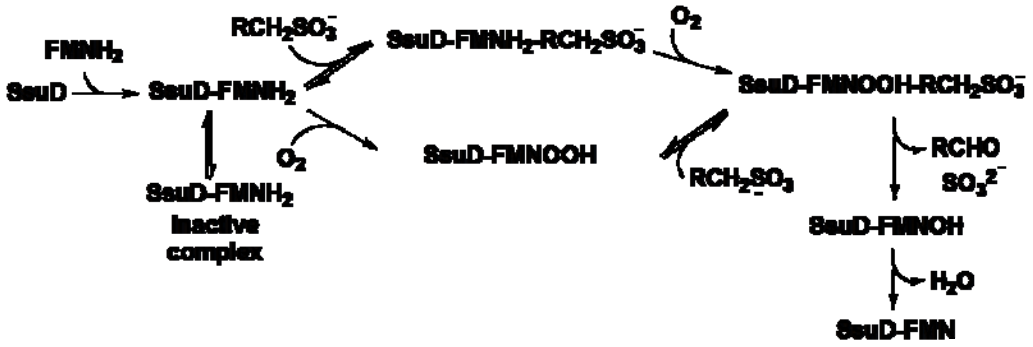

Scheme 1.11. Order of substrate binding for SsuD (Adpated from (*39*)).

1.11 Comparison of SsuD with related TIM-barrel enzyme structures

The alkanesulfonate monooxygenase, SsuD, is structurally and mechanistically related to other proteins that can be classified as TIM-barrel enzymes. Triosephosphate isomerase (TIM) is a glycolytic enzyme that catalyzes the interconversion of D-glyceraldehyde 3-phosphate and dihydroxyacetone phosphate (*59*). The three-dimensional crystal structure of the TIM monomer is composed of a $(\beta/\alpha)_8$ barrel motif, and contains an intriguing flexible loop that is close to the active site. The three-dimensional crystal structures of SsuD and several other enzymes that are structurally related to SsuD have been solved in recent years (*60-63*). These members of the bacterial luciferase family include Mer, an F_{420}-dependent methylenetetrahydromethanopterin reductase; LadA, a long-chain alkane monooxygenase; and bacterial luciferase from *Vibrio harveyi*, as well as SsuD. The locations of the known active sites of enzymes exhibiting a TIM-barrel fold have been shown to be located at the C-terminal end of the β barrel (*64*). The LuxA, and Mer monomers contain a non-prolyl *cis* bond which creates an outward extension at the entrance of the active sites of these enzymes. In contrast, no non-prolyl *cis* bond is present at the equivalent position in either the LadA or SsuD monomers. The SsuD enzyme shows striking structural relationship to LuxA, LadA, and Mer, which use $FMNH_2$ or the flavin analog F_{420} as a substrate; however, the structural relatedness of SsuD to TIM-barrel enzymes that use flavins as a tightly bound cofactor is poor.

1.11.1 Bacterial luciferase from Vibrio harveyi (LuxA)

Bioluminescent organisms have captivated people for centuries. These living organisms that radiate light such as fireflies, glowworms, mushrooms, fish, or bacteria are very widely dispersed throughout the natural environment. The enzymes responsible for these bioluminescence reactions are called luciferases, and respresent a very large and diverse group. In fact, the only common bond between theses enzymes from different organisms is the absolute requirement of O_2 needed to catalyze their respective reactions.

Luminous bacteria are the most widely distributed of all the bioluminescent organisms, being found in marine, freshwater, and terrestrial environments. Bacterial luciferase is a flavoprotein monooxygenase and has been the most extensively studied of all known luciferases. Like SsuD, bacterial luciferase employs reduced flavin as a substrate, which is supplied by a reductase, rather than as a tightly bound cofactor. The enzyme catalyzes the reaction of $FMNH_2$, O_2, and a long-chain aliphatic aldehyde to yield the corresponding carboxylic acid, FMN, and a photon of blue-green light. All bacterial luciferases studied so far appear to be homologous and catalyze the same reaction:

$$FMNH_2 + O_2 + RCHO \rightarrow FMN + RCOOH + H_2O + h\nu \ (\lambda_{max} = 490 \text{ nm})$$

The reaction has been shown to proceed through various intermediates, including a C4a-(hydro)peroxyflavin (Scheme 1.7) (*47*). Light emission occurs when this flavin intermediate dehydrates to yield FMN.

The three dimensional crystal structure of luciferase has been solved, but the binding sites for reduced flavin and aldehyde substrate have not been identified (*61*).

However, studies have been performed in which $FMNH_2$ has been modeled into the crystal structure of bacterial luciferase (*65*). Unlike SsuD, bacterial luciferase is a heterodimeric enzyme composed of α and β subunits with a molecular weight of 77 kDa. These α and β subunits have different topologies with molecular masses of 40 and 37 kDa, respectively (Figure 1.10). Both polypeptides are encoded on the same *lux* operon, designated *luxA* and *luxB* for the α and β subunits, respectfully. The two *lux* genes display sequence homology that may have arisen during a gene duplication event (*66*). The α subunit of the luciferase heterodimer contains the active center and binds one reduced flavin molecule. The role of the β subunit has been shown to be essential for a high quantum yield reaction (*55*). These two subunits are very similar in overall structure and share about 32% amino acid sequence homology. However, there is a 29 amino acid region in the α subunit that is not present in the β subunit. Dimerization of the α and β subunits is mediated through a parallel four-helix bundle (*61*). Each subunit contributes two α-helices (α2 and α3) to form this bundle. Interestingly, there is an intersubunit hydrogen bond between amino acid residues His45 and Glu88. These residues are conserved among the two subunits with αHis45 H-bonding to βGlu88 and βHis45 H-bonding to αGlu88. Both of these residues are conserved throughout all bacterial luciferase enzymes, and mutation of His45 in the α subunit of *V. harveyi* luciferase resulted in a dramatic decrease in the bioluminescence activity (*46*). The high resolution crystal structure also revealed a non-prolyl *cis* peptide bond in the α subunit of luciferase between residues Ala74 and Ala 75, but not the β subunit (*61*). No non-prolyl *cis* peptide

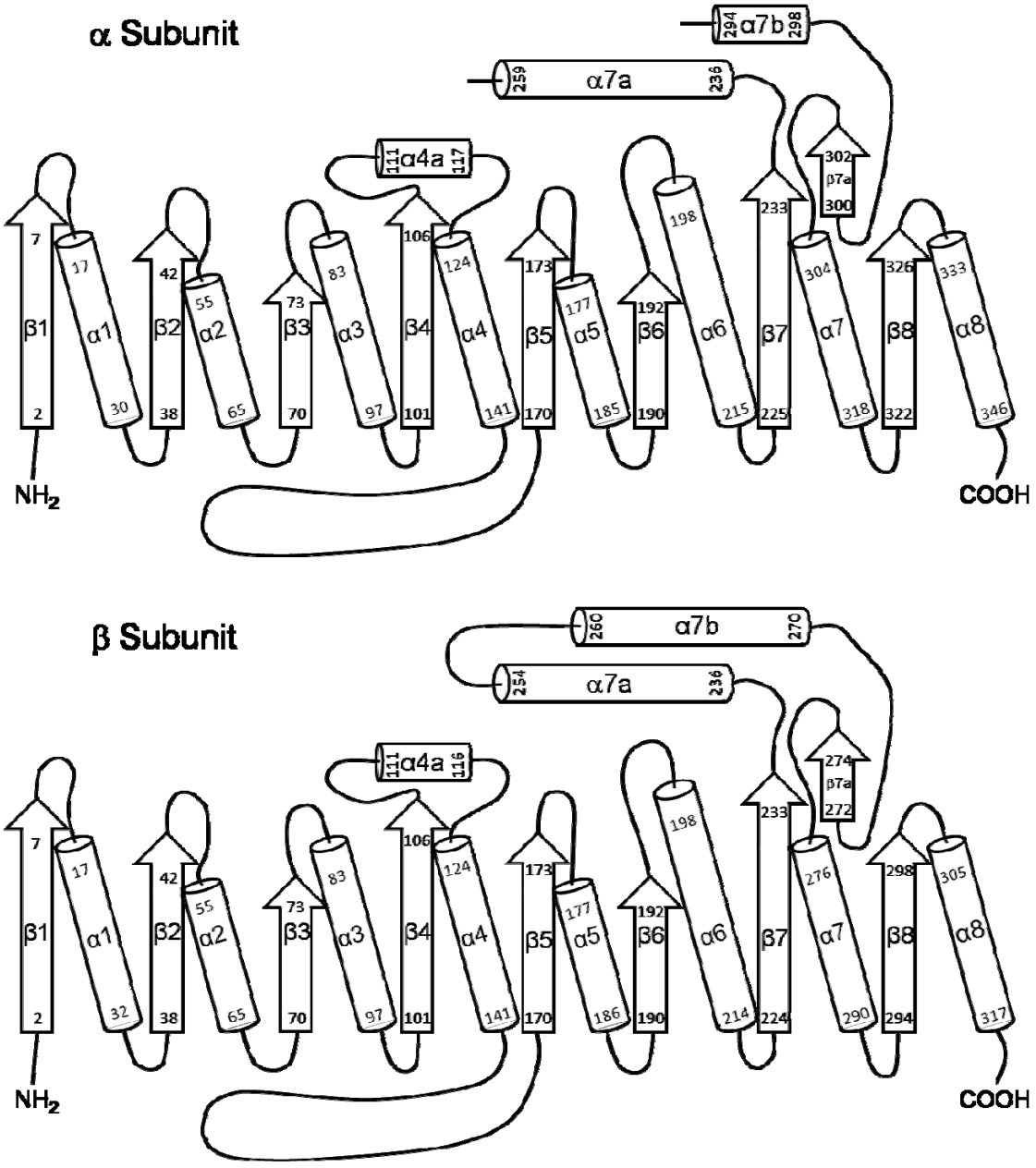

Figure 1.10 Topology diagram showing the secondary structural elements of the α and β subunits of luciferase, represented as arrows for β-strands and cylinders for α-helices (Adapted from (*61*)).

bond was identified at the equivalent position between residues Ala76 and Leu77 in the crystal structure of either SsuD subunit (*60*).

The mechanism of bacterial luciferase has been extensively studied through stopped-flow kinetics, site-directed mutagenesis, and flavin binding studies (*45-49*). A model of the luciferase:FMN complex has been developed based on structural activity data, energetic criteria, and geometric requirement for catalysis (Figure 1.11) (*65*). Site-directed mutagenesis was performed to elucidate the role of specific residues in the reaction catalyzed by bacterial luciferase. It has been known for many years that luciferase contains a reactive cysteinyl residue located in the active site that is protected from alkylation by the binding of flavin (Figure 1.12). It was demonstrated that alkylation of the reactive thiol, which resides in a hydrophobic pocket, leads to inactivation of the enzyme (*67*). Substitutions of Cys106 were constructed to determine whether this reactive cysteine residue is required for the formation of the C4a-(hydro)peroxyflavin intermediate, substrate binding, or the emission of visible light. The cysteine residue was replaced with either alanine, serine, or valine. The light intensities exhibited a 3-, 2-, and 50-fold decrease compared to wild-type for the serine, alanine, and valine variants, respectively (*48*). It is interesting to note that luciferase enzymes from *Vibrio fischeri*, *Photobacterium leiognathi*, and *Photobacterium phosphorium* contain a valine residue at this same position in the α subunit (*55*). There is also a strictly conserved neighboring threonine residue in the three-dimensional crystal structure of *V. harveyi* luciferase; however the functional role of this amino acid residue is not known.

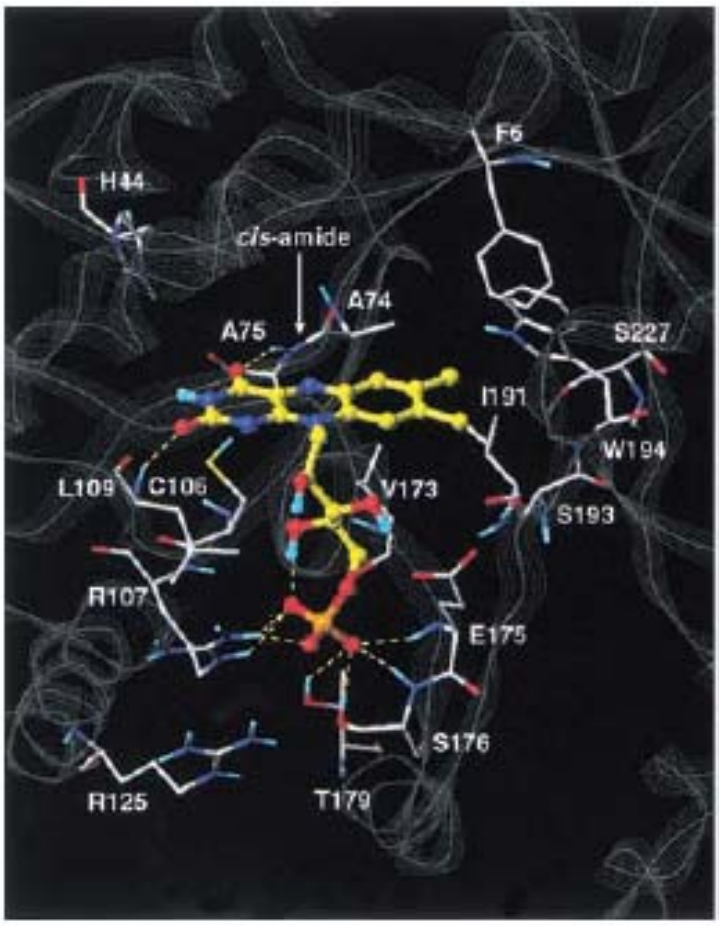

Figure 1.11. Model of the luciferase:flavin complex. Flavin is shown in a ball-and-stick representation with the carbon atoms colored in yellow. Hydrogren bonds formed between amino acid residues and the FMN moiety are shown as dashed lines (*65*) (Reprinted with permission).

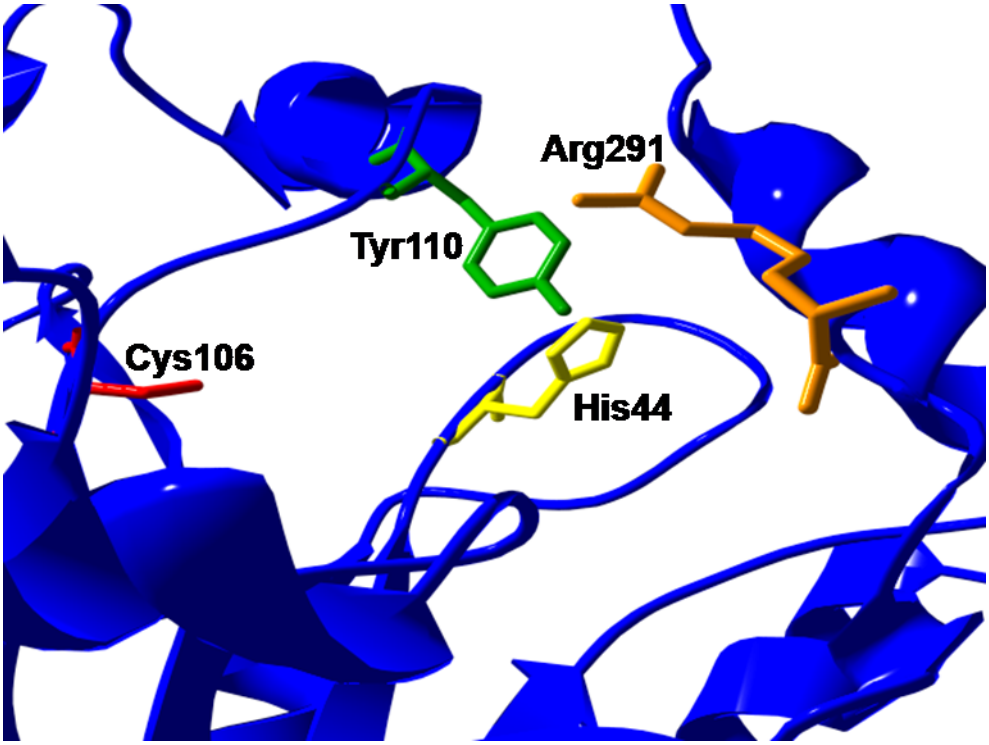

Figure 1.12. Three-dimensional crystal structure of the active site of luciferase from *Vibrio harveyi* (PDB ID: 1LUC) (*61*).

The mechanistic role of Cys106 in bacterial luciferase was also investigated using rapid reaction kinetic analyses and substrate binding studies (*45, 48*). The formation of a C4a-(hydro)peroxyflavin intermediate was previously shown to be required for the emission of visible light by bacterial luciferase (*47*). This intermediate has a maximum absorption at approximately 380 nm. The variant luciferase enzymes also catalyzed the formation of the C4a-(hydro)peroxyflavin intermediate with the same rate as the wild type protein. However, the decay of this intermediate was two orders of magnitude faster than with the wild type enzyme. The binding affinity for $FMNH_2$ to all luciferase variants was decreased with the serine variant being the most altered and the valine variant being the least altered. The Cys106Ser and Ala variant enzymes had lower affinities for *n*-decanal substrate than wild type. However, under the same conditions, the Cys106Val mutant was apparently a poor aldehyde binding enzyme. The apparent dissociation constants for a variety of aldehyde substrates were greater than one millimolar, making it difficult to obtain saturation. Also, the C106A and C106S luciferase variant enzymes catalyzed the bioluminescence reaction with similar efficiencies compared to wild-type luciferase. However, the bioluminescence of the C106V luciferase variant catalyzed reaction was about 50-fold less than wild-type enzyme. These experiments demonstrated that the cysteine at position 106 in the α subunit of luciferase from *V. harveyi* is critical for the stabilization of the C4a-(hydro)peroxyflavin intermediate.

The α subunits of all bacterial luciferase species have five conserved histidine residues in which a sequence is known. Mutation of these residues all resulted in marked decreases in bioluminescence activity, but the degree to which each mutant was

inactivated depended on the position of the histidyl residue mutated, and the type of mutation which was introduced (*47*). Of the five histidyl residues which were mutated, His44 and His45 seemed to be the most crucial to the bioluminescence activity of bacterial luciferase. The His44 and His45 variants replaced with an aspartate, alanine, or lysine were examined further. Although it is known that the bioluminescence activity of bacterial luciferase is coupled to the oxygenation of aldehyde substrate, these six variants retained little or no significant activity for the monooxygenation of aldehyde (*47*). The C4a-(hydro)peroxyflavin intermediate was not detected in experiments performed on the H45D, H45A, or H45K luciferase variants, while 14, 45, and 20% bioluminescence yields were obtained from absorption spectroscopy for the H44D, H44A, and H44K variants, respectfully, compared to wild-type luciferase (*47*). Isotope effects on the His44 and His45 variants using [1-^{2}H]decanal as a substrate were similar to those obtained for wild type enzyme, suggesting that neither histidine residue was crucial for the abstraction of the C1 hydrogen of the aldehyde substrate.

Replacement of the histidine at position 44 in the α subunit of *V. harveyi* luciferase by alanine was previously shown to reduce the bioluminescence activity by 5 orders of magnitude compared to wild type luciferase (*47*). This activity could be reconstituted with the addition of imidazole, and other simple amines, to the enzymatic reaction mixture (*58*). The efficiency of imidazole in enhancing the activity of the H44A mutant luciferase was also found to be pH dependent. Through these chemical rescue experiments it was suggested that this histidine at position 44 was the catalytic base in the

reaction catalyzed by luciferase from *V. harveyi*. However, no pH profile studies were performed to solidify these observations.

1.11.2 Long-chain alkane monooxygenase (LadA)

LadA is a key initiating enzyme in the long-chain alkane degradation pathway in thermophilic bacillus *Geobacillus thermodenitrificans*. This flavoprotein monooxygenase is involved in the conversion of long-chain alkanes, ranging from C_{15} to C_{36}, to the corresponding alcohol, where $R = 13 \leq n \geq 34$ (Scheme 1.12). The three dimensional

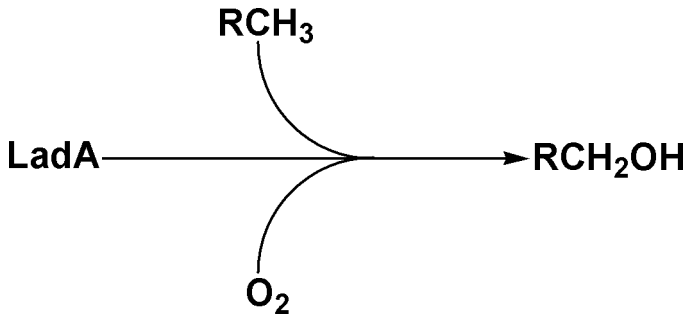

Scheme 1.12. Overall reaction catalyzed by LadA (Adapted from (*68*)).

crystal structure for LadA has been solved in the absence and presence of bound FMN cofactor (*68*). The results identify LadA as a homodimer containing two separate active sites in which the flavin cofactor is bound. The structure of LadA is composed of a $(\beta/\alpha)_8$ barrel or TIM barrel fold. The LadA protein is very structurally similar to other flavin-dependent enzymes designated as bacterial luciferase family members: the F_{420}-dependent N^5,N^{10}-methylenetetrahydromethanopterin reductase Mer, the F_{420}-dependent secondary alcohol dehydrogenase Adf, *V. harveyi* luciferase LuxA, and the alkanesulfonate monooxygenase SsuD from *E. coli* (*60-63*). All of these enzymes fold as

TIM barrel proteins and utilize flavin or the flavin analogue F_{420} as a substrate. The dimerization between both subunits of LadA is promoted by a parallel four-helix bundle formed by α_2 and α_3 of each subunit, which is also found in bacterial luciferase. In contrast to the structures of LuxA, Mer, and Adf, there exists no non-prolyl *cis* peptide bond at the equivalent position of either LadA or the LadA:FMN complex. Furthermore, a C-terminal extension of the β barrel fold of LadA was also observed in SsuD but not in LuxA, Mer, or Adf. In the FMN binding pocket of LadA, Ser230 is involved in interactions with the phosphate group of the flavin moiety and is conserved in SsuD and LuxA. LadA also contains five insertion regions and an extension at the C terminal end of the polypeptide chain, similar to SsuD. These insertion segments (IS) are located between β strands and α helices with IS1 – IS4 covering the C-terminal end of the β barrel (Figure 1.13). Since the active sites of all TIM barrel enzymes are located in this region, it is safe to say that these insertion segments may play a pivotal role in substrate binding and/or dimer formation. From this crystal structure, IS5 appears to play an important role in dimer formation. From gel filtration experiments with a Cys14Ala mutant there was no observed dimer formation, due to the essential location of Cys14 in IS1. This is proposed to perturb the hydrophilic interactions between IS1 and IS2 which is postulated to affect interactions in neighboring subunits to prevent LadA from dimerization.

LadA contains a large, deep pocket at the C-terminal end of the β barrel with enough space to accommodate flavin, O_2, and the terminal parts of a long-chain *n*-alkane. It is believed that the reaction mechanism proceeds through a C4a-(hydro)peroxyflavin

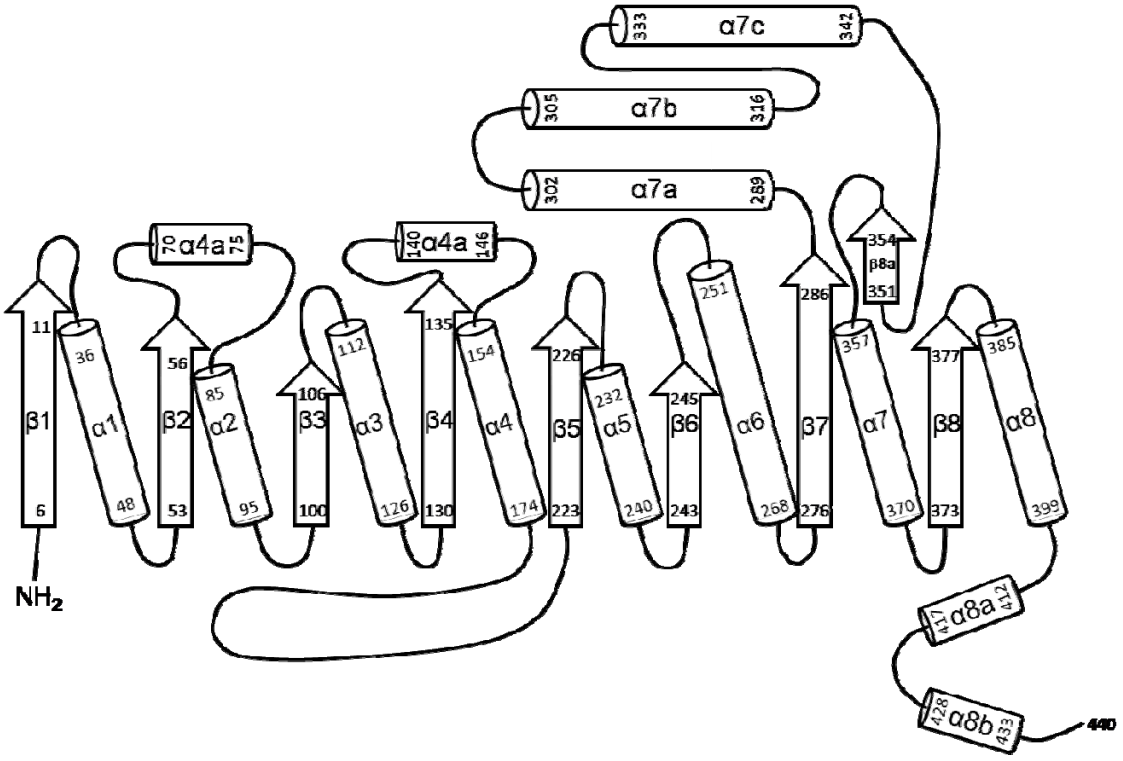

Figure 1.13 Topology diagram showing secondary structural elements of each LadA monomer, represented as arrows for β-strands and cylinders for α-helices (Adapted from (*68*)).

intermediate as with SsuD and bacterial luciferase. There are amino acid residues that line the flavin binding cavity that could sequester the isoalloxazine ring of FMN to protect any intermediates during catalysis. There is also a His138 residue that is postulated to act as a hydrogen bond donor to prevent the rapid breakdown of the proposed C4a-(hydro)peroxyflavin intermediate. The other amino acids His17, Tyr63, Gln79, and His311 are postulated to be located above the terminal carbon of the alkane from *in silico* alkane substrate docking experiments (*68*). Enzyme inactivation assays performed on variants of these four residues suggest that these amino acids may play a critical role in substrate activation and electron transfer. The Cys14, His311 and Tyr63 residues of LadA have spatial counterparts in LuxA at Cys106, His44, and Tyr110 and in SsuD at Cys54, His228, and Tyr331. The roles of the cysteine and histidine residues in bacterial luciferase and SsuD have been elucidated; however, the role of Tyr110 and Tyr331 of LuxA and SsuD, respectively, has not been fully investigated. The observation that the residues of each of these enzymes exist in a similar spatial arrangement provides further evidence of the similarities between the putative active sites of LadA and SsuD and the well characterized active site of LuxA.

1.11.3 Alkanesulfonate monooxygenase (SsuD)

The $FMNH_2$-dependent alkanesulfonate monooxygenase SsuD catalyzes the conversion of alkanesulfonates to the corresponding aldehyde and sulfite. This enzyme is synthesized under sulfur starvation conditions and allows *E. coli* to utilize a wide variety of 1-substituted alkanesulfonates as sulfur sources for growth when cysteine and inorganic sulfate are not available. The three-dimensional crystal structure of SsuD has

been solved and shown to be a homotetramer with a molecular weight of 181 kDa (*60*). The results indicate that SsuD folds similarly to a class of enzymes designated by a TIM-barrel fold, although the amino acid sequence identity is low. The structure of SsuD differs from the prototypical TIM-barrel structure with the addition of four insertion regions connecting β-strands and α-helices, plus an extension at the C-terminal region of the polypeptide chain (Figure 1.14). The SsuD crystals contain two monomers related by a 2-fold axis. Dimerization is mediated by a parallel four-helix bundle centered on this 2-fold axis. Each monomer contributes helices α2 and α3 to this four-helix bundle. In addition to this four-helix bundle, dimer formation is promoted by contacts between a β-hairpin structure of one monomer (insertion region 3) and insertion region 2 of the other monomer. In the tetrameric structure of SsuD the four subunits come in close contact at the center of the tetramer. The major interactions involve two four-helix bundles interacting in a head-to-tail fashion between the α1-helices of units A and C and α8-helices of units B and D (Figure 1.15) (*60*). Contacts between subunits A and C involve interactions between the α7a helices of the two subunits. In addition, there are significant contacts through the C-terminal extensions of A and D and equivalently B and C.

The crystal structure reveals that the distribution of amino acid residues Cys54, His228, and Tyr331 of SsuD are in a similar spatial arrangement to putative active site residues Cys14, His311, and Tyr63 of LadA and catalytically relevant residues Cys106, His44, and Tyr110 of bacterial luciferase. As mentioned, SsuD has been shown to fold similarly to bacterial luciferase, even though their amino acid sequence identity is low

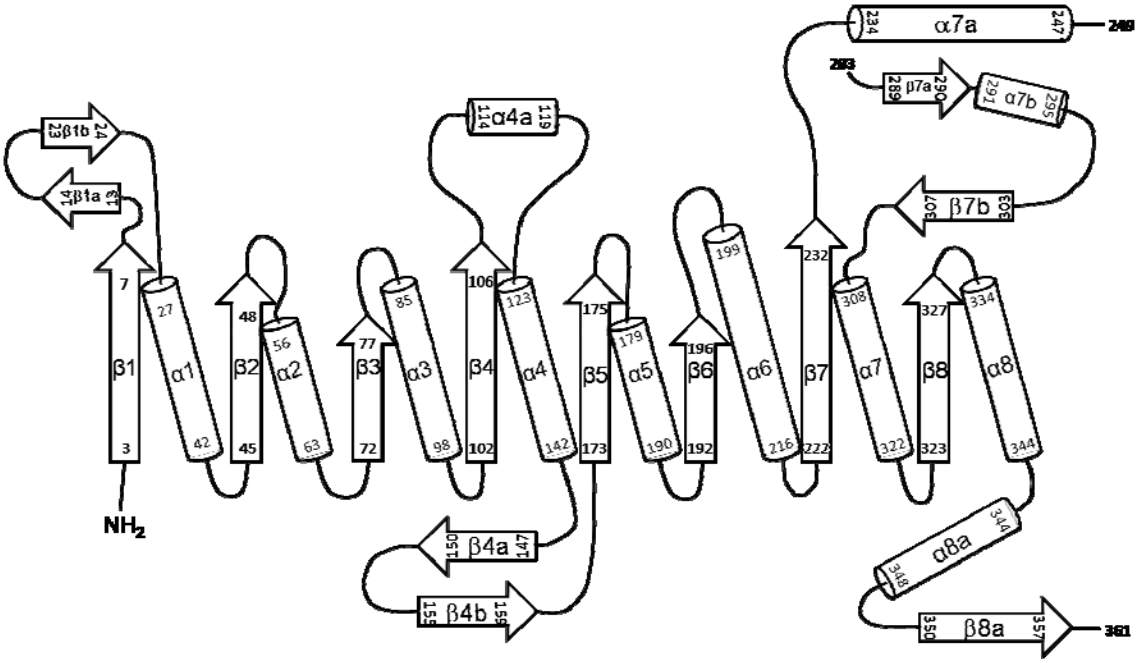

Figure 1.14 Topology diagram showing secondary structural elements of each SsuD monomer, represented as arrows for β-strands and cylinders for α-helices (Adapted from (*60*)).

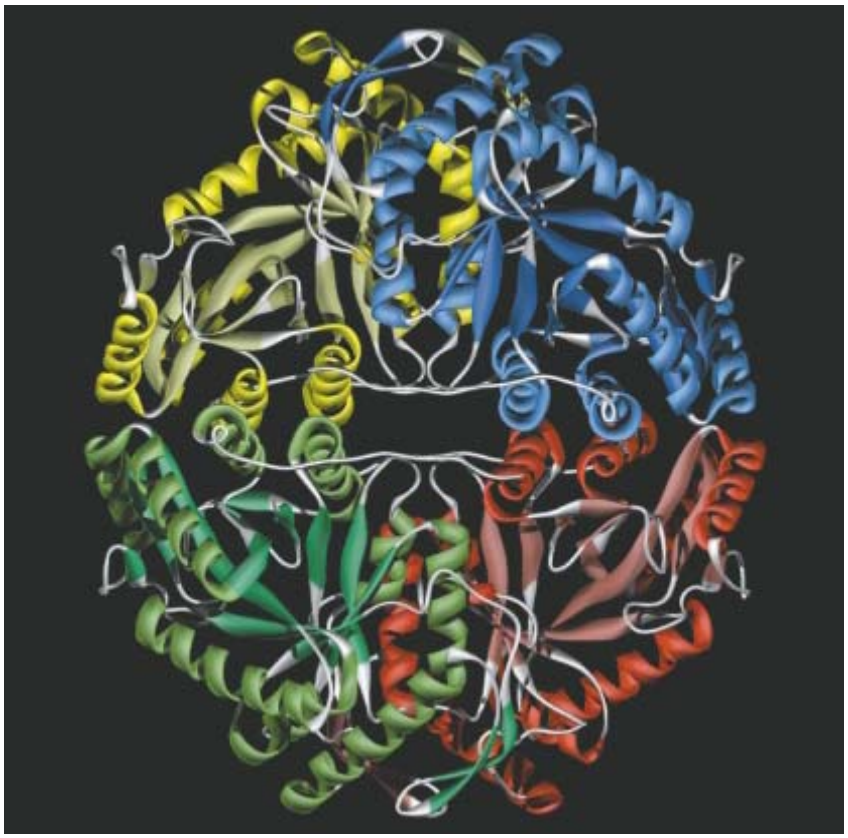

Figure 1.15 Tetrameric structure of SsuD showing the four-helix bundles mediating contact between subunits A (yellow), B (blue), C (green), and D (red) involved in dimerization and tetramerization (*60*) (Reprinted with permission).

(15%). Unfortunately, the three dimensional crystal structure of SsuD does not contain the $FMNH_2$ substrate. Attempts to co-crystallize SsuD with reduced or oxidized flavin and/or various alkanesulfonates has been unsuccessful, therefore the active site of this enzyme has not been clearly identified. However, the amino acid residues Tyr331, His228, and Cys54 are highly conserved throughout all known SsuD sequences from other bacterial organisms and are arranged in a structurally similar orientation as the active site residues in bacterial luciferase (Figure 1.16). Previous studies with SsuD have shown that enzymatic activity is abolished upon cysteine-labeling with methylmercury indicating that the lone cysteine at position 54 is crutial in the catalytic reaction. The location of this putative active site cavity is in agreement with the observation that the active sites of all TIM-barrel enzymes are located at the C-terminal end of the β-barrel (*64*). The active-site arrangements in both enzymes are similar, but the absolute location within the TIM-barrel is not identical. However, both SsuD and LuxA contain a disordered loop located in insertion region 4 which contains an Arg297 and Arg291, respectively. Experiments in which the entire disordered loop of bacterial luciferase was deleted suggest that the disordered loop of LuxA would cover the active site once substrates are bound to protect any intermediates formed in the luciferase catalyzed reaction (*80*).

The proposed active site residues Cys54, His228, Tyr331, and Arg297 of SsuD have counterparts of Cys106, His44, Tyr110 and Arg291 in the α subunit (LuxA) of luciferase and Cys14, His311, and Tyr63 in LadA. It is also important to note that the

SsuD enzyme activity is completely abolished when the Arg297 is mutated to cysteine (*57*). It is postulated that the loss of activity is due to a disulfide bridge between the aberrant Arg297Cys mutation due to the conformational flexibility of this region. The role of the tyrosine residues in both SsuD and LuxA have not been determined, however studies have been performed on the histidine residues from both enzymes. The His44 in bacterial luciferase was been proposed to act as a catalytic base in the oxidation of aliphatic aldehydes (*58*). Several substitutions of His228 SsuD were generated, and experiments were performed to determine the effect of these mutations on the binding of substrate, activity, and C4a-(hydro)peroxyflavin formation. These substitutions of His228 had no effect on the binding of flavin or octanesulfonate substrate (unpublished results). However, the steady-state kinetic parameters for each of the His228 variants were different. The k_{cat}/K_m for octanesulfonate was decreased by 50-fold for H228A and H228K SsuD, and 200-fold for H228D SsuD compared to wild type SsuD. It was determined that the activity for H228A SsuD could be reconstituted, at pH values above 7.0, by chemical rescue with imidazole. About 10 – 15% of the activity could be rescued in the pH range of 7.0 – 9.0, indicating that the deprotonated form of the imidazole ring is required for catalysis. The C4a-(hydro)peroxyflavin intermediate was also observed in the reaction of $FMNH_2$ with H228A in air-saturated buffer. The mutation of His228 to alanine had little effect on the rate of formation or decay of the C4a-(hydro)peroxyflavin

intermediate. To further determine whether the His228 is the catalytic base in the reaction catalyzed by SsuD the pH dependence on the k_{cat} and k_{cat}/K_m values was evaluated from pH 5.8-9.5. Two pKa values of 6.66 and 9.77 for the k_{cat} pH profile and 6.72 and 9.89 for the k_{cat}/K_m pH profile were also determined for the H228A variant. Differences between the pKa values between H228A and wild-type SsuD were within error. Even though the addition of imidazole could rescue H228A SsuD activity at pH values higher than 7.0, this only indicates that the deprotonated form of H228 is the active form during catalysis. If the histidine at position 228 was the catalytic base, one would expect the pH profiles of H228A and wild-type SsuD to be different; however, the pH profiles are similar. The results from studies on His228 SsuD variants suggest that this histidine residue is not the catalytic base in the desulfonation reaction catalyzed by SsuD; however, the His228 could be involved in stabilization of the active site in the proper conformation for catalysis to occur. A conserved Tyr331 is also located in a similar spatial position as Tyr110 of bacterial luciferase; however, no information is available about the role of this amino acid residue. The roles of Cys54 and Arg297 will be discussed in a later section.

1.12 Flexible loop

Surface loops are a common structural feature in many globular proteins. These loops are irregular segments of protein structure that link together other regular secondary structural elements like α-helices and β-sheets. Many times loops are found to contribute to the structure of an enzyme active site or play a functional role both in the binding of

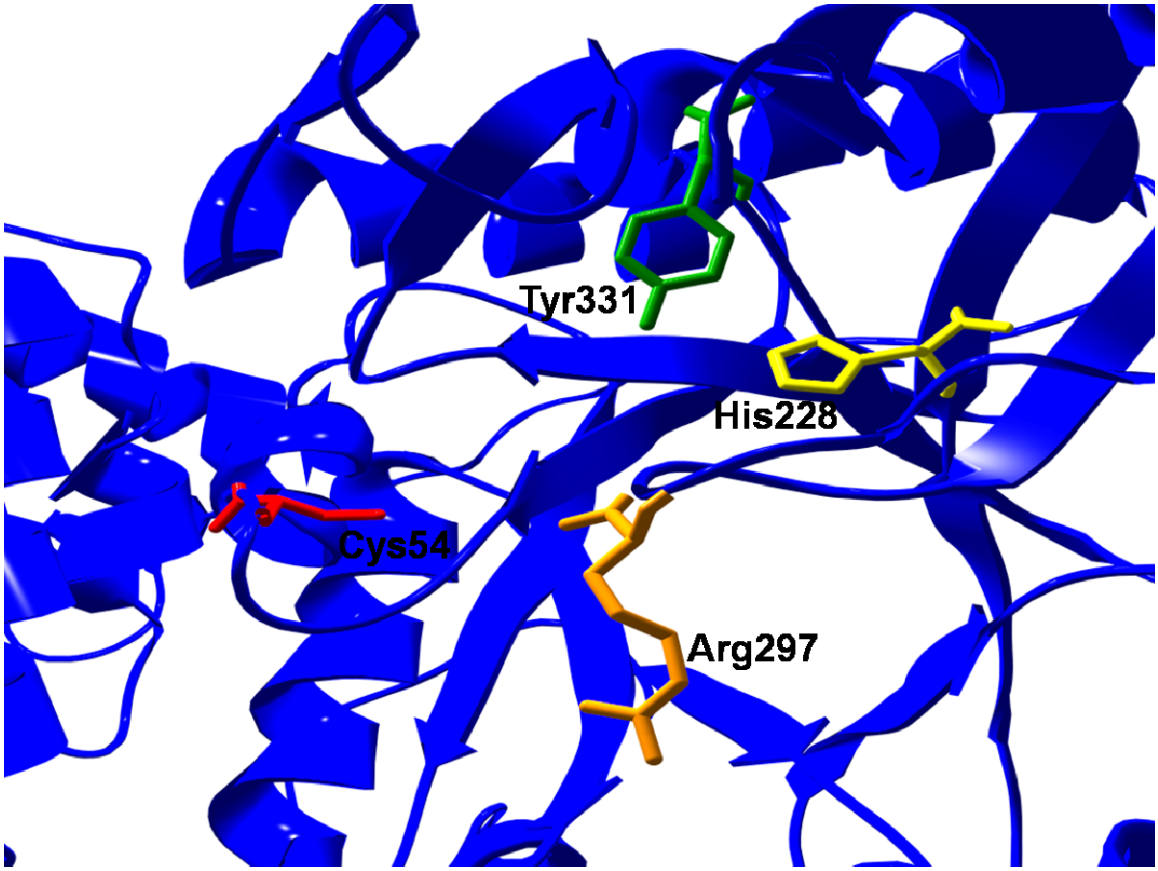

Figure 1.16. Putative active site of the alkanesulfonate monooxygenase, SsuD (*60*).

ligands and in enzyme catalysis. In these lid-containing β/α barrel enzymes, it is postulated that loop closure sequesters the substrate from solvent as well as prevents the premature release of catalytic intermediates. Three-dimensional crystal structures of many enzymes that exhibit TIM-barrel folds have provided evidence for movement of a flexible loop upon substrate binding (*69-71*). In each case, the loop is poorly defined in electron density maps indicating a high degree of conformational flexibility.

The flexible loop of triosephosphate isomerase has been extensively characterized. It has been shown that upon substrate binding in triosephosphate isomerase, this flexible loop closes over the active site to protect the substrates and/or intermediates during catalysis. The active site loop of triosephosphate isomerase consists of about ten residues and exhibits a hinged-lid motion between an "open" or "closed" conformation. In this fashion this "flexible loop" can exclude bulk solvent from the active site and position key residues for catalysis. In the crystal structures of both chicken muscle and yeast triosephosphate isomerase residues 168-177 leave the active site open to solvent in the apo form of the enzyme, but close down upon the binding of dihydroxyacetone phosphate or the competitive inhibitors phosphoglycolate, phosphoglycolohydroxamate, or even inorganic phosphate (*72,73*). The phosphate group of the bound substrate (or inhibitor) is near the mouth of the active site, while the triose part fills the active site pocket. Differences in the crystal structures of unliganded and liganded enzyme suggest a movement of the loop residues of around 10 Å toward the

active site when the substrate binds. Mutation of this loop resulted in failure to protect the highly reactive enediol intermediate causing elimination of the phosphate group and production of methylglyoxal, a compound which is toxic to cells (*74*).

Bacterial luciferase belongs to the family of enzymes described earlier as TIM-barrel enzymes, first observed in the structure of triosephosphate isomerase. The structural design of the αβ-barrel has eight repeating sections of the β-sheet-loop-α-helix motif with each section connected by an intervening loop to form a core of parallel β-sheets confined by a solvent exposed cage of α-helices (*64*). The main feature that distinguishes the α-subunit from the β-subunit of bacterial luciferase is a 29-residue loop between α7a-helix and β7a-sheet. This region is consistent with high mobility and is unresolved in the previously determined three-dimensional crystal structure (*61*). This disordered loop is located near the active site of bacterial luciferase and has been previously reported to be extremely susceptible to proteolysis, where cleavage in this region by any number of proteases rapidly inactivates the enzyme (*75, 76*). However, the loop seems to be protected from proteolysis by the binding of $FMNH_2$, suggesting that the loop becomes more ordered and unavailable to proteases upon substrate binding (*77*). Mutations were made to conserved residues located on the flexible loop in the α-subunit of luciferase to determine whether specific residues were required to stabilize any active site intermediates during catalysis. Residues Gly275 and Phe261, when mutated to Pro

and Asp, respectively, showed a decrease in the V_{max} value by 4-5 orders of magnitude (*78*). The formation of the C4a-(hydro)peroxyflavin intermediate was investigated with these variants. The G275P mutant was able to catalyze the formation of a C4a-(hydro)peroxyflavin intermediate with the same efficiency as wild-type luciferase, while the F261D mutant exhibited a 3-fold decrease in intermediate formation. Studies were also performed in which the entire 29 amino acid residue loop was removed from the enzyme. Deletion of this loop did not affect the overall secondary structure of the protein. The luciferase variant, designated $\alpha\Delta_{262\text{-}290}\beta$, retained its ability to bind flavin and aldehyde substrates with wild-type affinity and could carry out the chemistry of the bioluminescence reaction with nearly wild-type efficiency. However, the bioluminescence quantum yield of the $\alpha\Delta_{262\text{-}290}\beta$ luciferase variant was decreased by 2 orders of magnitude compared to wild-type luciferase (*79*). These experiments provide evidence that this "mobile loop" is an integral component of the active site or in close proximity to the active site of the enzyme.

The flexible loops located in SsuD and bacterial luciferase are very similar to ones found in triosephosphate isomerase from different organisms. These loops in SsuD and bacterial luciferase are proposed to close over the active site after the binding of substrates to protect any intermediates from being oxidized during the enzyme catalyzed reaction. In the initial purification and characterization of SsuD there contained a

mutation of Arg297 to Cys. This mutated enzyme had no detectible activity and it was postulated that a disulfide bond was formed between the Arg297Cys and Cys54. The fact that mutation of Arg297 located on the flexible loop in SsuD to Cys abolished all activity suggests that this region is conformationally flexible. Results from experiments performed on Arg297 SsuD variants will be discussed in a later section.

1.13 Summary

Flavoproteins, which are widely distributed in many different organisms, catalyze a variety of reactions. They play essential roles in metabolism and the degradation of harsh chemicals. Specifically, the flavin monooxygenases are essential in detoxification, degradation, and biosynthesis of certain compounds in bacterial organisms. Along with a number of single-component flavoproteins monooxygenases, many two-component flavin-dependent monooxygenases have been identified in bacteria. All two-component monooxygenase systems contain a flavin reductase and a flavin-dependent monooxygenase. The reductive and oxidative half-reactions are carried out on separate enzymes. Although there are many different flavin monooxygenases catalyzing a variety of different reactions, the overall catalytic mechanisms are quite similar. Flavin is reduced by the coenzyme NAD(P)H, and reduced flavin subsequently activates molecular oxygen to form a enzyme-bound C4a-(hydro)peroxyflavin, which serves as a oxygenating agent to directly insert an oxygen atom into the substrate. Both protonated

(FlOOH) and deprotonated ($FlOO^-$) are able to oxidize substrates. The FlOOH is usually involved in the oxygenation of aromatic substrates as an electrophilic agent, while FlOO- acts as a nucleophilic agent to attack the substrate.

The alkanesulfonate monooxygenase system in *E. coli* is only synthesized under sulfur starvation conditions. This system is able to desulfonate a wide range of sulfonated compounds including 1-substituted alkanesulfonates from ethanesulfonate to tetradecanesulfonate and various sulfonated buffers. It belongs to a family of flavin dependent monooxygenases that utilize $FMNH_2$ as a co-substrate instead of a tightly bound cofactor. The flavin reductase, SsuE, transfers the reduced flavin to SsuD after subsequent reduction with NAD(P)H. While the mechanism of the flavin reductase, SsuE, has been elucidated, the catalytic mechanism of the SsuD catalyzed desulfonation reaction remains unclear. In the following chapters, two conserved amino acids located in the putative active site of SsuD will be discussed regarding their role in catalysis.

CHAPTER TWO

Catalytic Role of a Conserved Cysteine Residue in the Desulfonation Reaction by the Alkanesulfonate Monooxygenase Enzyme

2.1 INTRODUCTION

Sulfur is a critical element for the growth of bacterial organisms. All bacteria have inorganic sulfur requirements for the production of sulfur-containing compounds. Inorganic sulfur is poorly represented in aerobic soil, therefore bacteria in these environments must have an alternative process for obtaining this crucial element (*2*,*4*). To meet its sulfur requirements under sulfate-starvation conditions, *E. coli* synthesizes taurine dioxygenase and alkanesulfonate monooxygenase proteins for the acquisition of sulfur from alternative sulfur sources (*1*,*57*). The expression of these proteins allows the organism to utilize a broad range of alkanesulfonates during growth when inorganic sulfur is limiting. The two-component alkanesulfonate monooxygenase system is comprised of both an NAD(P)H[1]-dependent flavin reductase (SsuE) and a monooxygenase (SsuD). SsuD is part of a family of reduced flavin-dependent

monooxygenases that use flavin as a substrate instead of a bound prosthetic group (*57*). It catalyzes the oxygenolytic cleavage of 1-substituted alkanesulfonates in the presence of $FMNH_2$ and dioxygen, producing the corresponding aldehyde and sulfite (Scheme 2.1).

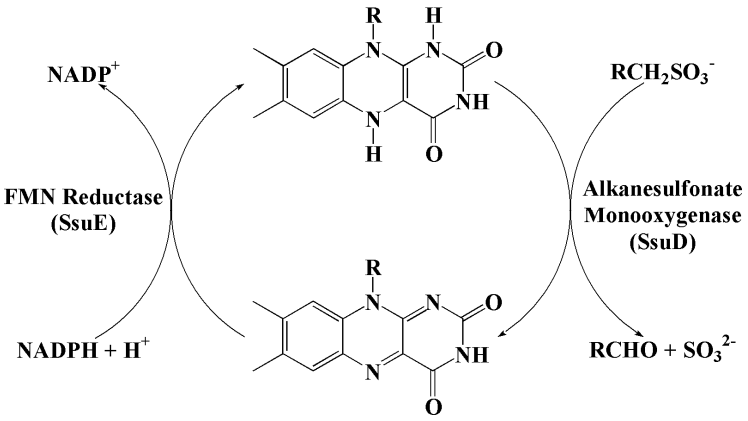

Scheme 2.1 Overall reaction mechanism of the alkanesulfonate monooxygenase system

The reaction catalyzed by SsuD has been previously studied through steady-state and rapid reaction kinetic analyses (*39*). The octanesulfonate substrate is unable to bind to SsuD unless reduced flavin was present, suggesting that reduced flavin binds first to induce a protein conformational change that allows the alkanesulfonate to bind. The formation of a C4a-(hydro)peroxyflavin intermediate when $FMNH_2$ is mixed with SsuD and oxygenated buffer at low octanesulfonate concentrations is observed in rapid reaction kinetic studies. Interestingly, the C4a-(hydro)peroxyflavin intermediate is not observed when SsuD is premixed with $FMNH_2$ under anaerobic conditions prior to mixing with oxygenated buffer and octanesulfonate. The absence of any accumulated flavin intermediate corresponded with a decrease in the amount of octanal product formed in the reaction. These results suggested that an inactive form of the enzyme is generated when

SsuD is first premixed with reduced flavin under anaerobic conditions, which must undergo a conversion back to the active enzyme form in the presence of dioxygen or alkanesulfonate before catalysis can occur.

The SsuD enzyme exists as a homotetramer containing four active sites, with each subunit composed of a TIM-barrel fold. The location of the SsuD active site has been proposed to be located at the C-terminal end of the β-barrel, where the active sites of most TIM-barrel enzymes are found (*64*). The identification of the active site is supported by earlier biochemical studies and the location of conserved amino acid residues in SsuD. Although the amino acid sequence identity is low, SsuD is strikingly similar in overall structure with bacterial luciferase and long-chain alkane monooxygenase (LadA) (*60, 61, 68*). While luciferase uses a long-chain aliphatic aldehyde as a substrate to catalyze the production of visible light and a corresponding carboxylic acid, LadA oxidizes long-chain alkanes to primary alcohols. These enzymes catalyze distinctly different biochemical reactions; however, they all are members of the flavin-dependendent monooxygenase family (*2,57*).

Several amino acids located in the putative active site of SsuD (His228, Tyr331, Arg297, and Cys54) are in a similar spatial arrangement as catalytically relevant amino acids from bacterial luciferase (His44, Tyr110, Arg291, and Cys106) and LadA (His311 and Tyr63). The His44 residue in the α-subunit of bacterial luciferase has been reported to be the catalytic base in the bioluminescence reaction. Mutation of this histidine residue to alanine showed marked differences in the intensity of light emitted (*46*). However, it was found that the bioluminescence activity could be reconstituted by chemical rescue

with the addition of imidazole to the reaction (*58*). A corresponding residue has also recently been identified in the three-dimensional structure of LadA (*68*). The catalytic role of the conserved tyrosine residue common in all three enzymes has not been evaluated. The tyrosine residue in SsuD is within hydrogen bonding distance to the Nδ1 nitrogen atom in the imidazole ring of His228, and may play a role in the stabilization of this residue during catalysis. A conserved arginine residue in SsuD is also located in a similar position to Arg291 in bacterial luciferase. In both enzymes, this residue is located in an insertion region containing an unstructured loop that is thought to cover the active site with the binding of substrates. Deletion of this unstructured loop region in bacterial luciferase resulted in a decrease in bioluminescence; however, direct substitution of Arg291 has not been performed (*79*). The catalytic role of Cys106 in bacterial luciferase has been studied in extensive detail. Initial studies demonstrated that chemical modification of the reactive thiol of Cys106 resulted in the inactivation of the enzyme, leading to the assumption that this residue was directly involved in catalysis (*67, 80, 81*). Mutation of the cysteine residue at position 106 to alanine, serine, and valine was shown to reduce bioluminescence; however, it was not directly involved in catalysis (*45, 48*). The reactions catalyzed by many flavin-dependent monooxygenases have been shown to involve a C4a-(hydro)peroxyflavin intermediate. It was previously determined through rapid reaction kinetic analyses that the active site cysteine is involved in the stabilization of the C4a-(hydro)peroxyflavin intermediate in bacterial luciferase. Although this group of enzymes contains spatially conserved residues, the corresponding role of these residues in the desulfonation reaction catalyzed by SsuD has not been evaluated.

It was previously demonstrated that cysteine-labeling of SsuD with methylmercury leads to inactivation of the enzyme (*60*). Due to the expression of this protein under times of sulfur limitation, there is only one cysteine residue located in the putative active site pocket of SsuD. The inactivation of cysteine-modified SsuD combined with the spatial similarity of this residue to the functionally significant Cys106 in bacterial luciferase suggests that Cys54 may be important in catalysis. In order to determine the function of Cys54 in the desulfonation reaction, two variants of the SsuD enzyme were constructed in which the cysteinyl residue was replaced by either alanine or serine. The experiments described in this work define the functional role of the conserved cysteine residue in the catalytic mechanism of SsuD.

2.2 MATERIALS METHODS

2.2.1 Materials

QuikChange site directed mutagenesis kit and super-competent cells *Escherichia coli* BL21(DE3) were from Stratagene (La Jolla, CA). Oligonucleotide primers were from Invitrogen (Carlsbad, CA). Flavin mononucleotide phosphate (FMN), nicotinamide adenine dinucleotide phosphate (NADPH), N-ethylmaleimide (NEM), 5-5′-dithio-bis(2-nitrobenzoic acid) (DTNB), dimethyl sulfoxide (DMSO), guanidine·HCl, EDTA, sodium chloride, urea, D-glucose, and glucose oxidase were purchased from Sigma (St. Louis, MO). Potassium phosphate (monobasic and dibasic) and glycerol were obtained from Fisher (Pittsburgh, PA). Octanesulfonate was from Fluka (Milwaukee, WI). The standard phosphate buffer contained 25 mM potassium phosphate, pH 7.5, and 10% glycerol unless otherwise noted.

2.2.2 Site-Directed Mutagenesis

Mutagenesis of the *ssuD* gene was performed with the Stratagene QuikChange site-directed mutagenesis kit. The TGC codon for Cys54 was replaced with GCT and GCG for Ser and Ala, respectively. The pET21a plasmid containing the *ssuD* gene was used as the template for these mutations. The *ssu*D Cys54 variants were identified by sequence analysis at Davis Sequencing (Davis, CA). Plasmids harboring the appropriate *ssuD* Cys54 variants were transformed into *E. coli* BL21(DE3) super-competent cells for

protein expression and stored at ⁻80 °C. The mutants generated are referred to as C54S (Cys54 to Ser) and C54A (Cys54 to Ala) SsuD.

2.2.3 Expression and purification of variant and wild-type SsuD

The variant and wild-type SsuD proteins were expressed from a pET21a expression vector in *E. coli* strain BL21(DE3), and the purification of each protein was performed as previously described (*39*). Following purification, stocks of the variant and wild-type SsuD enzymes were stored in standard buffer with 100 mM NaCl at ⁻80 °C. The enzyme concentrations were determined spectrophotometrically by using an absorption coefficient of 47 900 M^{-1} cm^{-1} at 280 nm. Wild-type SsuE was also expressed and purified as previously described and the concentration determined spectrophotometrically by using an absorption coefficient of 20 340 M^{-1} cm^{-1} at 280 nm (*82*).

2.2.4 Far-UV circular dichroism

The spectra of the variant and wild-type SsuD enzymes were obtained with an enzyme concentration of 1.2 μM in 25 mM potassium phosphate buffer, pH 7.5, at 25 °C. Buffer exchange was performed to remove all NaCl and glycerol using an Amicon Ultra Centrifugal Filter (Millipore, Billerica, MA) with a MWCO of 10 000 kDa. Buffer exchanges were performed four times by centrifugation at 3000 RPM. Far-UV circular dichroism spectra were recorded on a JASCO J-810 spectropolarimeter (Easton, MD). Measurements were taken in 0.2 nm increments in continuous scanning mode from 270 to 180 nm in a 0.1 cm path length cuvette with a bandwidth of 1 nm and a scanning speed of 20 nm/min. Each spectrum is the average of eight accumulated scans. Background

correction and smoothing of the data were performed using the JASCO J-720 software provided with the instrument.

2.2.5 Cysteine Accessibility Assays

The accessibility of Cys54 to thiol modifying agents was probed with the use of NEM and DTNB. A 200 μM solution of DTNB or NEM was added to 20 μM of SsuD (1 mL total volume) in standard buffer and the absorbance recorded at the corresponding wavelengths. Similar experiments were performed under denaturing conditions with 2.0 M guanidine-HCl at a final concentration of 2.0 M. The release of TNB was monitored at 412 nm, and the amount of TNB released per subunit was calculated using a molar extinction coefficient of 14 150 M^{-1} cm^{-1} (*83*). The reaction of the cysteine thiol with NEM was determined by monitoring the total change in absorbance at 305 nm, and the amount of NEM bound to each SsuD monomer determined using the molar extinction coefficient 620 M^{-1} cm^{-1} (*84*).

2.2.6 Steady-state kinetic studies

A coupled assay was utilized to determine the steady-state kinetic parameters of the variant and wild-type SsuD enzymes. The NAD(P)H-dependent flavin reductase, SsuE, was included in the reaction to supply $FMNH_2$ to SsuD. For C54S and wild-type SsuD the reaction was initiated with the addition of NADPH (500 μM) into a reaction mixture containing SsuD (0.2 μM), SsuE (0.6 μM), FMN (2 μM), NADPH (500 μM), and varying concentrations of octanesulfonate (10–500 μM) in standard buffer with 100 mM NaCl at 25°C. Because of decreased enzymatic activity, assays with C54A contained a final concentration of 1.0 μM protein. The reaction was quenched with urea (2 M final

concentration) following a 3 min incubation. The resulting solution was centrifuged for 4 minutes to remove precipitated protein and an aliquot (200 μL) of the reaction mixture was added to 50 μL of 1 mM DTNB. Following a 2 min incubation at room temperature, the amount of sulfite product formed was quantified spectrophotometrically at a wavelength of 412 nm (ϵ = 14 150 M^{-1} cm^{-1}). The steady-state kinetic parameters were determined using the Michaelis-Menten equation.

2.2.7 Flavin binding studies

Flavin binding to variant and wild-type SsuD enzymes was monitored by spectrofluorimetric titration with either oxidized or reduced flavin. Spectra were obtained on a Perkin Elmer LS 55 luminescence spectrometer (Palo Alto, CA) with an excitation wavelength of 280 nm and emission wavelength of 345 nm. For the titration of SsuD with FMN, a 1.0 mL solution of variant or wild-type SsuD enzyme (1 μM) in standard buffer containing 100 mM NaCl was titrated with a solution of FMN (1.5–65.0 μM for C54S and 4.4–90.8 μM for C54A), and the fluorescence spectra recorded after each addition as previously described (*39*). Similar experiments were performed with $FMNH_2$, however care had to be taken to keep the solution anaerobic. Anaerobic SsuD enzyme solutions were prepared in a glass titration cuvette by at least 15 cycles of evacuation followed by equilibration with ultra high purity argon gas. An oxygen scavenging system composed of 20 mM glucose and 10 units of glucose oxidase was also included to ensure the solution was kept anaerobic. Anaerobic solutions of $FMNH_2$ were prepared as previously described (*39*). The SsuD variants (0.5 μM) were titrated with $FMNH_2$ (0.21–6.0 μM for

C54S and 0.21–9.4 μM for C54A). The bound FMN or $FMNH_2$ was determined by the following equation (*39*):

$$[\text{FMN}]_{\text{bound}} = [\text{SsuD}]\frac{I_0 - I_c}{I_0 - I_f}, \quad (1)$$

where [SsuD] is the initial concentration of enzyme, I_0 is the initial fluorescence intensity of SsuD prior to titration, I_c is the fluorescence intensity of SsuD following each addition of FMN or $FMNH_2$, and I_f is the final fluorescence intensity. The concentration of bound FMN or $FMNH_2$ was plotted against the total FMN or $FMNH_2$ to obtain the dissociation constant (K_d) according to Eq. 2:

$$Y = \frac{B_{\max} X}{K_d + X} \quad (2)$$

where B_{max} is the maximum binding at equilibrium with the maximum concentration of substrate, and K_d is the dissociation constant for the substrate (*39*).

2.2.8 Octanesulfonate binding

Octanesulfonate binding to wild-type or variant SsuD was investigated by similar fluorimetric titration methods employed for flavin binding. A 1.0 mL solution of SsuD (1 μM), with reduced flavin (2 μM), was made anaerobic in a glass titration cuvette as described previously (*39*). Aliquots of an anaerobic solution of octanesulfonate (1.3–57.5 μM for C54S and 1.3–73.2 μM for C54A) in an air-tight titrating syringe were added to the SsuD-$FMNH_2$ complex. The fluorescence spectra were recorded with an excitation wavelength at 280 nm and emission intensity measurements at 344 nm. The concentration of bound octanesulfonate was determined by Eq. 1, and plotted against the

concentration of free octanesulfonate to determine the dissociation constant (K_d) according to Eq. 2.

2.2.9 Rapid reaction kinetic experiments

Rapid reaction kinetic analyses were carried out using an Applied Photophysics SX.18 MV stopped-flow spectrophotometer. The stopped-flow instrument was made anaerobic by repeated filling and emptying of the drive syringes with an oxygen scrubbing system. The oxygen scavenging system contained standard buffer with 100 mM NaCl, 20 mM glucose, and 10 units of glucose oxidase. The protein solutions were prepared in an anaerobic chamber in standard buffer containing 100 mM NaCl. Reduced flavin solutions were prepared as previously described (*39*). The protein and $FMNH_2$ solutions were transferred to a glass tonometer, and incubated in an anaerobic chamber (95% N_2 and 5% H_2 gas) for 2–3 hours before being transferred to the stopped-flow spectrophotometer. All experiments contained 45 μM enzyme and 15 μM $FMNH_2$ (initial concentration before mixing) in one drive syringe mixed against air-saturated buffer in the other drive syringe. When included in the reaction, the concentration of octanesulfonate was varied from 50–2000 μM (before mixing) in air-saturated buffer. All experiments were carried out at 4 °C in single-mixing mode by mixing equal volumes of the solutions, and monitoring the reactions by single wavelength analyses at 370 and 450 nm. The initial analyses of single-wavelength traces at 370 and 450 nm were performed using the PROKIN software (Applied Photophysics, Ltd.) installed in the stopped-flow spectrophotometer. A global analysis was applied to determine the steps involved in flavin oxidation. Kinetic fits of the data were performed using the KaleidaGraph software

(Abelbeck Software, Reading, PA). The single-wavelength traces of each mutant were fitted to a double or triple exponential using the following equations:

$$A = A_1 \exp(-k_1 t) + A_2 \exp(-k_2 t) + C \quad (3)$$

$$A = 1 - [A_1 \exp(-k_1 t) + A_2 \exp(k_2 t) + A_3 \exp(-k_3 t) + C] \quad (4)$$

where k_1, k_2, and k_3 are the apparent rate constant for the different phases, A is the absorbance at time t, A_1, A_2, and A_3 are amplitudes of each phase, and C is the absorbance at the end of the reaction.

The data for the concentration dependence of octanesulfonate on k_1 were fitted with a simplified hyperbolic equation:

$$k_{obs} = k_{lim}[S]/K_d + [S] \quad (5)$$

where k_{obs} is the observed rate constant, k_{lim} is the limiting rate constant for flavin reduction, K_d is the dissociation constant for the enzyme-substrate complex, and S is the substrate concentration.

2.3 RESULTS

2.3.1 Structural properties of the SsuD variants

Because of the role of the alkanesulfonate monooxygenase enzymes in sulfur acquisition during times of sulfur starvation, sulfur-containing amino acids are limiting in each enzyme. The SsuE protein contains no cysteine residues, while SsuD contains only one cysteine residue located in the putative active site. To determine whether Cys54 was accessible to solvent in the active site, assays were performed employing NEM and DTNB. Results from the DTNB assays showed that there was one mole of equivalent thiol per mole of SsuD protein, but DTNB was only reactive with the cysteine thiol when the protein was first denatured with guanidine·HCl (data not shown). However, when NEM was added before denaturation followed by the addition of DTNB there was no absorbance detected from the TNB anion. The cysteine SsuD variants were not labeled with either NEM or DTNB. These results indicated that Cys 54 in the native SsuD protein was inaccessible to the bulkier DTNB label unless the protein was first denatured. The smaller NEM label was able to react with the cysteine thiol, thereby rendering the cysteine unreactive to further labeling by DTNB upon denaturation.

Circular dichroism spectroscopy was performed on C54S, C54A, and wild-type SsuD to ensure that mutations introduced into the SsuD enzyme did not cause any gross secondary structural changes. The results revealed that there were no major perturbations in the overall secondary structure between the variants and wild-type SsuD suggesting

that substitution of Cys54 did not cause any major consequences to the protein structure (Figure 2.1).

2.3.2 Steady-state kinetic parameters for octanesulfonate

Steady-state kinetic analyses were performed with each cysteine variant to determine if the substitution of Cys54 led to an alteration in the kinetic parameters previously determined for wild-type SsuD. Because SsuD requires reduced flavin for activity, a coupled assay that includes SsuE in the reaction must be employed. This assay included an excess of SsuE so $FMNH_2$ would not be limiting in the reaction. The steady-state kinetic parameters for C54S, C54A and wild-type SsuD were obtained by measuring the amount of TNB anion formed at 412 nm from the reaction of DTNB with the sulfite product. The steady-state kinetic parameters were determined by a fit of the data to the hyperbolic dependence of each enzyme on octanesulfonate concentration (Figure 2.2A and B). The K_m and k_{cat} values determined for C54S SsuD were 7.45 ± 0.86 μM and 28.1 ± 0.4 min^{-1}, respectively (Table 2.1). The C54S SsuD enzyme showed an approximate 6-fold decrease in the K_m value and a 2-fold decrease in the k_{cat} value compared to wild-type (K_m, 44.0 ± 8.3 μM; k_{cat}, 51.7 ± 2.1 min^{-1}). The value for the catalytic efficiency (k_{cat}/K_m) of the C54S SsuD variant actually increased 3-fold compared to wild-type SsuD. Conversely, the K_m and k_{cat} values determined for C54A SsuD were 26.43 ± 1.73 μM and 5.59 ± 0.08 μM^{-1} min^{-1}, respectively. The K_m value for C54A SsuD showed a 2-fold decrease in the K_m value and a 9-fold decrease in the k_{cat} value compared to wild-type. There was a 5-fold decrease in the k_{cat}/K_m value for the C54A SsuD variant compared to wild-type SsuD. These results suggest that serine was effectively able to substitute for

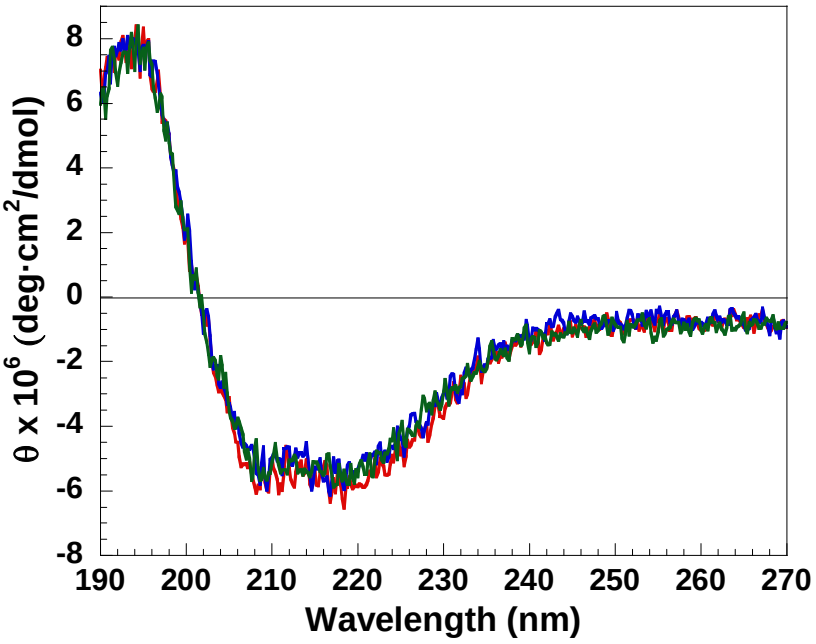

Figure 2.1: Far-UV circular dichroism spectra of C54S, C54A, and wild-type SsuD. Each spectra was obtained with an enzyme concentration of 1.2 μM in 25 mM potassium phosphate buffer, pH 7.5, at 25 ºC. Measurements were taken in 0.1 nm increments from 270 to 190 nm in a 0.1 cm path length cuvette. Each spectrum is the average of eight accumulated scans; smoothing of the data was performed using the default parameters within the Jasco J-720 software. The spectra correspond to wild-type SsuD (red), C54S SsuD (blue), and C54A SsuD (green).

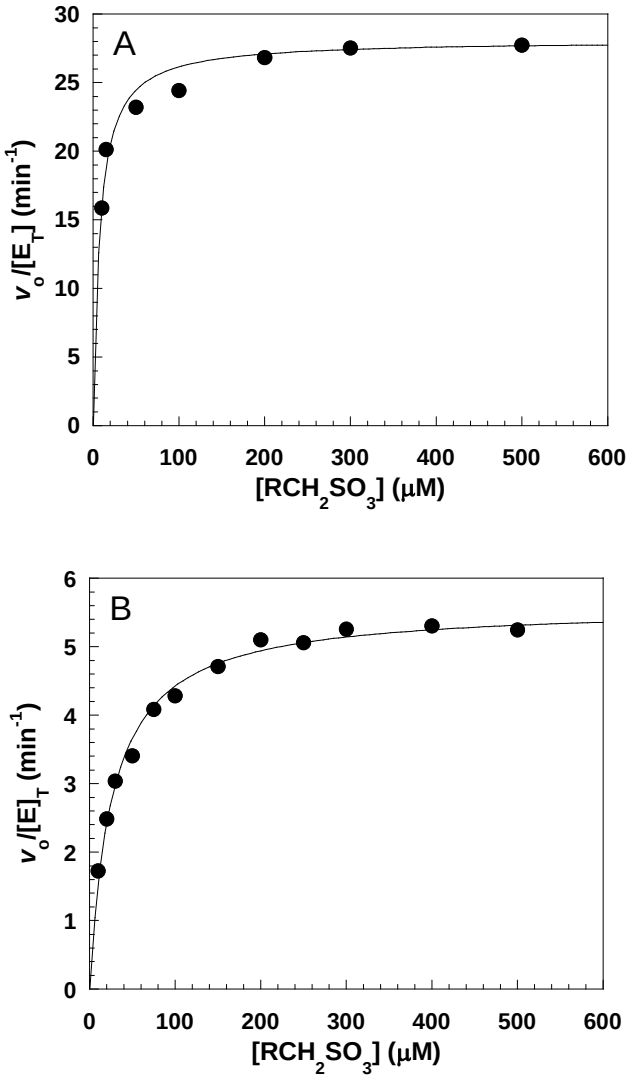

Figure 2.2: Steady-state kinetic analyses of C54S and C54A SsuD. A: Initial rates as a function of octanesulfonate concentration for: A: C54S SsuD B: C54A SsuD. The assay measured the sulfite product formed from the reaction of C54S (0.2 μM) or C54A (1.0 μM) SsuD, 2 μM FMN, 500 μM NADPH, and varying concentrations of octanesulfonate substrate (10-600 μM) in standard buffer with 100 mM NaCl at 25 °C. Sulfite product was quantified as described in *Experimental Procedures*. Each assay was performed in triplicate and the solid lines represent fits of the data to the Michaelis-Menten equation.

Table 2.1: Dissociation Constants and Steady-state Kinetic Parameters for C54S, C54A, and wild-type SsuD.

	K_d, FMN (μM)	K_d, $FMNH_2$[a] (μM)	K_m, octanesulfonate (μM)	k_{cat} (min^{-1})	k_{cat}/K_m (μM^{-1} min^{-1})
WT SsuD[b]	10.2 ± 0.4	0.32 ± 0.15	44.0 ± 8.3	51.7 ± 2.1	1.17 ± 0.22
C54S SsuD	11.3 ± 0.6	0.47 ± 0.09	7.4 ± 0.9	28.1 ± 0.4	3.75 ± 0.68
C54A SsuD	13.7 ± 0.4	0.53 ± 0.09	26.4 ± 1.7	5.6 ± 0.1	0.21 ± 0.01

[a] Determined under anaerobic conditions as described in *Experimental Procedures*
[b] Previously reported (*39*).

cysteine under steady-state conditions, while the cysteine to alanine substitution decreased the catalytic efficiency.

2.3.3 Substrate binding to the C54 SsuD variants

Spectrofluorimetric titrations were performed to determine whether Cys54 substitutions affect the binding of FMN or $FMNH_2$. The dissociation constants for the binding of oxidized and reduced flavin to the SsuD variants were determined by titrating either FMN or $FMNH_2$ into a sample of C54S or C54A SsuD. The decrease in the intrinsic protein fluorescence emission due to the binding of FMN or $FMNH_2$ was monitored at 344 nm for each variant. The concentration of bound and free flavin was calculated using Eq. 1, and the concentration of flavin bound to each variant was plotted against the concentration of free flavin. The dissociation constants (K_d) for FMN and $FMNH_2$ are summarized in Table 2.1. The average K_d value for $FMNH_2$ binding to each SsuD variant was 0.47 ± 0.09 μM and 0.53 ± 0.09 μM for C54S or C54A SsuD, respectively. The dissociation constants for FMN binding to C54S and C54A SsuD were determined to be 11.3 ± 0.6 μM and 13.7 ± 0.4 μM, respectively (data not shown). These results indicate that mutation of the putative active site cysteine residue to either alanine or serine had little effect on FMN or $FMNH_2$ binding when compared to the previously reported K_d value of 0.32 ± 0.15 μM ($FMNH_2$) and 10.2 ± 0.4 μM (FMN) for wild-type SsuD (*39*).

It was previously shown that ordered substrate binding occurs in the SsuD reaction, with reduced flavin cofactor binding first before the octanesulfonate substrate

can bind (*39*). The binding of octanesulfonate to the C54S or C54A SsuD/$FMNH_2$ complex was performed to determine whether the binding of substrate was affected by the cysteine substitutions. To ensure that all of the $FMNH_2$ was bound to SsuD, a 2:1 ratio of $FMNH_2$ to SsuD was used in these experiments. Dissociation constants for the binding of octanesulfonate to the SsuD variants were obtained under anaerobic conditions similar to those previously described for titration of each SsuD variant with $FMNH_2$. The concentration of octanesulfonate substrate bound to each SsuD variant/$FMNH_2$ complex was calculated according to Eq. 1 and plotted against the concentration of free octanesulfonate after each addition (Figure 2.3, titration of C54S SsuD). The K_d value for the binding of octanesulfonate to each SsuD variant/$FMNH_2$ complex was 2.68 ± 0.60 μM and 4.97 ± 0.58 μM for C54S and C54A SsuD, respectively. The K_d values obtained for these SsuD variants are distinctly different from those obtained for wild-type SsuD (17.5 ± 0.9 μM) by similar methods (*39*). These results suggest that each variant has an increased affinity for octanesulfonate and indicate that the binding of octanesulfonate is affected by the substitution of Cys54 with either Ala or Ser.

2.3.4 Kinetic studies of flavin oxidation by the SsuD variants

A C4a-(hydro)peroxyflavin intermediate has been observed through rapid reaction kinetics in the reaction of bacterial luciferase with the aldehyde substrate, and the active site Cys106 was shown to be involved in stabilizing this intermediate (*47*,*48*,*85*). This active site cysteine in bacterial luciferase is homologous to Cys54 located in the putative active site of SsuD. The formation of a C4a-(hydro)peroxyflavin intermediate has previously been detected in similar experiments with wild-type SsuD (*39*). This

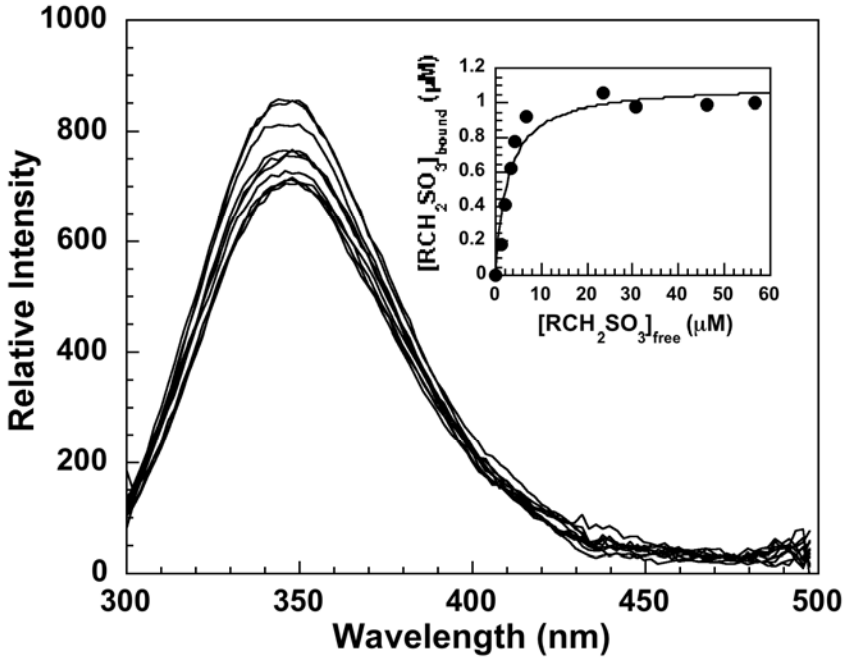

Figure 2.3: Fluorimetric titration of the C54S SsuD/$FMNH_2$ complex with octanesulfonate. C54S SsuD (1.0 μM) was titrated with octanesulfonate (1.3-57.5 μM). Emission intensity measurements at 344 nm were obtained with an excitation wavelength of 280 nm. The change in the intrinsic fluorescence intensity for the SsuD/$FMNH_2$ complex following the addition of octanesulfonate was converted to concentration of bound octanesulfonate (Eq. 1) and plotted against the concentration of free octanesulfonate. Inset: Change in fluorescence emission intensity at 344 nm. The solid line represents a fit of the titration curve to Eq. 2.

intermediate was only observed when $FMNH_2$ was mixed against SsuD in air-saturated buffer, not when SsuD was premixed with $FMNH_2$ and then mixed against air-saturated buffer. Rapid reaction kinetic studies were performed to further define the role of Cys54 in catalysis. Stopped-flow kinetic studies were initially performed in the absence of the alkanesulfonate substrate to monitor the oxidation of $FMNH_2$ by the SsuD variants at 370 and 450 nm (data not shown). The SsuD variants were maintained at a higher concentration (45 μM) relative to $FMNH_2$ (15 μM) to ensure single-turnover conditions. Single-wavelength kinetic traces were obtained for each SsuD variant premixed with $FMNH_2$ followed by mixing against air-saturated buffer in the stopped-flow. Under these experimental conditions the C54S and C54A SsuD variants displayed kinetic traces that increased at similar rates at 370 and 450 nm. The kinetic traces at 370 nm were best fit to a double exponential equation with rates of 0.044 s^{-1} (k_1) and 0.12 s^{-1} (k_2) for C54S SsuD, and 0.042 s^{-1} (k_1) and 0.10 s^{-1} (k_2) for C54A SsuD. The rates obtained from kinetic traces at 450 nm were 0.046 s^{-1} (k_1) and 0.096 s^{-1} (k_2) for C54S SsuD, and 0.042 s^{-1} (k_1) and 0.095 s^{-1} (k_2) for C54A SsuD. The k_1 values obtained for the SsuD variants were approximately 10-fold lower than the values obtained for wild-type SsuD, while the k_2 values were similar. There was no evidence for the formation of a C4a-(hydro)peroxyflavin intermediate generated under these experimental conditions. As previously observed with wild-type SsuD, the two phases observed in the kinetic traces at 370 and 450 nm can be attributed to direct flavin oxidation (*39*).

An additional set of stopped-flow kinetic experiments were performed in an attempt to determine if the C4a-(hydro)peroxyflavin was detectable with the SsuD

variants by mixing $FMNH_2$ against C54S and C54A SsuD in air-saturated buffer. An initial fast phase was observed in the reaction of C54S SsuD with $FMNH_2$ that was not observed with C54A SsuD (Figure 2.4). The kinetic trace at 370 nm was best fit to a triple exponential equation with rates of 111 s^{-1} (k_1), 24.1 s^{-1} (k_2), and 0.33 s^{-1} (k_3) for SsuD C54S (○, Figure 2.4A). The rates of flavin oxidation for the C54S SsuD variant were increased approximately 10-fold, 20-fold, and 40-fold over wild-type for k_1, k_2, and k_3, respectively. The kinetic trace at 450 nm was best fit to a double exponential with rates of 9.76 s^{-1} (k_1) and 0.33 s^{-1} (k_2) (●, Figure 2.4A). The C54A SsuD kinetic trace at 370 nm, did not exhibit an initial fast step and was best fit to a double exponential with rates of 4.70 (k_1) and 0.35 (k_2) at 370 nm (○, Figure 2.4B). Rates of 1.99 (k_1) and 0.32 (k_2) for C54A SsuD were obtained from the fit of the kinetic traces at 450 nm (●, Figure 2.4B). The initial fast phase observed at 370 nm for the C54S SsuD catalyzed reaction may be attributed to formation of the C4a-(hydro)peroxyflavin intermediate as shown for wild-type SsuD (*39*). These results suggest that the C4a-(hydro)peroxyflavin is only observed with the more conservative cysteine to serine substitution, while substitution of Cys to Ala led to decreased accumulation of this flavin intermediate. Table 2.2 summarizes the single-turnover kinetic rate constants obtained for WT, C54S, and C54A SsuD.

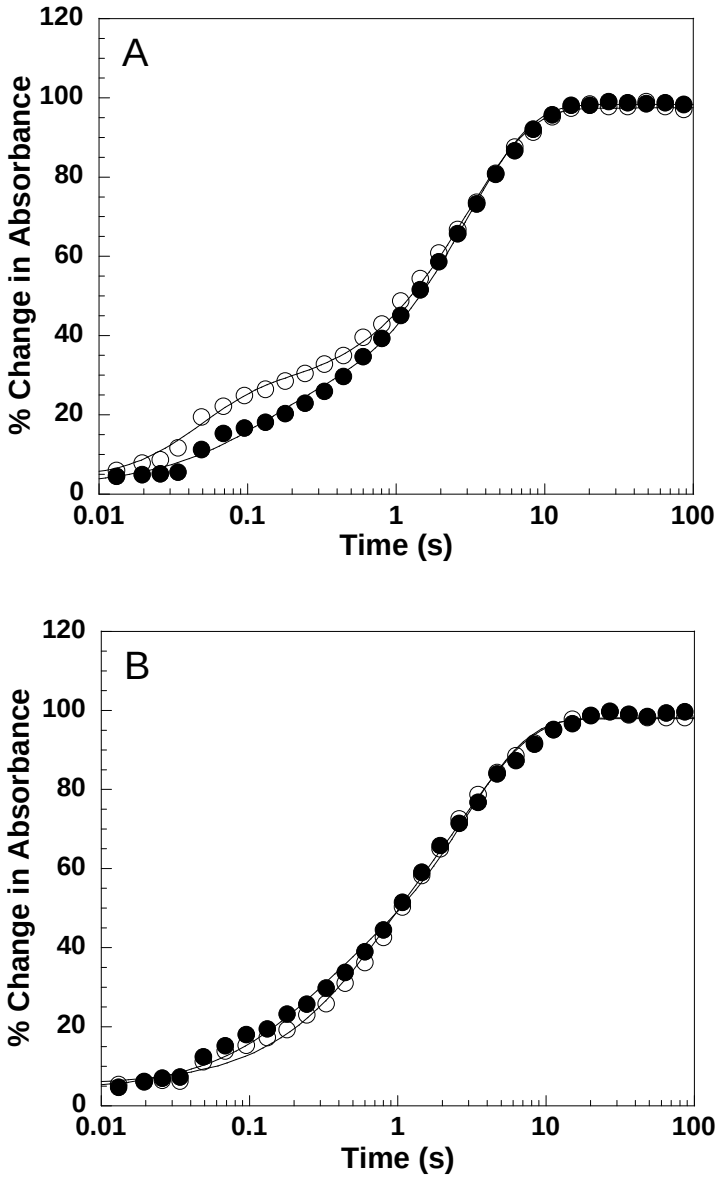

Figure 2.4: Kinetics of flavin oxidation by C54S and C54A SsuD in the absence of octanesulfonate substrate. A: Free $FMNH_2$ mixed against C54S SsuD in air-saturated buffer. B: Free $FMNH_2$ mixed against C54A SsuD in air-saturated buffer. The kinetic traces shown are an average of three separate experiments following flavin oxidation at 370 (○) and 450 nm (●). The solid lines are the fits of the kinetic traces to Eq. 3 or 4.

Table 2.2: Single-turnover kinetic rate constants for the oxidation of $FMNH_2$ for WT, C54S, and C54A SsuD in the absence of octanesulfonate

	370 nm			450 nm	
	k_1, s^{-1}	k_2, s^{-1}	k_3, s^{-1}	k_1, s^{-1}	k_2, s^{-1}
SsuD WT[a]	12.9	0.95	0.08	1.3	0.09
SsuD C54S	111	24.1	0.33	9.76	0.33
SsuD C54A	—	4.7	0.35	1.99	0.32

[a] Previously reported (*39*)

2.3.5 Kinetic studies of flavin oxidation by SsuD variants in the presence of octanesulfonate

Rapid reaction kinetic analyses were also employed to determine if the presence of the octanesulfonate substrate had an effect on the rate of formation of the C4a-(hydro)peroxyflavin intermediate. The oxidation of flavin by the SsuD variants in the presence of octanesulfonate substrate was monitored by stopped-flow analyses at 370 and 450 nm by mixing free $FMNH_2$ (15 μM) with either C54S or C54A SsuD (45 μM) and octanesulfonate (50-2000 μM) in air-saturated buffer (concentrations given are before mixing). The kinetic trace for wild-type SsuD showed an initial fast phase at 370 nm at low octanesulfonate concentrations (≤ 100 μM). However, this initial fast phase at 370 nm was not observed for either the C54S or C54A SsuD variants even at low octanesulfonate concentrations, and all kinetic traces were best fit to a double exponential (Figure 2.5A and B). With both SsuD variants, the k_{obs} values for the second phase at 370 nm showed a hyperbolic dependence on substrate concentration, giving a K_d and limiting

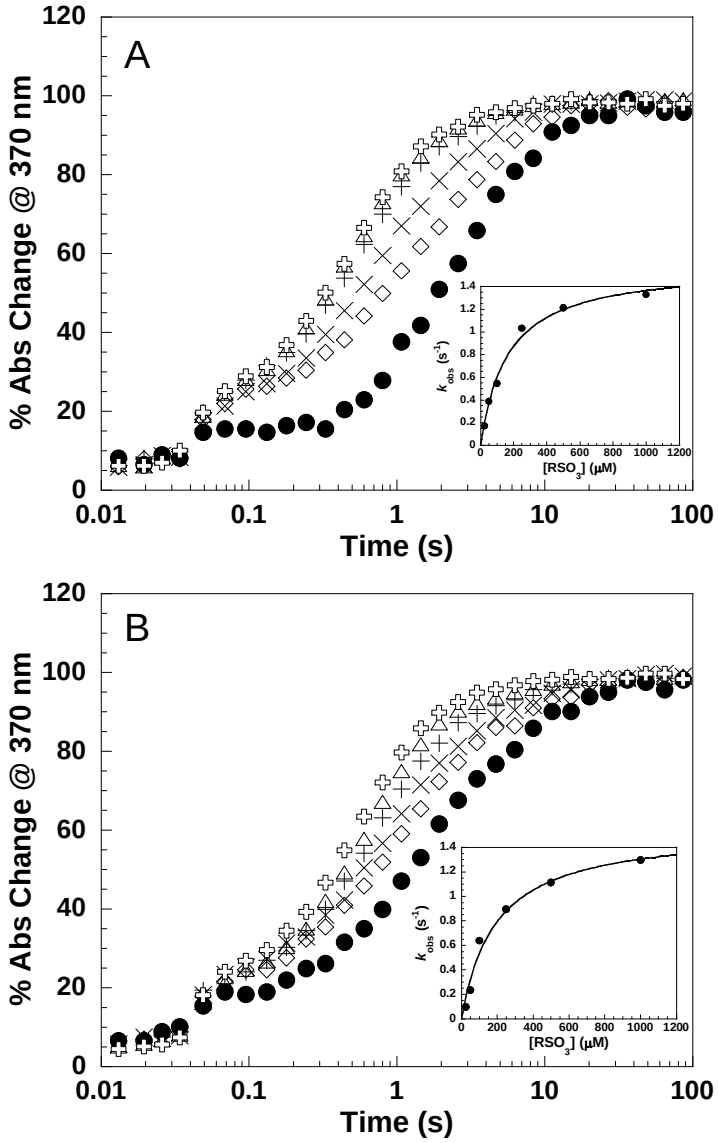

Figure 2.5: Kinetics of flavin oxidation by C54S and C54A SsuD in the presence of variable amounts of octanesulfonate (25 (●), 50 (◇), 100 (×), 250 (+), 500 (△), and 1000 μM (✣)) in oxygenated buffer. A: Anaerobic $FMNH_2$ mixed against C54S SsuD with varying concentrations of octanesulfonate substrate. B: Anaerobic $FMNH_2$ mixed against C54A SsuD with varying concentrations of octanesulfonate substrate. Insets: Dependence on the k_{obs} at varying octanesulfonate concentrations for the second phase at 370 nm. The solid lines are the fits of the kinetic traces to Eq. 3.

rate constant of 163 ± 23 μM and 1.58 ± 0.08 M^{-1} s^{-1} for C54S SsuD, and 190 ± 44 μM and 1.55 ± 0.11 M^{-1} s^{-1} for C54A SsuD, (Figure 2.5A and B, Insets). These results show a 2-fold increase in the K_d value for octanesulfonate and 2-fold decrease in the k_{obs} values for each variant compared to the values obtained for wild-type SsuD. The absence of a fast phase with each of the SsuD variants suggest that the C4a-(hydro)peroxyflavin does not accumulate with the SsuD variants in the presence of octanesulfonate.

2.4 DISCUSSION

The catalytic mechanism for several $FMNH_2$-dependent monooxygenase enzymes has been defined through various kinetic approaches (*44, 85-87*). While there are certain catalytic features that are maintained by this group of enzymes, there is low amino acid sequence similarity. Interestingly, the alkanesulfonate monooxygenase from *E. coli* is similar in overall structure to bacterial luciferase and LadA, although they share low amino acid sequence identity (*60, 61*). The monomeric units of these enzymes adopt a TIM-barrel fold, however the quaternary structure of each enzyme is different. Bacterial luciferase exists as a heterodimer, LadA forms a homodimer, and SsuD forms a homotetrameric structure. There are several conserved amino acid residues in SsuD with spatial counterparts in the active site of bacterial luciferase and LadA. The spatial correlation between conserved amino acid residues in these enzymes suggests that the active site of SsuD is located at the C-terminal end of the TIM-β-barrel (*60*). In addition, the catalytic role of several of these amino acid residues has been determined for bacterial luciferase from *V. harveyi*. The amino acid Cys106 lies along a wall of a small cavity that projects off a larger pocket, and is proposed to be in close contact with the pyrimidine structure of the isoalloxazine ring of the flavin (*61*). It was established that chemical modification of this active site cysteine results in the complete loss of enzymatic activity (*67, 80, 81*). However, it has been clearly shown that this cysteine is not directly involved in the catalytic reaction. These results were identified by substitution of the cysteine

residue to alanine, valine, and serine, resulting in an active luciferase enzyme with decreased bioluminescence. Furthermore, the luciferase enzyme from *V. fischeri* contains a valine residue at position 106 in the α subunit, in an identical position as the cysteine in luciferase from *V. harveyi*, indicating that a thiol is not directly essential for bioluminescence activity (*45, 48*). While the rate of formation of the C4a-(hydro)peroxyflavin intermediate was not compromised in these variants, the rate of decay for the flavin intermediate was increased relative to wild-type (*39*). It was therefore concluded that the cysteine is involved in the stabilization of the C4a-(hydro)peroxyflavin.

Due to its role in sulfur assimilation the SsuD enzyme only contains a single cysteine residue. This residue is highly conserved in all putative SsuD enzymes from a diverse group of bacteria. Previous studies have shown that labeling of the conserved Cys54 residue in the active site of SsuD also leads to inactivation of the enzyme as observed for bacterial luciferase. The role of Cys54 was evaluated in order to determine if this residue was involved in stabilizing the C4a-(hydro)peroxyflavin intermediate similar to the correlating residue in bacterial luciferase, or if this residue possessed an alternative role in catalysis. The cysteine residue was solvent accessible to the smaller cysteine label N-ethylmaleimide. However, the bulkier thiol modifying reagent DTNB was unable to react with cysteine unless the protein was first denatured, suggesting limited solvent accessibility within the active site. Site-directed mutagenesis was used to substitute the Cys54 residue with serine and alanine. Following the purification of each enzyme, circular dichroism spectroscopy was performed to determine if the secondary

structure of the SsuD variants was affected by these substitutions. The results from these experiments indicated that the substitution of Cys54 to serine or alanine caused no major perturbations in the overall secondary structure of SsuD. Therefore, the cysteine substitutions did not result in any overt changes in structure, and kinetic analyses were performed to investigate the role of Cys54 in catalysis.

In steady-state kinetic assays, the substitution of Cys54 altered the catalytic efficiency of SsuD when compared to wild-type. The C54S and C54A SsuD variants had k_{cat}/K_m values that were 3-fold greater and 5-fold lower than wild-type SsuD, respectively. However, the concentration of the C54A SsuD enzyme had to be increased 5-fold over the concentration of C54S and wild-type SsuD in order to detect any appreciable activity. The increase in the catalytic efficiency of C54S SsuD is largely attributed to the 6-fold decrease in the K_m value. These results suggest that the less conservative cysteine to alanine substitution had a more distinct impact on the steady-state kinetic parameters, while the serine was able to adequately substitute for cysteine.

The conserved cysteine residue in bacterial luciferase has been proposed to be involved in the stabilization of the C4a-(hydro)peroxyflavin intermediate. Similar steady-state kinetic parameters obtained for the conservative cysteine to serine SsuD variant as wild-type indicated that Cys54 may be involved in substrate binding through hydrogen bonding, as Ser would also be able to provide similar interactions. The effect of the cysteine to serine and alanine substitutions on reduced and oxidized flavin binding was probed through fluorescence spectroscopy. The K_d values determined for reduced or oxidized flavin binding to the SsuD variants were similar to those obtained for wild-type

SsuD indicating that Cys54 was not directly involved in flavin binding. This is in contrast to the results from fluorescence titration experiments with bacterial luciferase, where mutation of the cysteine at position 106 to alanine, serine, or valine resulted in an increase in the K_d value for $FMNH_2$ (*45*). Previous kinetic evaluation of SsuD demonstrated that two conformational changes likely occur with the binding of reduced flavin and octanesulfonate. Therefore, optimal contacts by the cysteine residue may only be obtained with both substrates bound, and flavin binding to the SsuD variants in the absence of octanesulfonate would be similar to wild-type SsuD.

The K_d values for octanesulfonate binding were also determined with each of the SsuD variants by titrating $FMNH_2$-bound C54A or C54S SsuD with octanesulfonate. The K_d value for both variants led to an increase in the binding affinity. It was previously demonstrated that incubation of wild-type SsuD with reduced flavin in the absence of oxygen results in the conversion of the complex to an inactive form that must undergo an isomerization to the active form of the enzyme before catalysis can occur (*39*). Because this conversion may only occur in the presence of dioxygen, octanesulfonate is likely binding to the inactive complex. Titration of octanesulfonate into the inactive form of the $FMNH_2$-bound SsuD variants may lead to alternative interactions of the substrate and active site amino acid residues in the absence of dioxygen leading to a greater affinity of SsuD for octanesulfonate. However, these interactions may not be optimal for catalysis.

The C4a-(hydro)peroxyflavin intermediate was previously identified in the SsuD catalyzed reaction by rapid reaction kinetic studies using stopped-flow analyses (*39*). The flavin intermediate was only detectable if SsuD and reduced flavin were not premixed in

the tonometer, leading to conversion of the complex to a proposed inactive form. As shown in Scheme 2.2, this species could be more specifically called a C4a-peroxyflavin intermediate (FMN-OO^-) to proceed with a nucleophilic attack on the sulfonate group of the alkanesulfonate to form an alkanesulfonate peroxyflavin adduct. The reaction would then proceed through a Baeyer-Villiger rearrangement leading to the generation of sulfite and the corresponding aldehyde product. Since SsuD and bacterial luciferase are structurally similar, a peroxyflavin intermediate should be observed spectrally in the 300–400 nm region; however, this intermediate was not observed in solutions of SsuD pre-mixed with $FMNH_2$ (*39*). The kinetic traces obtained at 370 nm for the $FMNH_2$-bound SsuD variants in the absence of octanesulfonate were similar, showing two distinct phases at 370 nm (data not shown). In these experiments there was no direct evidence for the formation of a C4a-(hydro)peroxyflavin intermediate, therefore the observed kinetic traces represent the auto-oxidation of $FMNH_2$ to FMN. However, the fast phase (k_1) was 10-fold slower for the SsuD variants than for wild-type SsuD, with the second phase (k_2) for each variant having comparable rates to wild-type SsuD. The results correlate with studies performed to determine the binding affinity of each SsuD variant for octanesulfonate. In the absence of dioxygen, the binding of octanesulfonate to the proposed inactive $FMNH_2$-SsuD in the fluorimetic titrations showed a higher binding affinity for each of the SsuD variants compared to wild-type. This increased affinity for octanesulfonate may result in a slower conversion to the active complex leading to a decrease in flavin oxidation when the SsuD variants are premixed with reduced flavin.

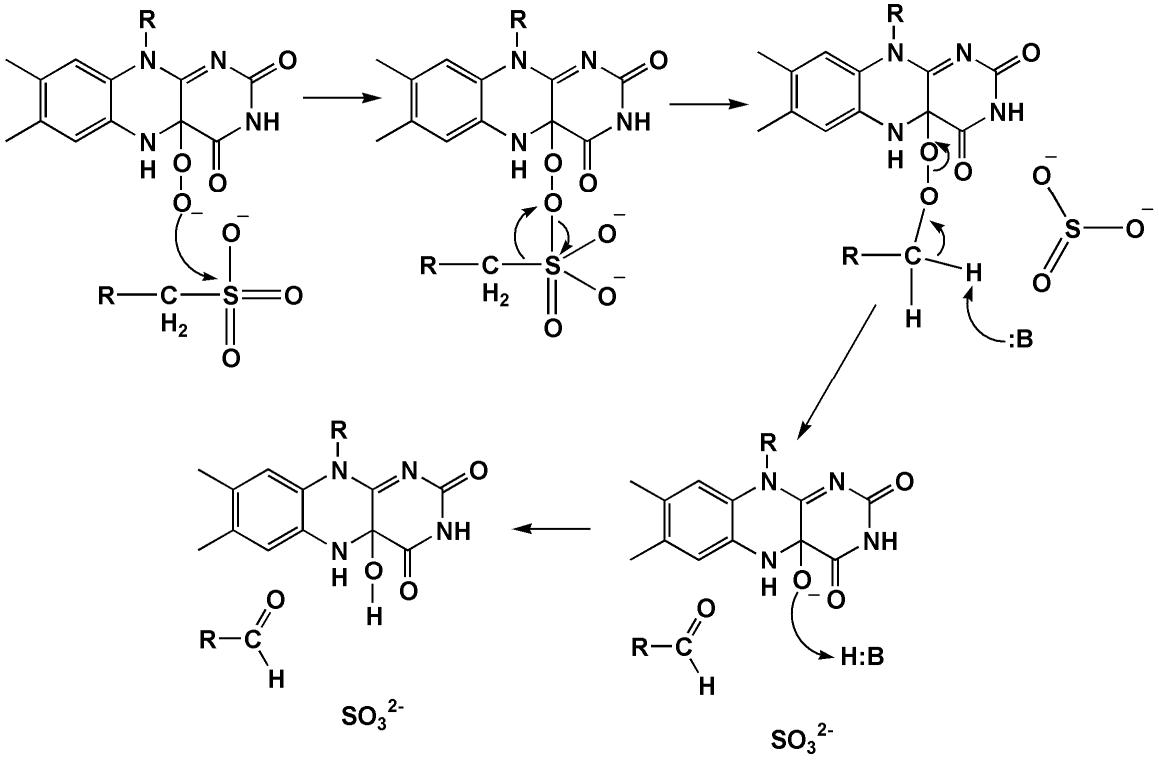
R
N
N
O
NH
N
H
O
O
O
R
C
H2
S
O
O
O

Kinetic studies were also performed to determine if the C4a-(hydro)peroxyflavin intermediate was observed in stopped-flow reactions when reduced flavin and the SsuD variants were not premixed. From the kinetic trace of C54S SsuD mixed against $FMNH_2$, three phases were identified with a fast phase (k_{obs} 111 s^{-1}) observed in the trace obtained at 370 nm that was not present in the kinetic traces obtained with premixed C54S SsuD and $FMNH_2$. This rate can be attributed to the formation of the C4a-(hydro)peroxyflavin intermediate and is 10-fold greater than the rate obtained with wild-type SsuD. As previously observed for wild-type, this fast phase was not present in the kinetic trace obtained at 450 nm. The rates obtained for the last two phases at 370 nm were approximately 25- and 4-fold greater for k_2 and k_3, respectively. The second phase (k_2) has been assigned to the decay of the peroxyflavin. Therefore, although there is increased accumulation of the flavin intermediate, the rate of breakdown for this intermediate has also increased. In addition, these results further confirm that identification of the C4a-(hydro)peroxyflavin intermediate in the reaction is dependent on the order of addition of $FMNH_2$ and O_2 to SsuD (*39*). The kinetic traces obtained at 370 and 450 nm for the C54A SsuD variant were similar with no initial fast phase observed at 370 nm, suggesting that there was no accumulation of the C4a-(hydro)peroxyflavin with this variant. Stopped-flow analyses on essential thiol variants of bacterial luciferase, where the reactive cysteinyl residue at position 106 in the α subunit was replaced with alanine, serine, and valine, were also performed in the absence of the aldehyde substrate (*48*). When mixing the luciferase variants and reduced flavin with oxygenated buffer, a C4a-(hydro)peroxyflavin intermediate was observed in all three mutants with rate constants

equal to that of wild-type luciferase. Rate constants obtained at 380 nm for the formation of a C4a-(hydro)peroxyflavin intermediate in the bacterial luciferase C106A, C106S, and C106V catalyzed reactions were essentially the same as the rate constants obtained for wild-type luciferase (*48*). The results with the SsuD cysteine variants support the importance of hydrogen bonding interactions in the stabilization of the C4a-(hydro)peroxyflavin intermediate either through direct interactions with the C4a-peroxy or by indirect interactions with the isoalloxazine ring. The cysteine thiol and not the thiolate is likely involved in stabilizing this intermediate, as the serine residue can compensate for cysteine in catalysis. The cysteine to alanine variant would be unable to stabilize the flavin intermediate through hydrogen bonding interactions, while the conservative cysteine to serine variant would still maintain these interactions. In several putative SsuD enzymes that have not been characterized, a serine or threonine replaces the conserved cysteine residue present in most bacteria further supporting the role of this residue in flavin stabilization.

Rapid reaction kinetic experiments were also performed for each SsuD variant in the presence of octanesulfonate. Similar kinetic experiments with wild-type SsuD showed an initial fast phase attributed to the formation of the C4a-(hydro)peroxyflavin only at low octanesulfonate concentrations ($\leq$ 100 μM). The reaction was thought to occur rapidly in the presence of increasing concentrations of the octanesulfonate substrate so that no appreciable levels of C4a-(hydro)peroxyflavin intermediate accumulated. With both SsuD variants there was no initial fast phase at 370 nm even at low octanesulfonate concentration, and the kinetic traces were best fit to a double exponential. At

concentrations of octanesulfonate greater than 100 μM, the first phase (representing flavin oxidation) at 370 nm displayed a hyperbolic dependence on octanesulfonate concentration (*39*). Values for k_{obs} at different octanesulfonate concentrations (50–2000 μM) were also obtained for the C54S and C54A SsuD variants. The k_{obs} values showed a similar hyperbolic dependence on substrate concentration with limiting rate constants of 1.58 and 1.55 s^{-1} for C54S and C54A SsuD, respectively. There was an alteration in the K_d value obtained using this method compared to fluorescent titration experiments with octanesulfonate. The K_d values for C54S and C54A SsuD were 3- and 4-fold greater than those obtained for wild-type SsuD. This increase in the K_d for octanesulfonate could be due to the octanesulfonate binding in a slightly altered conformation in the cysteine variants compared to wild-type SsuD. Alternatively, Cys54 may be directly involved in the binding of octanesulfonate to SsuD, coordinating both the flavin and octanesulfonate within the active site. These K_d values are also different from the values obtained from fluorescence titrations. This could be due to the octanesulfonate substrate binding to the inactive form of the SsuD-$FMNH_2$ complex in the titration experiments, and may not be relevant to experimental conditions. The increase in K_d values for the variants does not seriously impact catalysis, as the catalytic efficiency of C54S SsuD was actually 3-fold higher than wild-type.

In summary, these experiments performed on Cys54 SsuD variants have shown that the cysteine at position 54 is not directly essential for catalysis. The reaction catalyzed by C54S SsuD showed an increased rate of formation and decay for the C4a-(hydro)peroxyflavin intermediate compared to wild-type in the absence of

octanesulfonate, leading to a greater accumulation of this flavin intermediate. However, the C54A SsuD variant showed no detectable formation of this intermediate. Interestingly, there was no accumulation of the C4a-(hydro)peroxyflavin intermediate with either variant in the presence of octanesulfonate, suggesting that two separate events occur with each variant. The C54A SsuD variant is unable to stabilize the flavin intermediate in the presence or absence of octanesulfonate. However, based on both the steady-state and rapid reaction kinetic studies the C54S SsuD variant is able to substitute for cysteine, and appears to improve the catalytic efficiency of the enzyme. Although, the C4a-(hydro)peroxyflavin was observed in the absence of octanesulfonate in rapid reaction kinetic analyses with C54S SsuD, the reaction occurred too fast in the presence of octanesulfonate, and the flavin intermediate never accumulated. The data presented above suggest that the cysteine at position 54 could be involved in stabilizing the FMNOOH intermediate in the reaction catalyzed by the alkanesulfonate monooxygenase, either directly or indirectly through the isoalloxazine ring of the flavin.

CHAPTER THREE

Functional Role of the Active Site Arg297 Residue Located in a Postulated Mobile Loop of the Alkanesulfonate Monooxygenase

3.1 INTRODUCTION

Bacterial organisms, such as *E. coli*, have specific sulfur requirements that must be met to synthesize essential sulfur containing cofactors and metabolites. When bacteria are under sulfur starvation conditions they synthesize a certain set of proteins to obtain sulfur from alternative sulfur sources (*3*). The alkanesulfonate monooxygenase enzyme, SsuD, belongs to a two–component enzyme system that utilizes an NAD(P)H–dependent flavin reductase which catalyzes the reduction of FMN. The flavin reductase, SsuE, transfers the reduced flavin to SsuD, which catalyzes the liberation of sulfite from 1–substituted alkanesulfonates. (*57*). The sulfite is subsequently reduced by other enzymes and incorporated into essential sulfur–containing compounds. While SsuE has been well characterized, little mechanistic information exists regarding SsuD.

The alkanesulfonate monooxygenase, SsuD, is structurally related to a class of enzymes characterized by TIM-barrel folds. Although the amino acid sequence homology is low (<15%), SsuD has been shown to fold similarly to other flavin-dependent monooxygenases including bacterial luciferase and long-chain alkane monooxygenase (LadA). Unfortunately, a three-dimensional structure of SsuD complexed with either $FMNH_2$ and/or alkanesulfonate does not exist. However, the highly conserved amino acid residues Cys54, His228, Tyr331, and Arg297 of SsuD are in a similar spatial arrangement as the catalytically relevant residues of Cys106, His44, Tyr110, and Arg291 in bacterial luciferase, and the putative active site residues of Cys14, His311, and Tyr63 in LadA. The corresponding Cys and His residues in bacterial luciferase and SsuD have been characterized, but no detailed kinetic studies have been performed with LadA. Steady-state kinetic experiments performed on SsuD variants in which the amino acid residue Cys54 of SsuD was replaced with either Ser or Ala resulted in proteins with decreased activity; however, the binding of $FMNH_2$ was not affected by these substitutions. In rapid reaction kinetic traces obtained at 370 nm an initial fast phase was observed in C54S but not C54A SsuD. This phase was initially observed in stopped-flow kinetic traces obtained with wild-type SsuD, and has been attributed to the formation of a C4a-(hydro)peroxyflavin intermediate (*39*). These experiments provided evidence that the cysteine at position 54 in SsuD appears to be involved in the stabilization of the C4a-(hydro)peroxyflavin intermediate, similar to the role of Cys106 in bacterial luciferase (*48*). The His228 residue of SsuD has been reported to be the active site base in the desulfonation reaction. The binding of $FMNH_2$ and octanesulfonate substrate was not

affected by substitution of this His228 residue with Ala, Asp, or Lys; however, the steady-state kinetic parameters for octanesulfonate were significantly altered (unpublished results). It was shown that about 10-15% of wild-type activity could be rescued with addition of exogenous imidazole in the pH range of 7.0-9.0 with the H228A SsuD variant, indicating that only the deprotonated form of the imidazole ring is relevant for catalysis. The pH profiles of wild-type and H228A SsuD gave similar pK_a values for both k_{cat} and k_{cat}/K_m, which suggested that His228 in SsuD was not the catalytic base in the desulfonation reaction. These results are in contrast to the role of His44 in bacterial luciferase, which is proposed to be the active site base in the bioluminescence reaction (*58*).

Although the roles of the putative active site residues Cys54 and His228 have been elucidated, there is no information available on the conserved Arg297 located on a postulated flexible loop close to the active site of the enzyme. Surface loops have been identified in many globular proteins, and are known to play important roles in catalysis. These flexible loops are irregular segments of protein structure that link together secondary structural elements. Many times loops are found to contribute to the structure of an enzyme active site or play a functional role both in the binding of ligands and in enzyme catalysis. In these lid-containing β/α barrel enzymes, it is postulated that loop closure protects the substrate from solvent as well as preventing the premature release of catalytic intermediates. Along with SsuD, similar loops are found in the TIM-barrel enzyme family. It has been shown that upon substrate binding in triosephosphate isomerase, this flexible loop closes over the active site to protect the substrates and/or

intermediates during catalysis. Various members of the TIM barrel enzyme family possess a flexible loop at the active site with a similar function. The three-dimensional crystal structures of bacterial luciferase and SsuD contain a disordered region that is postulated to be part of a flexible loop. This putative flexible loop contains a conserved arginine residue at position 297 and 291 in SsuD and bacterial luciferase, respectively. In both enzymes, this residue is located in an insertion region containing an unstructured loop that is thought to cover the active site upon the binding of substrates. Although direct substitution of Arg291 has not been performed, deletion of this unstructured loop region in bacterial luciferase resulted in a decrease in bioluminescence (*79*). It is also interesting to note that when SsuD was first purified it contained an abherent Arg297 to Cys mutation that completely abolished enzymatic activity. It is postulated that a disulfide bond was formed between the Arg297Cys and Cys54, leading to the loss of activity. The arginine residue is located away from the cysteine, therefore this region would have to be flexible enough to move closer to the cysteine in order to form a disulfide bond. This evidence, along with the disordered region in the three dimensional crystal structure, gives validity to the flexibility of this region. In order to determine the role of Arg297 in the desulfonation reaction, two variants of the SsuD enzyme were constructed in which the arginine residue was replaced by either lysine or alanine. Various biochemical and mechanistic experiments were performed on the Arg297 SsuD variants and compared to wild-type SsuD. The data presented here provide information on the role of the conserved arginine residue located on a postulated flexible loop in SsuD.

3.2 MATERIALS AND METHODS

3.2.1 Materials

Oligonucleotide primers were from Invitrogen (Carlsbad, CA). Flavin mononucleotide phosphate (FMN), nicotinamide adenine dinucleotide phosphate (NADPH), 5-5′-dithio-bis(2-nitrobenzoic acid) (DTNB), dimethyl sulfoxide (DMSO), guanidine·HCl, EDTA, sodium chloride, urea, D-glucose, glucose oxidase, potassium phosphate (monobasic and dibasic), ammonium bicarbonate, phenylmethylsulfonyl fluoride (PMSF), and TPCK-treated trypsin were purchased from Sigma (St. Louis, MO). Glycerol was obtained from Fisher (Pittsburgh, PA). Octanesulfonate was from Fluka (Milwaukee, WI). The standard phosphate buffer contained 25 mM potassium phosphate (pH 7.5) and 10% glycerol, unless otherwise noted.

3.2.2 Site-Directed Mutagenesis

Mutagenesis of the *ssuD* gene was performed with the Stratagene QuikChange site-directed mutagenesis kit. The CGT codon for Arg297 was replaced with GCG and AAA for Ala and Lys, respectively. The pET21a plasmid containing the *ssuD* gene was used as the template for these mutations. The entire *ssuD* coding region containing the appropriate mutations was confirmed by sequence analysis at Davis Sequencing (Davis, CA). Each plasmid harboring the substituted *ssu* gene was transformed into *E. coli* BL21(DE3) super-competent cells (Invitrogen, Carlsbad, CA). The variants generated are referred to as R297K (Arg297 to Lys) and R297A (Arg297 to Ala) SsuD.

3.2.3 Expression and purification of wild type and variant SsuD

The SsuD wild-type and variant proteins were expressed from a pET21a expression vector in *E. coli* strain BL21(DE3), and the purification of each protein was performed as previously described. (*39*). Following purification, stocks of the variant and wild type SsuD enzymes were stored in 25 mM potassium phosphate buffer (pH 7.5), 100 mM NaCl, and 10% glycerol at ⁻80 °C. The enzyme concentrations were determined spectrophotometrically by using an absorption coefficient of 47 900 M^{-1} cm^{-1} at 280 nm. Wild-type SsuE was also expressed and purified as previously described and the concentration determined spectrophotometrically by using an absorption coefficient of 20 340 M^{-1} cm^{-1} at 280 nm (*82*).

3.2.4 Far-UV circular dichroism

The spectra of the variant and wild type SsuD enzymes were obtained with an enzyme concentration of 1.2 μM in 25 mM potassium phosphate buffer (pH 7.5) at 25 °C. Buffer exchange was performed to remove all NaCl and glycerol using an Amicon® Ultra Centrifugal Filter device (Millipore, Billerica, MA) with a MWCO of 10 000 kDa. Buffer exchanges were performed four times by centrifugation at 3 000 RPM. Far-UV spectra were recorded on a JASCO J-810 spectropolarimeter (Easton, MD). Measurements were taken in 0.1 nm increments in continuous scanning mode from 270 to 180 nm in a 0.1 cm path length cuvette with a bandwidth of 1 nm and a scanning speed of 20 nm/min. Each spectrum is the average of eight accumulated scans. Background correction and smoothing of the data was performed using the JASCO J-720 software

provided with the instrument. The CD data was analyzed by the CDPro software available online (*90*).

3.2.5 SsuD steady-state kinetic measurements

A coupled assay was utilized to determine the steady-state kinetic parameters of variant and wild-type SsuD enzymes, as described previously (*39*). The NAD(P)H dependent flavin reductase, SsuE, was included in the reaction to supply $FMNH_2$ to SsuD. For wild-type SsuD the reaction was initiated with the addition of NADPH (500 μM) into a reaction mixture containing SsuD (0.2 μM), SsuE (0.6 μM), FMN (2 μM), NADPH (500 μM), and varying concentrations of octanesulfonate (5–1500 μM) in standard buffer. Because of decreased enzymatic activity, assays with R297K and R297A contained a final concentration of 3.0 μM R297K SsuD, 9.0 μM SsuE, and 5 μM FMN. Assays performed with R297A SsuD gave no detectible activity, even with higher enzyme concentrations. All reactions were allowed to react for 3 minutes before quenching with urea (2 M final concentration). The resulting solution was centrifuged for 4 minutes to remove precipitated protein and an aliquot (200 μL) was added to 50 μL of DTNB (1 mM). Following a 2 min incubation at room temperature, the amount of sulfite product formed was quantified spectrophotometrically at a wavelength of 412 nm (ϵ = 14 150 M^{-1} cm^{-1}). The steady-state kinetic parameters were obtained using the Michaelis-Menten equation.

3.2.6 Flavin binding studies

Flavin binding to the variant and wild type SsuD enzymes was monitored by spectrofluorimetric titration with either oxidized or reduced flavin. Spectra were obtained

on a Perkin Elmer LS 55 luminescence spectrometer (Palo Alto, CA) with an excitation wavelength of 280 nm and emission wavelength of 345 nm. For the titration of SsuD with $FMNH_2$, a 1.0 mL solution of the variant SsuD enzymes (0.5 μM) in standard buffer containing 100 mM NaCl was titrated with a solution of $FMNH_2$, and the fluorescence recorded after each addition (0.26 – 9.19 μM for R297K and 0.26 -9.42 μM for R297A), as previously described (*39*). Anaerobic SsuD enzyme solutions were prepared in a glass titration cuvette by at least 15 cycles of evacuation followed by equilibration with ultra high purity argon gas. An oxygen scavenging system composed of 20 mM glucose and 10 units of glucose oxidase (1 unit is defined as the amount of enzyme needed to convert 1.0 μmole of β-D-glucose to D-gluconolactone and H_2O_2 per minute at pH 5.1 at 35 °C) was also included to ensure the solution was kept anaerobic. Anaerobic solutions of $FMNH_2$ were prepared as previously described (*39*). Bound $FMNH_2$ was determined by the following equation (*39*):

$$[\mathrm{FMN}]_{\mathrm{bound}} = [\mathrm{SsuD}]\frac{I_0 - I_c}{I_0 - I_f}, \qquad (1)$$

where [SsuD] is the initial concentration of enzyme, I_0 is the initial fluorescence intensity of SsuD prior to titration, I_c is the fluorescence intensity of SsuD following each addition of $FMNH_2$, and I_f is the final fluorescence intensity. The concentration of $FMNH_2$ bound was plotted against the total $FMNH_2$ to obtain the dissociation constant (K_d) according to

Equation 2 where B_{max} is the maximum binding at equilibrium with the maximum concentration of substrate. K_d is the dissociation constant for the substrate (*39*).

$$Y = \frac{B_{max} X}{K_d + X} \quad (2)$$

3.2.7 Octanesulfonate binding

Octanesulfonate binding to the variants and wild type SsuD was investigated by similar fluorimetric titration methods employed for flavin binding. A 1.0 mL solution of either R297K or R297A SsuD (1 μM), with reduced flavin (2 μM), was made anaerobic in a glass titration cuvette as described previously (*39*). Aliquots of an anaerobic solution of octanesulfonate in an air-tight titrating syringe were added to the variant SsuD-$FMNH_2$ complex. The fluorescence spectra were recorded with an excitation wavelength at 280 nm and emission intensity measurements at 344 nm. The concentration of bound octanesulfonate was determined by Eq. 1, and plotted against the concentration of free octanesulfonate to determine the dissociation constant (K_d) according to Eq. 2.

3.2.8 Rapid-reaction kinetics of flavin oxidation

Rapid reaction kinetic analyses were carried out using an Applied Photophysics SX.18 MV stopped-flow spectrophotometer. The stopped-flow instrument was made anaerobic by repeated filling and emptying of the drive syringes with an oxygen scrubbing system. The oxygen scavenging system contained standard buffer with 100 mM NaCl, 20 mM glucose, and 10 units of glucose oxidase. The protein solutions were prepared in an anaerobic chamber in standard buffer containing 100 mM NaCl. Reduced flavin solutions were prepared as previously described (*39*). The $FMNH_2$ solution was

transferred to a glass tonometer, and incubated in an anaerobic chamber (95% N_2 and 5% H_2 gas) for 2–3 hours before being transferred to the stopped-flow spectrophotometer. All experiments contained 15 μM $FMNH_2$ in one drive syringe mixed against 45 μM R297K, R297A, or wild-type SsuD enzyme in air-saturated buffer in the other drive syringe. When included in the reaction, the concentration of octanesulfonate was varied from 50–2000 μM (before mixing) in air-saturated buffer. All experiments were carried out in single-mixing mode by at 4 °C mixing equal volumes of the solutions, and monitoring the reactions by single wavelength analyses at 370 and 450 nm. The initial analyses of single-wavelength traces at 370 and 450 nm were performed using the PROKIN software (Applied Photophysics, Ltd.) installed in the stopped-flow spectrophotometer. A global analysis was applied to determine the steps involved in flavin oxidation. Kinetic fits of the data were performed using the KaleidaGraph software (Abelbeck Software, Reading, PA). The single-wavelength traces of each mutant were fitted to the following double or triple exponential equations:

$$A = A_1 \exp(-k_1 t) + A_2 \exp(-k_2 t) + C \quad (3)$$

$$A = 1 - [A_1 \exp(-k_1 t) + A_2 \exp(k_2 t) + A_3 \exp(-k_3 t) + C] \quad (4)$$

where k_1, k_2, and k_3 are the apparent rate constant for the different phases, A is the absorbance at time t, A_1, A_2, and A_3 are amplitudes of each phase, and C is the absorbance at the end of the reaction.

3.2.9 Rapid-reaction kinetics of flavin oxidation in the presence of SsuE

The single-turnover kinetics of flavin oxidation was determined for the variants and wild-type SsuD to determine whether substitution of the conserved arginine has an

effect on the kinetics of flavin oxidation in the presence of SsuE. Stopped-flow kinetic experiments were performed with aerobic solutions of R297K, R297A, or wild-type SsuD (35 μM), SsuE (35 μM), and FMN (25 μM) mixed against NADPH (25 μM) in air-saturated buffer at 4 °C. When included in the reaction, octanesulfonate (250 μM) was present in the drive syringe with NADPH. The concentrations given are before mixing. All experiments were carried out in single-mixing mode by mixing equal volumes of the solutions, and monitoring the reactions by single wavelength analyses at 450 nm.

3.2.10 Proteolytic susceptibility of the variants and wild-type SsuD

The susceptibility of the variants and wild-type SsuD to proteolysis was investigated with trypsin in the absence and presence of $FMNH_2$ and octanesulfonate substrates. Samples of the variant or wild-type SsuD enzymes (24 μM) were treated with 10 μg/mL TPCK-treated trypsin in 200 mM NH_4HCO_3, 1 mM $CaCl_2$ buffer (pH 8.4). When $FMNH_2$ was included in the incubation a ratio of 1:1.2, SsuD:$FMNH_2$, was kept to ensure that every flavin binding site in SsuD was occupied. An anaerobic solution of flavin (100 μM) was made containing 25 mM phosphate buffer, 10 mM EDTA and 10% glycerol at pH 7.5. The flavin solutions were bubbled with Ultra-High Purity argon gas for 20 minutes before being transferred to an anaerobic chamber. This FMN solution was reduced inside a gas-tight Hamilton syringe with a long wavelength UV lamp. The final concentration of $FMNH_2$ in each reaction mixture was 29 μM. The octanesulfonate concentration was 250 μM when included in the reaction. Reactions were performed in an anaerobic chamber to ensure that there was no presence of molecular oxygen. Samples (10 μL) were taken at various times (15, 30, 45, 60, 120, and 300 s) and added to 2 μL of

6 mg/ml phenylmethylsulfonyl fluoride (PMSF) to quench the reaction. These samples were run on 15% SDS-PAGE gels and analyzed using the LabImage 1D software (Kapelan, Halle, Germany) to determine the percent digestion.

3.3 RESULTS

3.3.1 Far-UV circular dichroism

Circular dichroism spectroscopy (CD) was performed on R297K, R297A, and wild-type SsuD to ensure that mutations to this conserved arginine residue did not result in any major overall secondary structural changes. Results revealed differences in the CD spectra for both variants in the 205-235 nm region compared to wild type (Figure 3.1), suggesting that substitution of this arginine residue with either lysine or alanine causes minor perturbations to the overall secondary structure of SsuD. Analysis of the CD data showed a 5% decrease in the α-helical content of the R297K and R297A SsuD variants compared to wild-type SsuD (Table 3.1). This decrease in a-helical content was replaced with a slight increase in the random coil (R297A) and unstructured secondary structural elements (R297K and R297A).

Table 3.1: % Secondary Structural Elements of R297K, R297A, and wild-type SsuD

	α-helix	β-sheet	Random Coil	Unstructured
WT SsuD	10	36	22	32
R297K SsuD	5	37	22	34
R297A SsuD	6	35	25	34

3.3.2 Steady-state kinetic parameters

Steady-state kinetic analyses were performed to determine whether the mutation of Arg297 to either Lys or Ala altered the kinetic parameters previously obtained for

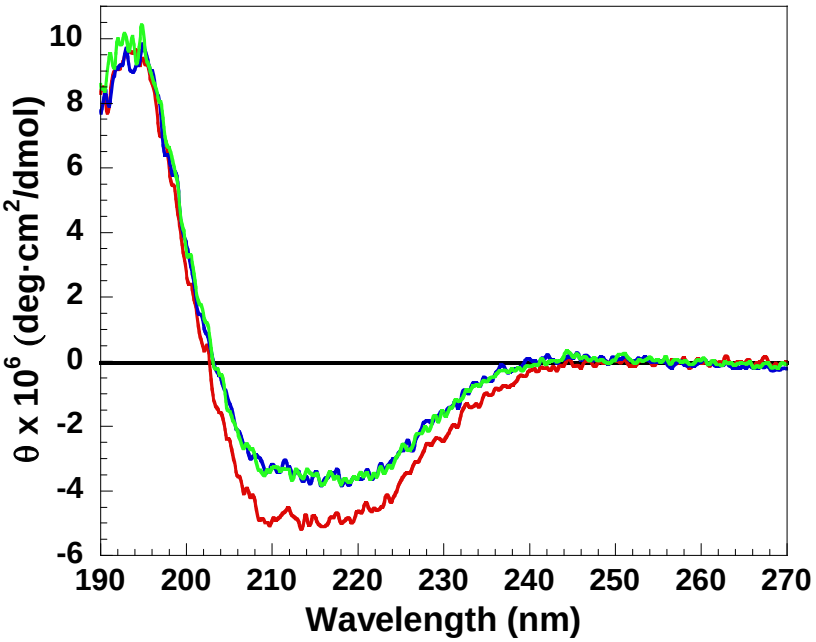

Figure 3.1: Far-UV circular dichroism spectra of R297K, R297A, and wild-type SsuD. Each spectra was obtained with an enzyme concentration of 1.2 μM in 25 mM potassium phosphate buffer, pH 7.5, at 25 ºC. Measurements were taken in 0.1 nm increments from 270 to 190 nm in a 0.1 cm path length cuvette. Each spectrum is the average of eight accumulated scans; smoothing of the data was performed using the default parameters within the Jasco J-720 software. The spectra correspond to wild-type SsuD (red), R297K SsuD (green), and R297A SsuD (blue).

wild-type SsuD. Because SsuD has an absolute requirement for $FMNH_2$, the FMN reductase, SsuE, was included in this assay to provide the reduced flavin to SsuD. The steady-state kinetic parameters for R297K and wild-type SsuD were obtained by monitoring the production of the TNB anion at 412 nm in the reaction of DTNB with the sulfite product. The data showed a hyperbolic dependence on octanesulfonate substrate concentration for the R297K SsuD variant (Figure 3.2). The K_m and k_{cat} values determined for R297K SsuD were 35.2 ± 4.6 μM and 1.5 ± 0.1 min^{-1}, respectively (Table 3.2). The K_m value for octanesulfonate with the R297K SsuD enzyme was essentially the same as wild-type, while the k_{cat} value was decreased about 35-fold compared to wild-type SsuD (K_m, 44.0 ± 8.3 μM; k_{cat}, 51.7 ± 2.1 min^{-1}). The value for the catalytic efficiency (k_{cat}/K_m) of the R297K SsuD variant decreased 30-fold compared to wild-type SsuD. The R297A SsuD variant exhibited no detectible production of sulfite, even at high concentration of octanesulfonate substrate. These results suggest that the charge on the amino acid is important for catalysis as the more conservative substitution of Arg to Lys, still retained some activity. The fact that substitution of Arg297 to Ala abolished all activity indicates that Arg297 could possibly have a direct role in catalysis.

3.3.3 Substrate binding to the R297 SsuD variants

Spectrofluorimetric titrations were performed to determine whether Arg297 substitutions had an effect on the binding of $FMNH_2$. The dissociation constants (K_d) for the binding of reduced flavin to the SsuD variants were determined by titrating $FMNH_2$ into a sample of R297K or R297A SsuD. The decrease in the intrinsic protein

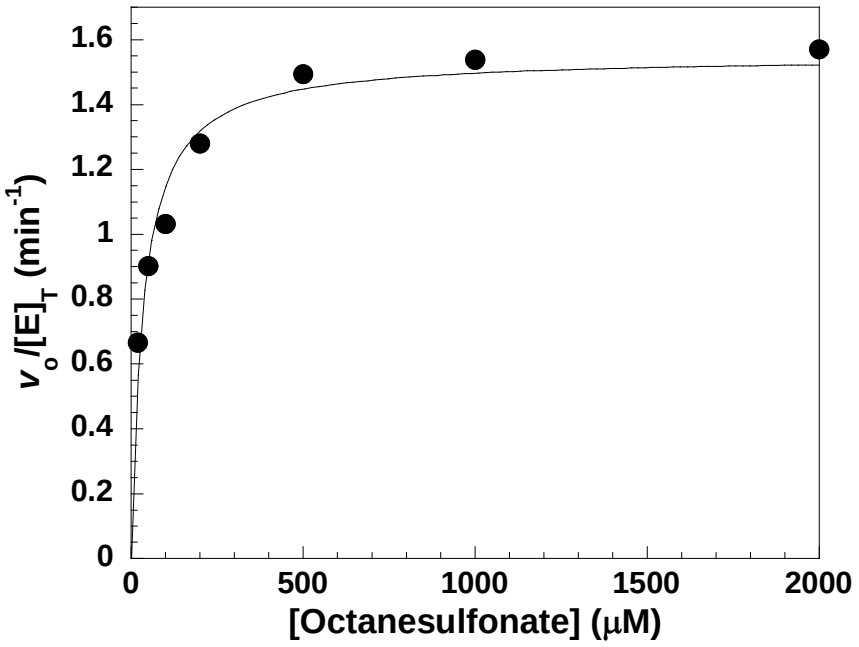

Figure 3.2 Steady-state kinetic analysis of R297K SsuD. The assay measured the sulfite product formed from the reaction of 3.0 μM R297K SsuD, 9.0 μM SsuE, 5.0 μM FMN, 500 μM NADPH, and varying concentrations of octanesulfonate substrate (10-2000 μM) in standard buffer with 100 mM NaCl at 25 °C. The amount of sulfite product was quantified as described in *Materials and Methods*. Each assay was performed in triplicate and the solid lines represent fits of the data to the Michaelis-Menton equation.

fluorescence emission due to the binding of $FMNH_2$ was monitored at 344 nm for each variant. The concentration of bound and free flavin was calculated using Eq. 1, and the concentration of flavin bound to each variant was plotted against the concentration of free flavin. The K_d values for $FMNH_2$ are summarized in Table 3.2. The average K_d value for $FMNH_2$ binding to each SsuD variant was 1.09 ± 0.16 μM and 1.46 ± 0.17 μM for R297K or R297A SsuD, respectively. This represents a 3-fold increase compared to the K_d value obtained for wild-type SsuD (0.32 ± 0.15 μM) (Figure 3.3, R297K fluorescence titrations with $FMNH_2$). These results indicate that mutation of the arginine residue located at position 297 to either lysine or alanine slightly altered the binding of $FMNH_2$ when compared to the previously reported K_d value for wild-type SsuD (*39*).

It was previously shown that ordered substrate binding occurs in the SsuD reaction, with reduced flavin cofactor binding first before the octanesulfonate substrate (*39*). The binding of octanesulfonate to the R297K or R297A SsuD/$FMNH_2$ complex was performed to determine whether the binding of substrate was affected by the arginine substitutions. To ensure that all of the $FMNH_2$ was bound to SsuD, a 2:1 ratio of $FMNH_2$ to SsuD was used in these experiments. Unfortunately, a K_d for octanesulfonate could not be obtained even with octanesulfonate additions over 300 μM. These results suggest that octanesulfonate does not bind to either variant and indicates that the binding of octanesulfonate is drastically affected by the substitution of Arg297 with either lysine or alanine. The residual activity associated with the R297K SsuD variant indicates that octanesulfonate must be binding; however, disrupted amino acid contacts caused by the substitution could prevent tight binding.

Table 3.2: Dissociation constants and steady-state kinetic parameters for R297K, R297A, and wild-type SsuD.

	K_d, $FMNH_2$[a] (μM)	K_m, octanesulfonate (μM)	k_{cat} (min^{-1})	k_{cat}/K_m (μM^{-1} min^{-1})
WT SsuD[b]	0.32 ± 0.15	44.0 ± 8.3	51.7 ± 2.1	1.17 ± 0.22
R297K SsuD	1.09 ± 0.16	35.2 ± 4.6	1.5 ± 0.1	0.04 ± 0.01
R297A SsuD	1.46 ± 0.17	ND*	ND*	ND*

[a] Determined under anaerobic conditions as described in *Experimental Procedures*

[b] Previously reported (*39*).

ND* No activity detected

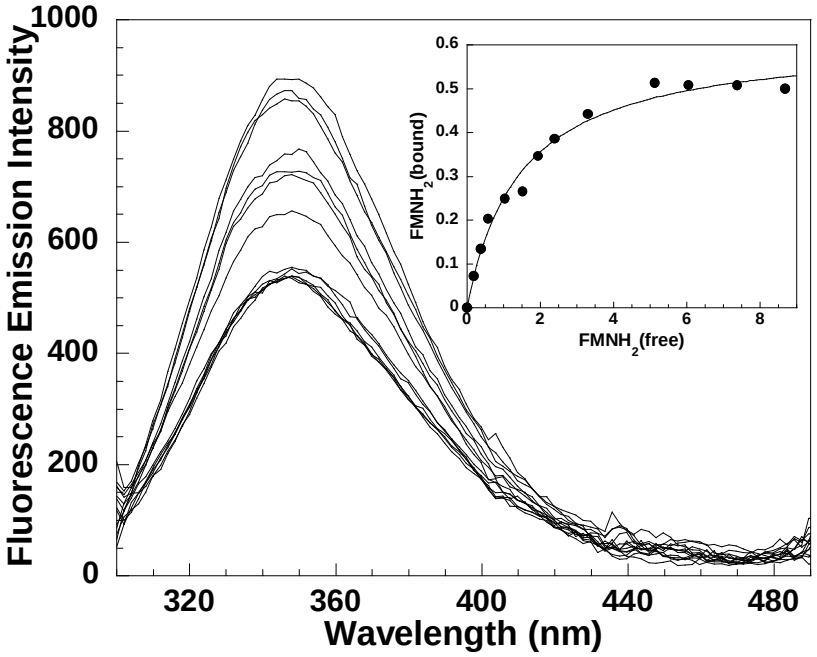

Figure 3.3: Fluorimetric titration of R297K SsuD with $FMNH_2$. R297K SsuD (0.5 μM) was titrated with $FMNH_2$ (0.26–9.19 μM). Emission intensity measurements at 344 nm were obtained with an excitation wavelength of 280 nm. The change in the intrinsic fluorescence intensity for R297K SsuD following the addition of $FMNH_2$ was converted to concentration of bound $FMNH_2$ (Eq. 1) and plotted against the concentration of free $FMNH_2$. Inset: Change in fluorescence emission intensity at 344 nm. The solid line represents a fit of the titration curve to Eq. 2.

3.3.4 Rapid reaction kinetics of flavin oxidation

Previous studies have identified the formation of a C4a-(hydro)peroxyflavin intermediate in stopped-flow kinetic experiments performed with wild-type SsuD, in the absence and presence of octanesulfonate substrate (*39*). Rapid reaction kinetic experiments performed with Cys54 variants of SsuD have shown that this cysteine residue stabilizes the formation of the C4a-(hydro)peroxyflavin intermediate (unpublished results). The similarities of SsuD and bacterial luciferase in the putative active site region extend away from the active site in the form of a flexible loop. The flexible loop is postulated to cover the active site of bacterial luciferase once substrates are bound to exclude bulk solvent from the active site during catalysis (*61*). This loop is disordered in the three-dimensional crystal structures of both SsuD and bacterial luciferase and contains an arginine at position 291 in luciferase and 297 in SsuD which is highly conserved among related $FMNH_2$-dependent monooxygenases (*60,61*). The role of Arg297 in the desulfonation reaction was probed through stopped-flow kinetic analyses. The SsuD variants were maintained at a higher concentration (45 μM) relative to $FMNH_2$ (15 μM) to ensure single-turnover conditions. It has been previously shown that the mixing order of $FMNH_2$ and SsuD is essential for a high accumulation of the C4a-(hydro)peroxyflavin intermediate (*39*). The flavin intermediate formation was observed when $FMNH_2$ was mixed against wild-type SsuD in oxygenated buffer; however, when SsuD and $FMNH_2$ were pre-mixed there was no detection of any flavin intermediate. Stopped-flow kinetic experiments were performed in an attempt to determine if the C4a-(hydro)peroxyflavin was detectable with the SsuD variants by mixing $FMNH_2$ against

either R297K or R297A SsuD in air-saturated buffer. Kinetic traces for $FMNH_2$ oxidation obtained at 370 nm for both variants in the absence of octanesulfonate substrate were best fit to a triple exponential with apparent rate constants of 26.6 s^{-1} (k_1), 1.3 s^{-1} (k_2), and 0.1 s^{-1} (k_3) for R297K and 22.0 s^{-1} (k_1), 1.8 s^{-1} (k_2), and 0.4 s^{-1} (k_3) for R297A SsuD (Figure 3.4). However, the kinetic traces obtained at 450 nm were fit to a double exponential equation with rate constants of 18.4 s^{-1} (k_1) and 1.4 s^{-1} (k_2) for R297K and 0.8 s^{-1} (k_1) and 1.9 s^{-1} (k_2) for R297A SsuD (Table 3.3).

Table 3.3: Single turnover kinetic rate constants for WT, R297K, and R297A SsuD in the absence of octanesulfonate

	370 nm			450 nm	
	k_1, s^{-1}	k_2, s^{-1}	k_3, s^{-1}	k_1, s^{-1}	k_2, s^{-1}
SsuD WT[a]	12.9	0.95	0.08	1.3	0.09
SsuD R297K	26.6	1.3	0.1	18.4	1.4
SsuD R297A	22	1.8	0.4	0.8	1.9

[a] Previously reported (*39*)

The first phase of flavin oxidation for both SsuD variants at 370 nm exhibited a 2-fold increase in comparison to wild-type SsuD. The rates obtained for the first and second phases for flavin oxidation at 450 nm with the R297K SsuD variant exhibited a 10-fold increase compared to wild-type. The second and third phases at 370 nm for R297K SsuD were similar to those obtained for wild-type SsuD; however, the rates obtained for the second and third phases of flavin oxidation for R297A SsuD were 2- and 4-fold higher that wild-type SsuD. These two phases obtained at 370 nm for flavin oxidation are attributed to the decomposition of the C4a-(hydro)peroxyflavin intermediate.

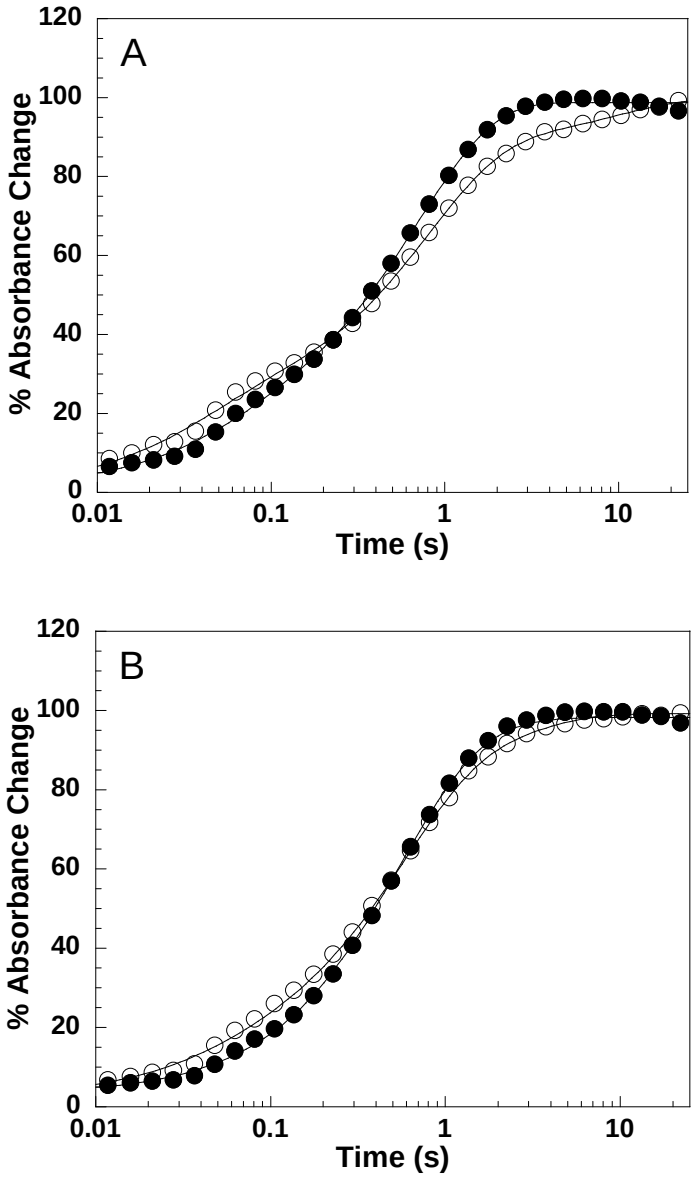

Figure 3.4: Kinetics of flavin oxidation by R297K and R297A SsuD in the absence of octanesulfonate substrate. A: Free $FMNH_2$ mixed against R297K SsuD in air-saturated buffer. B: Free $FMNH_2$ mixed against R297A SsuD in air-saturated buffer. The kinetic traces shown are an average of three separate experiments following flavin oxidation at 370 nm (○) and 450 (●). The solid lines are the fits of the kinetic traces to Eq. 3 or 4.

3.3.5 Kinetic studies of flavin oxidation by SsuD variants in the presence of octanesulfonate substrate

Rapid reaction kinetic analyses were also employed to determine if the presence of the octanesulfonate substrate had an effect on the rate of formation of the C4a-(hydro)peroxyflavin intermediate. The oxidation of flavin by the SsuD variants in the presence of octanesulfonate substrate was monitored by stopped-flow analyses at 370 and 450 nm by mixing free $FMNH_2$ (15 μM) with either R297K or R297A SsuD (45 μM) and octanesulfonate (50-2000 μM) in air-saturated buffer (concentrations given are before mixing). For wild-type SsuD, an initial fast phase at 370 nm was observed in kinetic traces obtained at low octanesulfonate concentrations (≤ 100 μM) (*39*). The rapid-reaction kinetic traces following the oxidation of $FMNH_2$ at 370 nm with R297K SsuD in the presence of octanesulfonate substrate were best fit to a triple exponential equation (Figure 3.5A). The initial fast phase for each octanesulfonate concentration, attributed to the formation of the C4a-(hydro)peroxyflavin intermediate, was similar to the rate obtained in the absence of octanesulfonate. Single-turnover kinetic traces obtained for the oxidation of flavin with R297K SsuD at 450 nm in the presence of increasing concentrations of octanesulfonate substrate were fit to a double exponential equation (Figure 3.5B). Rate constants are summarized in Table 3.3. The kinetic traces following flavin oxidation in the presence of octanesulfonate substrate at 370 and 450 nm exhibited no dependence on octanesulfonate concentration. The initial fast phase first observed with wild-type SsuD was not observed in any of the kinetic traces of flavin oxidation with R297A SsuD in the presence of increasing concentrations of octanesulfonate. Each

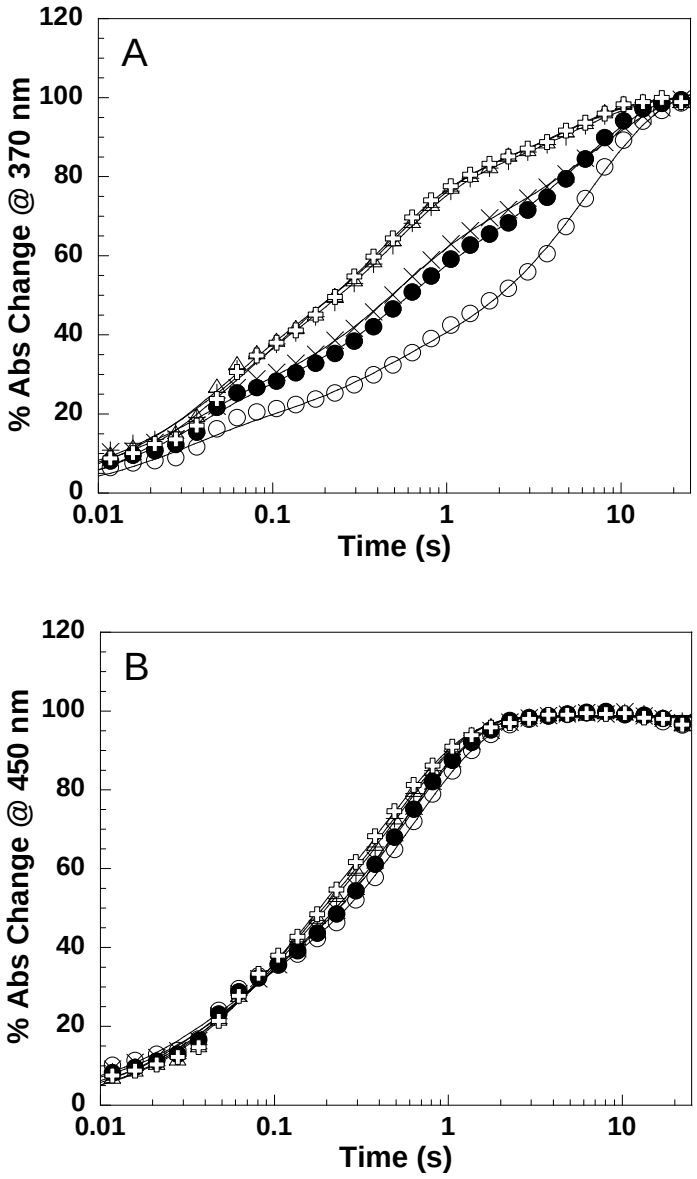

Figure 3.5: Kinetics of flavin oxidation by R297K SsuD in the presence of variable amounts of octanesulfonate (25 (○), 50 (●), 100 (×), 250 (+), 500 (△), and 1000 μM (✣)) in oxygenated buffer. A: Kinetics of flavin oxidation in the presence of R297K SsuD at 370 nm. B: Kinetics of flavin oxidation in the presence of R297K SsuD at 450 nm. The solid lines are the fits of the kinetic traces to Eq. 3.

Table 3.4: Single turnover kinetic rate constants for R297K and R297A SsuD in the presence of octanesulfonate substrate

	R297K SsuD					R297A SsuD			
	370 nm			450 nm		370 nm		450 nm	
[RCH_2SO_3]	k_1, s^{-1}	k_2, s^{-1}	k_3, s^{-1}	k_1, s^{-1}	k_2, s^{-1}	k_1, s^{-1}	k_2, s^{-1}	k_1, s^{-1}	k_2, s^{-1}
25 μM	34.6	3.13	0.15	25.0	1.57	11.6	1.43	6.6	1.57
50 μM	30.9	2.18	0.17	23.8	1.77	10.5	1.47	5.4	1.63
100 μM	32.9	2.17	0.14	20.0	1.82	8.9	1.47	4.7	1.56
250 μM	23.1	2.26	0.19	16.0	1.99	6.2	1.35	4.0	1.29
500 μM	22.1	2.50	0.22	16.4	2.03	6.1	1.29	4.0	1.37
1000 μM	22.1	2.51	0.22	13.9	2.11	5.6	1.23	4.0	1.42

rapid reaction kinetic trace at 370 nm was fit to a double exponential equation (Eq. 3) and essentially overlapped each other showing no dependence on octanesulfonate substrate concentration (Figure 3.6A). The stopped-flow kinetic traces following flavin oxidation at 450 nm for the R297A SsuD variant were similar, and also exhibited no dependence on octanesulfonate substrate concentration (Figure 3.6B). These results are in correlation to the results obtained from steady-state kinetic experiments which showed no detectible activity.

3.3.6 Rapid reaction kinetics of $FMNH_2$ oxidation in the presence of SsuE

The kinetics of flavin oxidation in the presence of the flavin reductase, SsuE, were obtained using stopped-flow analysis. It has been previously shown that flavin oxidation is faster in the presence of SsuE only (unpublished results). However, it is not well established how the $FMNH_2$ is transferred from SsuE to SsuD. Since the arginine at position 297 is located on a flexible loop, it is possible that this amino acid residue could facilitate the transfer of reduced flavin and/or help keep substrates bound in the active site through electrostatic interactions with a negatively charged group. Single-turnover experiments were performed to determine whether mutation of Arg297 had an effect on the oxidation of flavin in the presence of SsuE. In stopped-flow kinetic traces following the reduction and oxidation of flavin at 450 nm in the absence of octanesulfonate substrate by wild-type SsuD there is an apparent lag phase after the reduction of flavin by SsuE (Figure 3.7A). Fitting of the kinetic data was attempted, but unfortunately a good fit was not obtained. Qualitatively speaking this phase is not present in stopped-flow kinetic

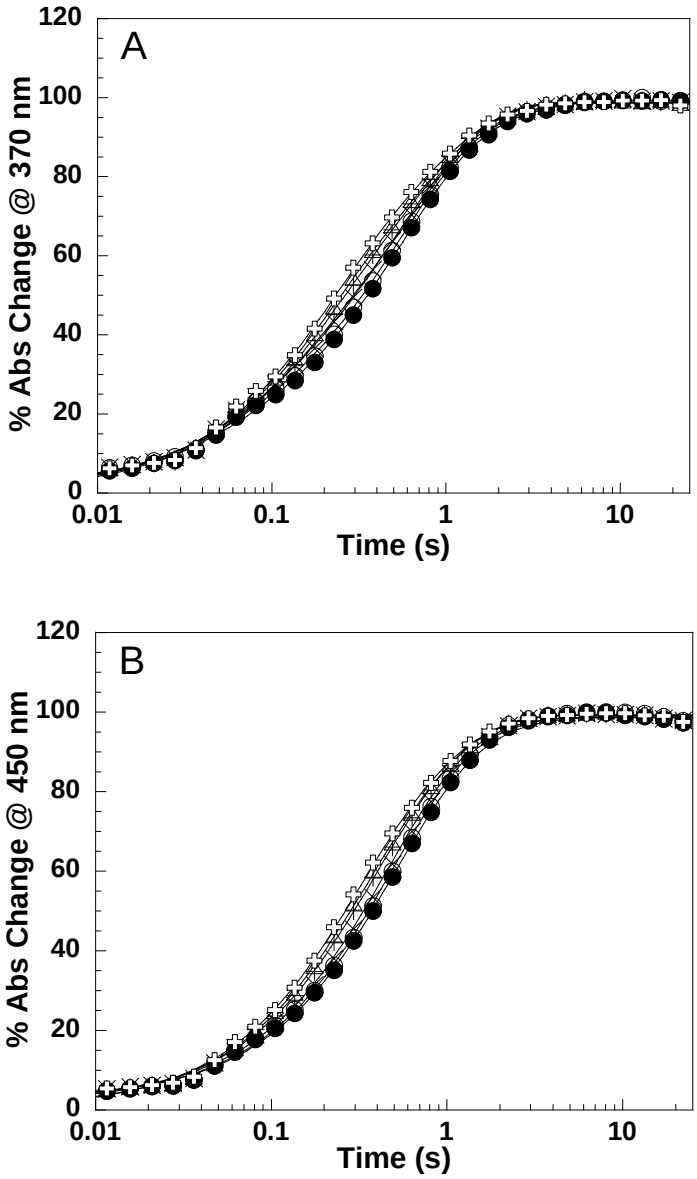

Figure 3.6: Kinetics of flavin oxidation by R297A SsuD in the presence of variable amounts of octanesulfonate (25 (●), 50 (◇), 100 (×), 250 (+), 500 (△), and 1000 μM (✣)) in oxygenated buffer. A: Kinetics of flavin oxidation in the presence of R297A SsuD at 370 nm. B: Kinetics of flavin oxidation in the presence of R297A SsuD at 450 nm. The solid lines are the fits of the kinetic traces to Eq. 3.

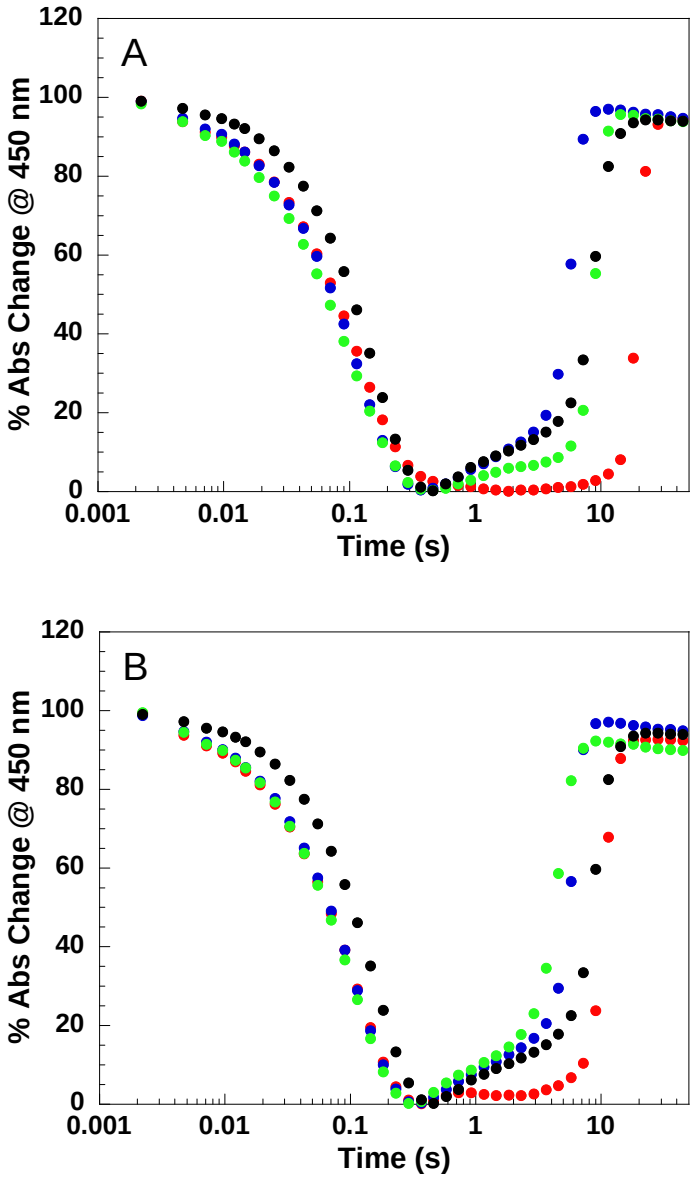

Figure 3.7: Kinetic traces following FMN reduction and $FMNH_2$ oxidation with R297K (●), R297A (●), and wild-type (●) at 450 nm in the presence of SsuE, or SsuE alone (●). A: Kinetic traces of R297K, R297A, wild-type SsuD, and SsuE alone at 450 nm. B: Kinetic traces of R297K, R297A, wild-type SsuD and SsuE alone at 450 nm in the presence of 250 μM octanesulfonate.

traces obtained with either R297K or R297A SsuD variant or the control experiment with SsuE alone. The rapid-reaction kinetic traces obtained at 450 nm with variants and wild-type SsuD in the presence of octanesulfonate substrate were similar to those obtained in the absence of octanesulfonate. Although the reduction of flavin was essentially the same, the oxidation of flavin was faster in the presence of octanesulfonate substrate (Figure 3.7B).

3.3.7 Proteolytic susceptibility of SsuD and variants

It was previously shown that bacterial luciferase is inactivated in the presence of trypsin in a time dependent manner (*75*-*77*). However, in the presence of $FMNH_2$ and aldehyde substrate the rate of inactivation is reduced. It is postulated that the mobile loop in bacterial luciferase closes down over the active site and reduces the susceptibility of the enzyme to proteolytic cleavage. The fate of wild-type SsuD after treatment with trypsin in the absence and presence of substrate(s) was investigated using SDS-PAGE to determine whether the binding of substrate(s) protects the enzyme from rapid proteolysis. If the arginine residue at position 297 facilitates the binding of substrates, one would expect proteolysis of the SsuD variants to proceed more rapidly than wild-type. For analysis, aliquots of the reaction mixtures of wild-type or variant SsuD enzyme with trypsin were withdrawn at specific times and the reaction quenched with PMSF. The SDS-PAGE gels displaying time-dependent proteolysis by trypsin for the variant and wild-type SsuD enzymes in the presence and absence of substrates is shown in Figures 3.8 and 3.9. The wild-type SsuD enzyme, in the absence of substrates, appeared to be rapidly digested, with no remaining protein left after 1 min (Figure 3.8A), whereas both

R297K and R297A SsuD variant enzymes were completely digested by trypsin in less than 15 seconds (Figure 3.8 I and Figure 3.9 IV) (Figure 3.8B and 3.9B). In the presence of $FMNH_2$, wild-type SsuD was digested significantly slower than in the absence of substrates, with complete digestion occurring after 5 minutes (Figure 3.8 II and Figure 3.9 V). Both R297K and R297A SsuD variants were completely digested after 5 minutes in the presence of $FMNH_2$ with 23 and 7% of protein remaining after 2 minutes, respectively (Figure 3.8B and 3.9B). This is in contrast to digestions with wild-type SsuD in which 11% of the native protein remained after incubation fro 5 minutes. These results indicate that there is a protective effect associated with $FMNH_2$ binding. When both octanesulfonate and $FMNH_2$ were included in the incubation, wild-type SsuD was digested significantly slower than in the presence of only $FMNH_2$, with 76% of the native protein still present after 5 minutes (Figure 3.8 III and Figure 3.9 VI). However, the R297K and R297A SsuD variants were completely digested between 2-5 minutes in the presence of both substrates. The difference between wild-type SsuD enzyme in the percent protein remaining when $FMNH_2$ or $FMNH_2$ and octanesulfonate were included in the digestion suggests that the binding of substrates has a protective effect on SsuD and limits proteolysis (Figure 3.8A). The R297K and R297A variant SsuD enzymes in the presence of $FMNH_2$ exhibited less proteolysis by trypsin compared to when reduced flavin was not included in the incubation (Figure 3.8B and 3.9B). The amount of proteolysis was essentially the same when both substrates were included in the reactions with the variant SsuD enzymes as compared to reactions with $FMNH_2$ only (Figure 3.8 III and Figure 3.9 VI). The similarity between the time-dependent digestion of R297K

and R297A SsuD with either $FMNH_2$ only or both $FMNH_2$ and octanesulfonate supports the previous observation, from fluorimetric titrations, that octanesulfonate may not be binding. The incubations with wild-type SsuD show that the binding of substrates protects the enzyme from being digested by trypsin. The R297K and R297A SsuD variants exhibited a greater amount of proteolysis than wild-type SsuD, even in the presence of substrates. This suggests that the arginine located at position 297 on the flexible loop in SsuD is important in protecting SsuD from proteolysis. This is possibly accomplished by contacts made with a negatively charged amino acid and/or stabilization of the binding of substrates.

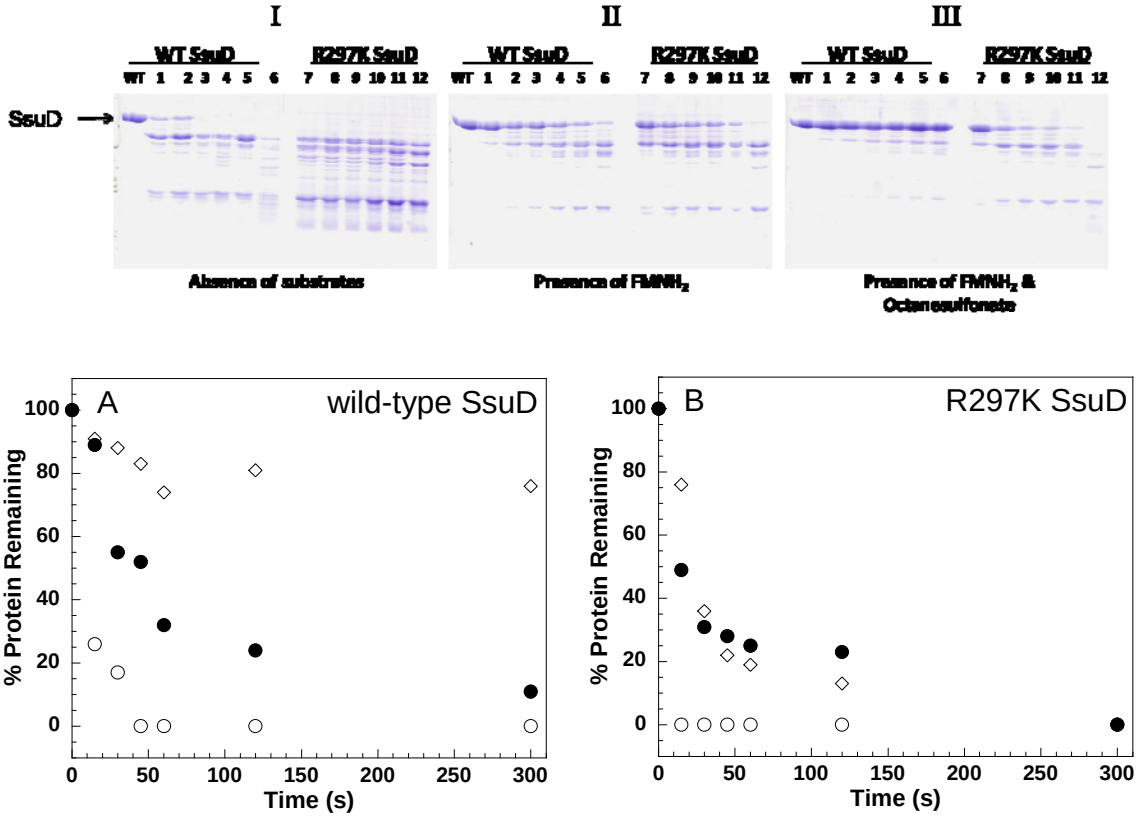

Figure 3.8: Effect of $FMNH_2$ on the time course of proteolysis of wild-type and R297K SsuD by low levels of trypsin. Aliquots were removed and quenched with PMSF after 15 s (lanes 1 and 7), 30 s (lanes 2 and 8), 45 s (lanes 3 and 9), 1 min (lanes 4 and 10), 2 min (lanes 5 and 11), or 5 min (lanes 6 and 12). A: % remaining wild-type SsuD without substrates (○), with $FMNH_2$ (●), and with both $FMNH_2$ and octanesulfonate (◇). B: % remaining R297K SsuD without substrates (○), with $FMNH_2$ (●), and with both $FMNH_2$ and octanesulfonate (◇).

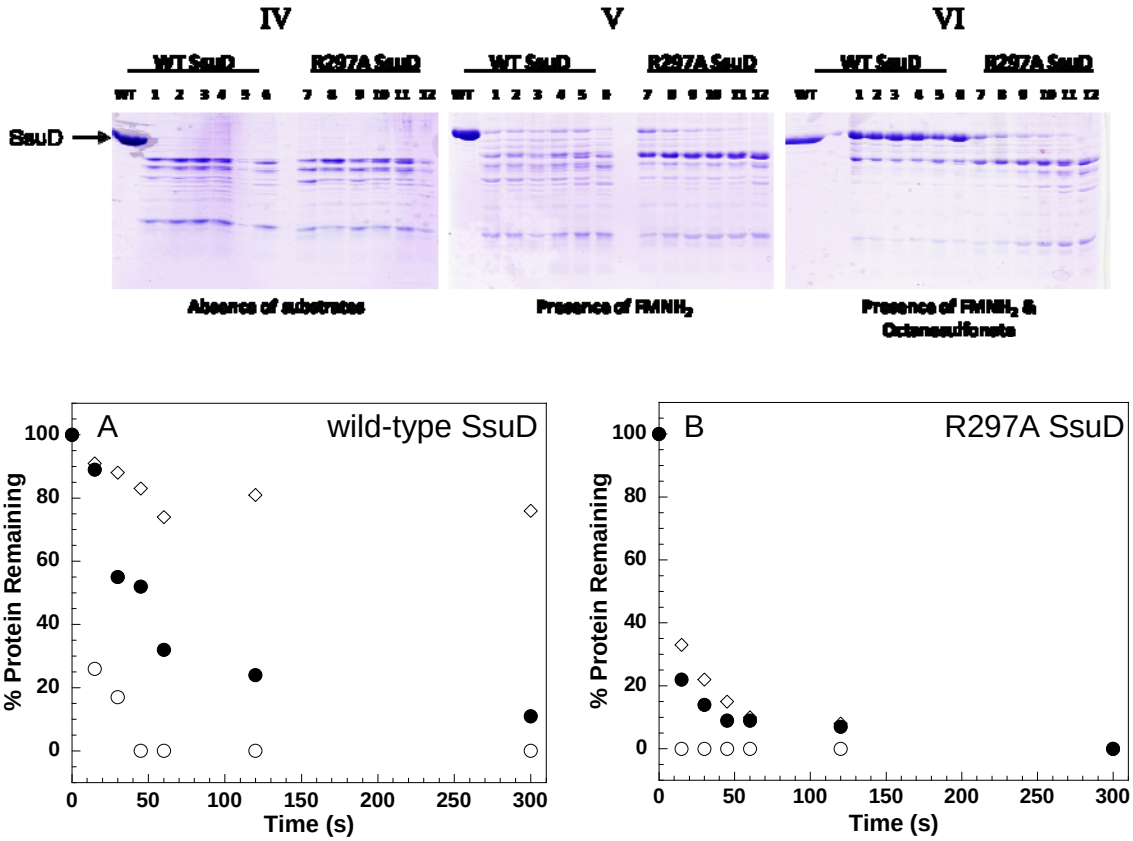

Figure 3.9: Effect of $FMNH_2$ on the time course of proteolysis of wild-type and R297A SsuD by low levels of trypsin. Aliquots were removed and quenched with PMSF after 15 s (lanes 1 and 7), 30 s (lanes 2 and 8), 45 s (lanes 3 and 9), 1 min (lanes 4 and 10), 2 min (lanes 5 and 11), or 5 min (lanes 6 and 12). A: % remaining wild-type SsuD without substrates (○), with $FMNH_2$ (●), and with both $FMNH_2$ and octanesulfonate (◇). B: % remaining R297A SsuD without substrates (○), with $FMNH_2$ (●), and with both $FMNH_2$ and octanesulfonate (◇).

3.4 DISCUSSION

While the catalytic mechanisms of several $FMNH_2$-dependent monooxygenases have been well studied, the mechanism of desulfonation by SsuD is not fully understood (*40-55*). The three-dimensional crystal structure of SsuD is strikingly similar in overall structure to the monomeric units of bacterial luciferase and LadA, although there is low amino acid sequence homology between them (*60, 61, 68*). While the quaternary structures of these three enzymes are different, the monomers have been shown to adopt a TIM-barrel fold. There is a conserved arginine residue located on a postulated mobile loop near the active site pocket of bacterial luciferase and SsuD. However, the role of the arginine residue in bacterial luciferase and SsuD has not been determined. The loop region is a distinguishing feature of bacterial luciferase family of enzymes. This loop is disordered in the crystal structures of luciferase and SsuD, indicating that it is located in a conformationally flexible region of the protein. It has previously been shown that both bacterial luciferase and SsuD have conformational changes associated with $FMNH_2$ binding (*79, 39*). It is postulated that the disordered loop in these enzymes may close over the active site following the binding of substrate(s), leading to conformational changes (*60, 61*).

Studies have been performed on bacterial luciferase from *V. harveyi* to determine whether the postulated mobile loop is required for bioluminescence activity. The mobile loop is located close to the active site pocket at amino acid positions 262-290 and is disordered in the three dimensional crystal structure of bacterial luciferase. *In vitro* assays

of a loop-deleted bacterial luciferase enzyme ($\alpha_{\Delta 262\text{-}290}\beta$) produced approximately 1% of the bioluminescence of the wild-type enzyme (*79*). Circular dichroism experiments showed that the loop deleted luciferase folds similarly to wild-type, however there is an increase in mean residue ellipticity around 222 nm. This suggests that the $\alpha_{\Delta 262\text{-}290}\beta$ luciferase has greater α-helical character than wild-type, which would be expected with the deletion of a disordered region of nearly 10% of the α subunit sequence (*79*). Since the light emission of the loop deleted enzyme is greatly reduced, experiments were performed to determine whether the ability to carry out the bioluminescence reaction was affected by loop deletion. Previous studies have shown that the βα7 loop of the α subunit of luciferase becomes ordered upon substrate binding and is postulated to cover the active site of luciferase during catalysis (*77*). Proteolytic inactivation experiments conducted on wild-type luciferase showed that the binding of $FMNH_2$ results in limited or no susceptibility to proteolysis. Since the binding of reduced flavin causes a decrease in the flexibility of the loop, investigations were carried out to determine the affect of the loop deletion on $FMNH_2$ binding. The dissociation constants for $FMNH_2$ binding to $\alpha_{\Delta 262\text{-}290}\beta$ and wild-type luciferase were determined by fluorescent titration to be 8.2 and 5.3 μM, respectively, suggesting that deletion of the loop caused no major changes in the binding affinity of $FMNH_2$. The binding affinity of aldehyde substrate was also determined to be similar for wild-type and the loop deleted enzyme. These findings indicate that the loop itself is essential for luciferase activity, but there is no clear evidence for the functional role of this loop in the enzyme catalyzed reaction. Site-directed substitutions to conserved residues on the disordered loop have raised questions as to whether the loop serves as a

gating mechanism (*78*). This loop might close over the active site and could sequester substrates and/or intermediates during the reaction, protecting them from oxidation by the bulk solvent.

The arginine residue located at position 297 in SsuD is conserved within all SsuD enzyme amino acid sequences and has a corresponding arginine residue at position 291 in bacterial luciferase. Site-directed mutagenesis was employed to substitute the conserved Arg297 residue with lysine and alanine to probe the role of this amino acid residue in the desulfonation reaction catalyzed by SsuD. Following over-expression and purification of the Arg297 variants, circular dichroism was performed to determine if there were any consequences to the overall secondary structure of SsuD because of the mutation. The experimental results indicated minor perturbations in the overall secondary structure in the 205-235 nm region for both mutants, compared to wild-type SsuD. This could possibly be due to the conformational flexibility of the loop which contains this conserved arginine. Part of the postulated flexible loop is disordered in the crystal structure of SsuD; however, the Arg297 residue is located after the disordered region on a random coil directly after helix α7b (Figure 1.14). Substitution of this Arg297 residue with either Lys or Ala could disrupt the formation of this α-helical segment of the enzyme. Since mutation of one amino acid appeared to cause minor changes in the overall secondary structure, kinetic analyses were also performed to determine the role of this Arg residue in the desulfonation reaction.

In steady-state kinetic assays, the substitution of Arg297 with either Lys or Ala altered the kinetic parameters compared to wild-type. The R297K SsuD variant had a 30

fold decrease in the k_{cat}/K_m value, while the R297A SsuD variant had no detectible activity. It is also important to note that the concentration of R297K SsuD had to be increased to obtain detectible activity. The decrease in the catalytic efficiency of the R297K SsuD variant is due to a 35-fold decrease in the k_{cat} value. The loss of activity of the R297A SsuD variant indicates that a positive charge on the amino acid at position 297 is important for efficient catalysis. These results indicate that the enzyme is unable to turnover with the substitution of Arg297 to Lys with a similar efficiency as wild-type SsuD. Previous results from pH profiles obtained for wild-type SsuD gives apparent pKa values of around 6.6 and 9.6 (unpublished results). These results suggest that there are two titratable amino acid residues that are important in catalysis. The amino acid with a pK_a around 6.6 would most likely be a histidine residue (His228), possibly in the deprotonated form acting as a catalytic base. The higher pK_a of 9.6 is in the correct range to correspond to an arginine residue. Recent results have also suggested that the histidine at position 228 could be involved in stabilizing the active site architecture or is needed for a catalytic step following the release of products (unpublished results). The results from these pH profile experiments performed on wild-type SsuD, combined with the abolished activity of R297A SsuD, suggest that it is possible that the arginine at position 297 could be acting as a catalytic base in the desulfonation reaction or important for the proper orientation of substrates for efficient catalysis.

The drastic reduction and complete loss of activity for the R297K and R297A SsuD variants, respectively, could be due the wrong orientation of substrates in the active site or the postulated flexible loop is unable to keep the substrates sequestered. Because

of the significant reduction in activity for both SsuD variants, the binding of $FMNH_2$ and octanesulfonate substrates was investigated through fluorescence spectroscopy. The K_d values determined for $FMNH_2$ with R297K and R297A SsuD exhibited a 3- and 5-fold increase compared to those obtained previously for wild-type SsuD, indicating that substitution of Arg297 with Lys or Ala caused a minor change in flavin binding. Results from previous studies probing the binding of substrates with wild-type SsuD demonstrated that two conformational changes are postulated to occur with the ordered binding of $FMNH_2$ and octanesulfonate substrates (*39*). Therefore, the binding of octanesulfonate to the R297K and R297A SsuD variants was also probed by fluorescence spectroscopy. The results from fluorescence titrations with octanesulfonate into either the R297K or R297A SsuD variant in complex with $FMNH_2$ exhibited no quenching of the intrinsic fluorescence signal with each addition. Two reasons for these results may be: 1.) unfavorable contacts between amino acids caused by the substitution of the arginine at position 297 with either lysine or alanine, or 2.) octanesulfonate is not binding in the proper orientation for quenching of the intrinsic protein fluorescence. The conformational change induced by substrate binding is possibly due to the flexible loop closing over the active site of the enzyme. Substitution of the arginine located on this mobile loop could have altered the movement of the loop, causing the octanesulfonate to not bind as tightly to the SsuD enzyme.

A C4a-(hydro)peroxyflavin intermediate, observed spectrally in the 300-400 nm range, was previously identified in the wild-type SsuD catalyzed reaction by single-turnover kinetics using stopped-flow analysis (*39*). This flavin intermediate was only

observed when $FMNH_2$ was mixed against wild-type SsuD in air-saturated buffer. As shown in Scheme 3.1, the C4a-(hydro)peroxyflavin intermediate could perform a nucleophilic attack on the alkanesulfonate substrate subsequently followed by a Baeyer-Villiger rearrangement to produce sulfite and the corresponding aldehyde. An initial fast phase in the absence of octanesulfonate substrate, representing the formation of the C4a-(hydro)peroxyflavin intermediate, was observed in stopped-flow kinetic traces obtained for both Arg297 variants at 370 nm with rate constants that were similar to those obtained previously for wild-type SsuD (*39*) (Table 3.3). The single-turnover kinetics of R297K and R297A SsuD variants in the presence of octanesulfonate substrate were also investigated by stopped-flow analyses. Kinetics traces obtained for the oxidation of $FMNH_2$ with the R297K SsuD variant in the presence of octanesulfonate substrate exhibited formation of the C4a-(hydro)peroxyflavin intermediate, even at high concentrations of octanesulfonate. The C4a-(hydro)peroxyflavin intermediate was only observed at low concentrations of octanesulfonate ($\leq$ 100 μM) in stopped-flow kinetic studies previously performed on wild-type SsuD, possibly due to the reaction proceeding faster at higher substrate concentrations (*39*). In contrast to rapid reaction kinetic traces performed on wild-type SsuD, the formation of the C4a-(hydro)peroxyflavin intermediate at high concentrations of octanesulfonate for the R297K SsuD variant may be due to a higher accumulation of this intermediate because of a slower turnover of the variant enzyme. The rates obtained from double exponential fits were not dependent on the concentration of octanesulfonate; however, the shape of the curve changed with increasing octanesulfonate concentration. This could be due to a conformational change

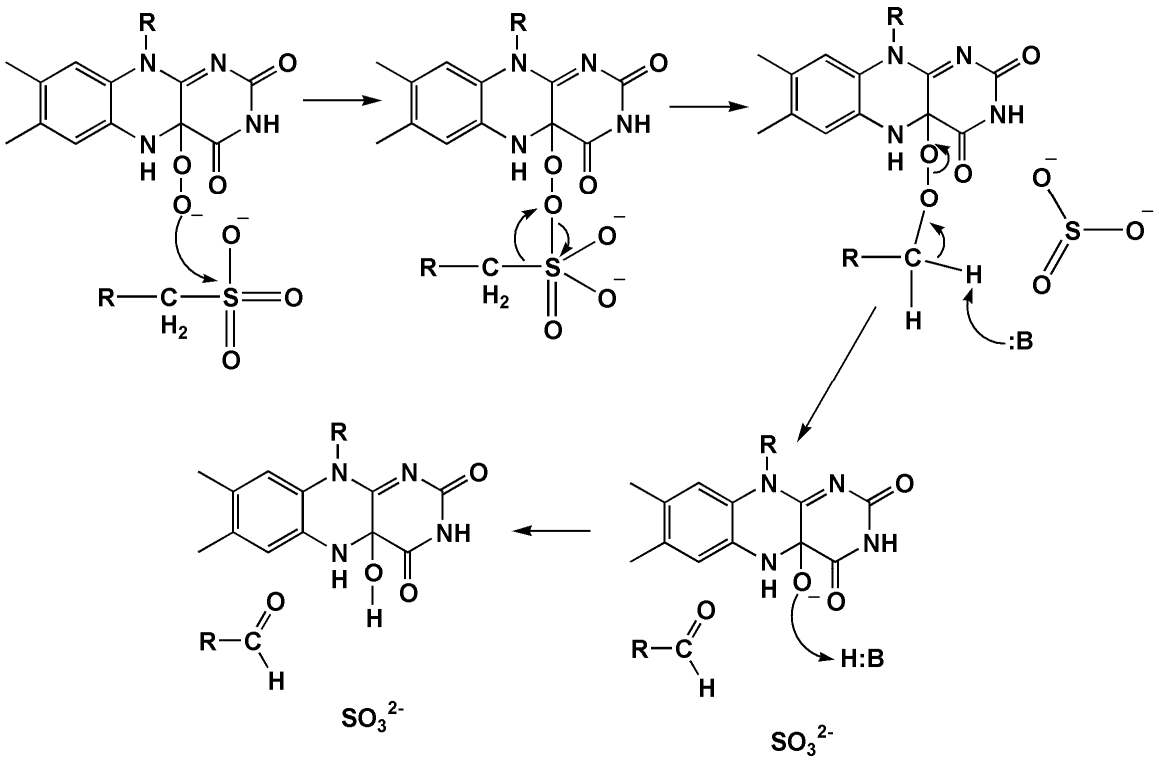

Scheme 3.1 Desulfonation recation catalyzed by SsuD (*39*).

associated with the flavin moiety within the active site. Consequently, the stopped-flow kinetic traces obtained for flavin oxidation at 450 nm did not appear to change with increasing octanesulfonate concentrations. The kinetic traces at 370 and 450 nm of R297A SsuD mixed against $FMNH_2$ were essentially the same, with no appreciable formation of the C4a-(hydro)peroxyflavin intermediate. The flavin intermediate was observed in the absence of octanesulfonate, but no activity was detected in the steady-state assays. This suggests that the R297A SsuD variant is possibly in the right conformation to form the C4a-(hydro)peroxyflavin intermediate, but the wrong conformation for catalysis to occur in the presence of octanesulfonate. This is in correlation to the previously mentioned experiments in which no activity was detected in steady-state assays with the R297A SsuD variant and in fluorescence titrations in which the binding of octanesulfonate did not appear to occur.

It has been previously shown that the flavin reductase, SsuE, and alkanesulfonate monooxygenase, SsuD, interact with each other through protein-protein interactions (*89*). Stopped-flow kinetic analyses were performed to determine if substitution of Arg297 with either Lys or Ala would affect $FMNH_2$ oxidation in the presence of SsuE. The kinetic traces obtained at 450 nm following flavin oxidation in the presence of wild-type SsuD showed a lag phase possibly due to the binding of $FMNH_2$ and/or the transfer of reduced flavin from SsuE to SsuD. Similar kinetic traces in the presence of either R297K or R297A SsuD were devoid of this lag phase. With the absence of this lag phase in R297K and R297A SsuD variants, it appears that the $FMNH_2$ is being released into the solvent to be non-enzymatically oxidized. If the arginine at position 297 is facilitating the

transfer of $FMNH_2$ from SsuE to SsuD, the substitution of this residue with lysine or alanine would have an affect on this step. The kinetic traces obtained in the presence of 250 μM octanesulfonate were similar, except the reaction appeared to be faster. These results suggest that substitution of Arg297 with either Lys or Ala impairs the ability of SsuD to receive the $FMNH_2$ from SsuE by possibly disrupting electrostatic interactions between the Arg297 on the mobile loop and another amino acid. If this Arg297 is essential for the loop to close over the active site properly, then mutation of this amino acid would cause the loop to not function correctly.

As mentioned previously, the SsuD enzyme contains an unstructured region in the three-dimensional crystal structure similar to bacterial luciferase (*60*). This region has been shown to be essential for a high yield of bioluminescence in bacterial luciferase (*80*). These flexible loops have been postulated to close over the active site to protect intermediates during the catalytic reaction. The sensitivity of variants and wild-type SsuD to proteolytic cleavage was investigated with trypsin in the absence and presence of substrates to determine whether the binding of substrates would affect the amount of proteolytic cleavage. In the absence of substrates the variant and wild-type SsuD enzymes were digested very rapidly. However, in the presence of $FMNH_2$ both variants and wild-type SsuD were digested much slower. It is known that the binding of $FMNH_2$ induces a conformational change in the SsuD enzyme. This conformational change associated with the binding of $FMNH_2$ could be due to the flexible loop closing over the active site, consequently protecting the enzyme from proteolysis. In the presence of both $FMNH_2$ and octanesulfonate substrates wild-type SsuD showed very limited proteolysis,

with about 80% of the native protein still remaining after a 5 min incubation (Figure 3.8A). Both R297K and R297A SsuD variants exhibited similar digestion patterns in the presence of both substrates as digestions in the presence of $FMNH_2$ only (Figure 3.8B and 3.9B). Therefore, the presence of octanesulfonate in the incubation with either R297K or R297A SsuD variants did not change the amount of proteolysis. These results, along with the results from fluorescence titrations, suggest that octanesulfonate does not bind to either SsuD variant enzyme. This could be due to disrupted contacts between the flexible loop and the rest of the protein after the binding of substrates, caused by the mutation of Arg297. This distorted conformation could possibly be favorable for $FMNH_2$ binding, but unfavorable for octanesulfonate binding.

In summary, the results presented herein use a combination of biochemical and mechanistic approaches to determine the functional role of Arg297 located on a postulated mobile loop near the active site of SsuD. The Arg297 residue, located on a flexible loop, may play a role in stabilizing the closed conformation of the SsuD-$FMNH_2$ complex, protecting the reduced flavin from non-enzymatic oxidation. This could be accomplished by electrostatic interactions between Arg297 and a negatively charged amino acid after substrates are bound or direct interactions with the substrate(s). The fact that substitution of Arg297 with Ala abolished all activity also suggests that this amino acid residue could act as a catalytic base in the desulfonation reaction. The previously described results from pH profiles exhibit a pK_a of 9.6, which is in the range for an arginine residue. Experiments in which the flavin reductase, SsuE, was included in the reaction suggest that this arginine residue could also be facilitating the transfer of

$FMNH_2$ from SsuE and sequestering the substrates in the active site with subsequent loop closure. There are still many unanswered questions as to the role of the arginine at position 297 in SsuD, but the experiments described in this paper give some insight as to the function of this residue in the desulfonation reaction.

CHAPTER FOUR

SUMMARY

The alkanesulfonate monooxygenase system from E. coli, composed of a NAD(P)H-dependent FMN reductase (SsuE) and a flavin-dependent monooxygenase (SsuD), is capable of desulfonating a wide range of linear 1-substituted alkanesulfonates in the presence of FMN, NAD(P)H and O_2 resulting in the liberation of sulfite and formation of a corresponding aldehyde (*57*). This enzymatic system is induced under sulfur starvation conditions and expressed from the same operon along with an ABC-type transporter which is involved in the uptake of alkanesulfonates into the cell. The FMN reductase supplies the monooxygenase with reduced flavin to activate molecular oxygen for the cleavage of the C-S bond of alkanesulfonates in the desulfonation reaction. Alkanesulfonates are very stable compounds and difficult to eliminate from the environment. The C-S bond cleavage and flavin transfer between SsuE and SsuD is mechanistically novel between these two enzymes.

While the flavin reductase of this two-component system has been well characterized and the flavin transfer mechanism explored, there is much less known about the monooxygenase component, SsuD (*82, 88, 89*). This research has focused on

elucidating the mechanistic roles of conserved amino acids in the alkanesulfonate monooxygenase with a combination of biochemical and kinetc approaches.

4.1 Flavin binding and transfer in the alkanesulfonate monooxygenase system

In the overall reaction of the two-component alkanesulfonate monooxygenase system, SsuE catalyzes the reduction of FMN to form $FMNH_2$ which is subsequently transferred to the monooxygenase, SsuD, for the oxygenation of alkanesulfonates. To understand the overall catalytic mechanism of the two-component alkanesulfonate monooxygenase system it is important to obtain information on flavin binding and transfer within this system.

Previous experiments have determined the binding affinities of FMN and $FMNH_2$ for SsuE and SsuD. The SsuE enzyme has a 1000-fold lower K_d than the SsuD enzyme for FMN. Since $FMNH_2$ is very unstable in the presence of O_2, the binding affinity of the reduced form of flavin might give insight into the mechanism of flavin transfer between the reductase and the monooxygenase. A spectrofluorimetric titration method was developed to determine the dissociation constants of $FMNH_2$ for SsuE and SsuD under anaerobic conditions because of the high reactivity of reduced flavin with molecular oxygen. The K_d value of $FMNH_2$ for SsuD was 40-fold lower than for SsuE, indicating that SsuE has a clear preference for the oxidized form of flavin while SsuD prefers the reduced form.

The preference for either the oxidized or reduced form of flavin has been observed in other members of the flavin-dependent two-component monooxygenase systems. Dissociation constants for the oxidized and reduced forms of FMN have only

been determined for the alkanesulfonate monooxygenase system from E. coli and the ActVA-ActVB system involved in actinorhodin biosynthesis from *Streptomyces colelicolor* (*86*). In both systems the monooxygenase enzymes were able to bind $FMNH_2$ with higher affinity than FMN and the reductase components were able to bind FMN with a higher affinity that $FMNH_2$. This preference for either oxidized or reduced flavin appears to play a role in the mechanism of flavin transfer between the two enzymes of two-component systems.

To elucidate the mechanism of flavin transfer between SsuE and SsuD a combination of kinetic analyses and biochemical experiments were performed. Results from single enzyme kinetic analyses performed on SsuE indicated that there is an ordered sequential mechanism involved in the reduction of flavin, with NADPH as the first substrate to bind and $NADP^+$ as the last product to dissociate. However, in the presence of SsuD and octanesulfonate the kinetic mechanism of SsuE is altered to a rapid equilibrium ordered mechanism, and the K_m value for FMN is increased 10-fold (*88*)**.** More recent research has detected stable protein-protein interactions between SsuE and SsuD through affinity chromatography and spectroscopic analyses (89). This information from binding affinity experiments, kinetic studies, and biophysical analyses support a model for the direct transfer of flavin from SsuE to SsuD.

4.2 Catalytic mechanism of the alkanesulfonate monooxygenase

Flavoprotein monooxygenases are capable of catalyzing a wide variety of biochemical reactions. These reactions involve three steps: 1) flavin reduction by NAD(P)H; 2) activation of molecular oxygen to form a C4a-(hydro)peroxyflavin

intermediate; 3) oxygenation of a substrate. These steps can be accomplished in two different ways. In single-component enzymes the FMN is tightly bound and all three reactions happen on the same enzyme. In the two-component systems the reductive and oxidative half-reactions are performed by two separate enzymes.

Initial characterization of SsuD has previously been performed to give insight into the catalytic mechanism of the desulfonation reaction. Results from fluorimetric titrations of SsuD with octanesulfonate indicate that the $FMNH_2$ moiety must be bound first before the octanesulfonate can bind (*39*). Rapid reaction kinetic experiments using a stopped-flow instrument indicated the formation of a C4a-(hydro)peroxyflavin intermediate, similar to other characterized flavoproteins monooxygenases. Results from single-turnover experiments employing different mixing modes gave rise to the idea of an isomerization step involved before catalysis could occur. Site-directed mutagenesis studies have shown that the His228 located in the putative active site is not the catalytic base, as was suggested before. In summary, the previous experiments performed on wild-type SsuD propose that an ordered substrate binding mechanism takes place in SsuD with multiple conformational changes associated with the binding of substrates. Also, results from studies performed on His228 SsuD variants suggest that this histidine residue is not the active site base in the desulfonation reaction.

4.3 Putative active site of SsuD and the catalytic role of Cys54

Although the amino acid sequence homology is low, SsuD is similar in overall structure to other flavin-dependent monooxygenases bacterial luciferase and long-chain alkane monooxygenase (LadA). All three of these enzymes exhibit a TIM-barrel fold first

characterized by triosephosphate isomerase. Interestingly, several amino acids located in the putative active site of SsuD (Cys54, His228, Tyr331, and Arg297) are in a similar spatial arrangement to the catalytically relevant residues of bacterial luciferase from (Cys106, His44, Try110, and Arg291). The Cys106 residue of bacterial luciferase has been shown to stabilize the C4a-(hydro)peroxyflavin intermediate formed in the enzyme catalyzed reaction and the His44 residue is the proposed active site base; however, no information is currently available about the Tyr110 and Arg291 residues.

Substitutions were made to the cysteine residue located at position 54 in the putative active site of SsuD (C54S and C54A) in order to determine the catalytic role of this amino acid in the desulfonation reaction. Results from substrate binding studies reveal that Cys54 is not directly involved in the binding of $FMNH_2$. However, the binding affininty for octanesulfonate substrate was increased with both substitutions. Results from steady-states kinetic assays showed a 3-fold increase and a 6-fold decrease in the k_{cat}/K_m for the C54S and C54A SsuD variants, respectfully. Based on the steady-state kinetic studies the C54S SsuD variant is able to substitute for cysteine to improve the catalytic efficiency of the enzyme. Stopped-flow kinetic analyses showed that replacement of the Cys54 with Ser increased the rate of C4a-(hydro)peroxyflavin formation by about 10-fold, whereas no intermediate formation was observed for the Cys54Ala SsuD variant. Single-turnover experiments in the presence of octanesulfonate exhibited no C4a-(hydro)peroxyflavin intermediate formation. These results suggest that Cys54 could be involved in stabilizing the FMNOOH intermediate in the reaction

catalyzed by the alkanesulfonate monooxygenase, either directly or indirectly through the isoalloxazine ring of the flavin, similar to the function of Cys106 in bacterial luciferase.

4.4 Functional role of Arg297 located on a flexible loop in SsuD

It was previously reported that an abarrent mutation of Arg297→Cys abolished all enzymatic activity. It was postulated that this was due to a disulfide bond between the Cys mutation at position 297 and Cys54 located in the putative active site of SsuD (57). This Arg297 is located on a postulated mobile loop which is thought to play an essential role in protecting any intermediates by closing over the active site during the enzymatic reaction. Circular dichroism experiments have shown that minor perturbations in the overall secondary structure result from the substitution of Arg297 with either Lys or Ala compared to wild-type SsuD. Results from fluorescence titrations showed a slight decrease in the binding affinity for $FMNH_2$ in both R297K and R297A SsuD variants compared to wild-type, suggesting that the Arg297 residue is not essential for flavin binding. Unfortunately, a K_d for octanesulfonate could not be obtained under similar experimental conditions. Steady-state kinetic assays revealed a 30-fold decrease in the k_{cat}/K_m value for octanesulfonate with R297K SsuD. Consequently, no detectable activity was observed for the R297A SsuD variant. Stopped-flow kinetic analyses showed that replacement of Arg297 with Lys or Ala did not affect the formation of the C4a-(hydro)peroxyflavin intermediate in the abence of octanesulfonate. However, single-turnover experiments in the presence of SsuE showed an altered step subsequently after flavin reduction with R297K and R297A SsuD variants. These stopped-flow kinetic traces suggest that the Arg297 located on the flexible loop could possibly facilitate the

transfer of $FMNH_2$ from SsuE and protect it during the enzyme catalyzed reaction. The SsuD variants and wild-type SsuD were shown to be more susceptible to proteolysis in the absence of reduced flavin, while SsuD was digested more slowly in the presence of $FMNH_2$. Proteolytic digestions performed on wild-type SsuD in the presence of both $FMNH_2$ and octanesulfonate showed limited proteolysis with most of the native protein remaining after 5 min. Similar digestions preformed with R297K and R297A variants in the presence of both $FMNH_2$ and octanesulfonate exhibited similar digestion patterns to the ones performed with $FMNH_2$ only. These results indicate that the binding of $FMNH_2$ and octanesulfonate substrates induces a conformational change that protects the SsuD enzyme from proteolysis, and the flexible loop is likely involved in this conformational change. These results suggest that the arginine located at position 297 in SsuD is essential for facilitating the transfer of $FMNH_2$ from SsuE to SsuD and/or the protection of the $FMNH_2$ from being oxidized during the course of the reaction by locking down over the active site.

The catalytic functions of another putative active site amino acid, Tyr331, and the disordered flexible loop are presently being performed. Substitution of Tyr331 with Ala, or Phe results in an enzyme with a similar catalytic function as wild-type SsuD (unpublished results). Experiments are currently being performed on an SsuD variant in which the entire flexible loop region is deleted from the amino acid sequence. Similar studies performed on loop deleted bacterial luciferase resulted in an enzyme variant with bioluminescence that was 2 orders of magnitude lower than that of wild-type luciferase, implying that the flexible loop is essential for high bioluminescence activity.

In summary, the catalytic mechanism of the alkanesulfonate monooxygenase enzyme has been extensively explored. The overall mechanism of SsuD shows some common properties with other flavin-dependent monooxygenases with a ordered substrate binding mechanism and a C4a-(hydro)peroxyflavin intermediate generated in catalysis. Conformational changes are involved in catalysis and play important roles in protecting the reactive intermediates and controling the substrate binding order. The catalytic role of Cys54 has been probed by substrate binding, steady-state, and rapid reaction kinetic studies. The Cys54 has been shown to be responsible for stabilizing the C4a-(hydro)peroxyflavin intermediate, as previously proposed, similar to Cys106 in bacterial luciferase. The SsuD enzyme contains an Arg297 located on a flexible loop that has been shown to protect the enzyme from proteolysis and possibly facilitate the transfer of $FMNH_2$ from SsuE. Determing the catalytic roles of other putative active site amino acids is essential to understanding the mechanism of the desulfonation reaction catalyzed by the alkanesulfonate monooxygenase, SsuD.

REFERENCES

1. Van der Ploeg, J. R., Weiss, M. A., Saller, E., Nashimoto, H., Saito, N., Kertesz, M. A., and Leisinger, T. (1996) Identification of sulfate starvation-regulated genes in *Escherichia coli*: a gene cluster involved in the utilization of taurine as a sulfur source, J. Bacteriol. *178*, 5438-5446.
2. Van der Ploeg, J. R., Eichhorn, E., and Leisinger, T. (2001) Sulfonate-sulfur metabolism and its regulation in *Escherichia coli*, Arch. Microbiol. *176*, 1-8.
3. Kahnert, A., Vermeij, P., Wietek, C., James, P., Leisinger, T., and Kertesz, M. A. (2000) The *ssu* locus plays a key role in organosulfur metabolism in *Pseudomonas putida*, *J. Bacteriol. 182*, 2869-2878.
4. Quadroni, M., Staudenmann, W., Kertesz, M., and James, P. (1996) Analysis of global responses by protein and peptide fingerprinting of proteins isolated by two-dimensional gel electrophoresis. Application to the sulfate-starvation response of *Escherichia coli*, *Eur. J. Biochem. 239*, 773-781.
5. Van der Ploeg, J. R., Iwanicka-Norwicka, R., Bykowski, T., Hryniewicz, M. M., and Leisinger, T. (1999) The *Escherichia coli ssu*EADCB gene cluster is required for the utilization of sulfur from aliphatic sulfonates and is regulated by the transcriptional activator Cbl, *J. Biol. Chem*. *274*, 29358-29365.

6. Hell, R., Schuster, G., and Gruissem, W. (1993) An O-Acetylserine (Thiol) Lyase cDNA from Spinach, *Plant Physiol*. *102*, 1057-1058.

7. Neuenschwander, U., Suter, M., and Brunold, C. (1991) Regulation of Sulfate Assimilation by Light and *O*-Acetyl-L-Serine in *Lemna minor* L., *Plant Physiol. 97*, 253-258.

8. Ellis, H.R. and Poole, L.B. (1997) Novel Application of 7-Chloro-4-nitrobenzo-2-oxa-1,3-diazole to Identify Cysteine Sulfenic Acid in the AhpC Component of Alkyl Hydroperoxide Reductase, *Biochemistry 36*, 15013-15018.

9. Ellis, H.R. and Poole, L.B. (1997) Roles for the Two Cysteine Residues of AhpC in Catalysis of Peroxide Reduction by Alkyl Hydroperoxide Reductase from *Salmonella typhimurium*, *Biochemistry 36*, 13349-13356.

10. Eichhorn, E., van der Ploeg, J. R., Kertesz, M. A., and Leisinger, T. (1997) Characterization of α-ketoglutarate-dependent taurine dioxygenase from *Escherichia coli*, *J. Biol. Chem. 272*, 23031–36.

11. Ryle, M. J., Padmakumar, R., and Hausinger, R. P. (1999) Stopped-flow kinetic analysis of *Escherichia coli* taurine/α-ketoglutarate dioxygenase: interactions with α-ketoglutarate, taurine, and oxygen, *Biochemistry 38*, 15278–15286.

12. Kredich, N.M. (1996) Biosynthesis of cysteine. In: Neidhardt FC, Curtiss R, Ingraham JL, Lin ECC, et al (eds) *Escherichia coli* and *Salmonella*, 2nd edn. ASM, Washington DC, pp 514–527.

13. Iwanicka-Norwicka, R. and Hryniewicz, M. M. (1995) A new gene, *cbl,* encoding a member of the LysR family of transcriptional regulators belongs to *Escherichia coli cys* regulon, *Gene 166*, 11-17.

14. Van der Ploeg J. R., Iwanicka-Nowicka R., Kertesz M. A., Leisinger T., and Hryniewicz M. M. (1997) Involvement of CysB and Cbl regulatory proteins in expression of the *tauABCD* operon and other sulfate starvation-inducible genes in *Escherichia coli*, *J Bacteriol 179*, 7671–7678.

15. Eichhorn, E., Van der Ploeg, J. R., and Leisinger, T. (2000) Deletion analysis of the *Escherichia coli* taurine and alkanesulfonate transport systems, *J. Bateriol. 182*, 2687-2795.

16. Van der Ploeg, J. R., Cummings, N. J., Leisinger, T., and Connerton, J.F. (1998) *Bacillus subtilis* genes for the utilization of sulfur from aliphatic sulfonates, *Microbiology 144***,** 2555–2561.

17. Massey, V. (1999) The Chemical and Biological Versatility of Riboflavin, *Biochemical Society Transactions 28*, 283-296.

18. Müller, F. (1987) Flavin radicals: chemistry and biochemistry, *Free Radical Biology & Medicine 3*, 215-230.

19. Ghisla, S. and Massey, V. (1989) Mechanisms of flavoproteins-catalyzed reactions, *J. Biol. Chem. 181*, 1-17.

20. Hemmerich, P. and Müller, F. (1973) Flavin-O_2 interaction mechanisms and the function of flavin in hydroxylation reactions, *Annals New York Academy of Sciences 212*, 13-26.

21. Job, V., Marcone, G. L., Pilone, M. S., and Pollegioni, L. (2002) Glycine oxidase from *Bacillus subtilis*. Characterization of a new flavoprotein, *J. Biol. Chem. 277*, 6985-6993.

22. Gibson, Q. H., and Hastings, J. W. (1962) The Oxidation of Reduced Flavin Mononucleotide by Molecular Oxygen, *Biochem. J. 83*, 368-377.

23. Kemal, C., Chan, T. W., and Bruice, T. C. (1977) Reaction of $^3O_2$ with dihydroflavins. 1. N3,5-dimethyl-1,5-dihydrolumiflavin and 1,5-dihydroisoalloxazines, *J. Am. Chem. Soc. 99*, 7272-7286.

24. Anderson, R.F. (1982) in *Flavins and Flavoproteins* (Massey, V., and Williams, *C.*H., Jr., eds) pp. 278-283, Elsevier/North-Holland, New York.

25. Mewies, M., Mcintire, W. S., and Scrutton, N. S. (1998) Covalent attachment of flavin adenine dinucleotide (FAD) and flavin mononucleotide (FMN) to enzymes: The current state of affairs, *Protein Sci. 7*, 7-20.

26. Swoboda, B. E. P., and Massey, V. (1965) Purification and Properties of the Glucose Oxidase from *Aspergillus niger*, *J. Biol. Chem. 240*, 2209-2215.

27. Kunst, F., Ogasawara, N., Moszer, I., Albertini, A. M., Alloni, G., Azevedo, V., Bertero, M. G., Bessières, P., Bolotin, A., Borchert, S., Borriss, R., Boursier, L., Brans, A., Braun, M., Brignell, S. C., Bron, S., Brouillet, S., Bruschi, C. V., Caldwell, B., Capuano, V., Carter, N. M., Choi, S. K., Codani, J. J., Connerton, I. F., Danchin, A., et al. (1997) The complete genome sequence of the gram-positive bacterium *Bacillus subtilis*, *Nature 390*, 249-256.

28. Nishiya, Y. and Imanaka, T. (1998) Purification and characterization of a novel glycine oxidase from *Bacillus subtilis*, *FEBS Lett. 438*, 263-266.

29. Binda, C., Mattevi, A., and Edmondson, D. E. (2002) Structure-Function Relationships in Flavoenzyme-dependent Amine Oxidations, *J. Biol. Chem. 277*, 23973-23976.

30. Venkataram, U. V. and Bruice, T. C. (1984) On the mechanism of flavin-catalyzed dehydrogenation α,β to an Acyl function. The mechanism of 1,5-dihydroflavin reduction of maleimides, *J. Am. Chem. Soc. 106*, 5703-5709.

31. Duane, W. and Hastings, J. W. (1975) Flavin mononucleotide reductase of luminous bacteria, *Mol. Cell. Biochem. 6*, 53-64.

32. Jablonski, E. and DeLuca, M. (1977) Purification and Properties of the NADH and NADPH Specific FMN Oxidoreductases from *Beneckea harveyi*, *Biochemistry 16*, 2932-2936.

33. Lei, B., Liu, M., Huang, S., and Tu, S-C. (1994) *Vibrio harveyi* NADPH-Flavin Oxidoreductase: Cloning, Sequencing, and Overexpression of the Gene and Purification and Characterization of the Cloned Enzyme, *J. Bacteriol. 176*, 3552-3558.

34. Fontecave, M., Eliasson, R., and Reichard, P. (1987) NAD(P)H:flavin oxidoreductase of *Escherichia coli*. A ferric iron reductase participating in the generation of the free radical of ribonucleotide reductase, *J. Biol. Chem. 262*, 12325-12331.

35. Bruns, C. M. and Karplus, P. A. (1995) Refined crystal structure of spinach ferredoxin reductase at 1.7 Å resolution: oxidized, reduced, and 2′-phospho-5′-AMP bound states, *J. Mol. Biol. 247*, 125–145.

36. Lei, B. and Tu, S-C. (1998) Mechanism of Reduced Flavin Transfer from *Vibrio harveyi* NADPH-FMN Oxidoreductase to Luciferase, *Biochemistry 37*, 14623-14629.

37. Müller, F. Chemistry and Biochemistry of Flavoenzymes, Vol I pp 402. 1991 by CRC Press.

38. Ballou, D. P., Entsch, B., Cole, L. J. (2005) Dynamics involved in catalysis by single-component and two-component flavin-dependent aromatic hydroxylases, *Biochem. Biophys. Res. Comm. 338*, 590-598.

39. Zhan, X., Carpenter, R. A. and Ellis, H. R. (2008) Catalytic importance of substrate binding order for the $FMNH_2$-dependent alkanesulfonate monooxygenase enzyme, *Biochemistry 47*, 2221-2230.

40. Massey, V. (1994) Activation of molecular oxygen by flavin and flavoproteins, *J. Biol. Chem. 269,* 22459-22464.

41. Sheng, D., Ballou, D. P. and Massey, V. (2001) Mechanistic studies of cyclohexanone monooxygenase: chemical properties of intermediates involved in catalysis, *Biochemistry 40*, 11156-11167.

42. Entsch, B., Ballou, D. P. and Massey, V. (1976) Flavin-Oxygen Derivatives Involved in Hydroxylation by *p*-Hydroxybenzoate Hydroxylase, *J. Biol. Chem. 251*, 2550-2563.

43. Nakamura, S., Ogura, Y., Yano, K., Higashi, N., and Arima, K. (1970) Kinetic Studies on the Reaction Mechanism of *p*-Hydroxybenzoate Hydroxylase, *Biochemistry 9*, 3235-3242.

44. Sucharitakul, J., Chaiyen, P., Entsch, B., and Ballou, D. P. (2006) Kinetic Mechanisms of the Oxygenase from a Two-component Enzyme, *p*-Hydroxyphenylacetate 3-Hydroxylase from *Acinetobacter baumannii*, *J. Biol. Chem. 281*, 17044-17053.

45. Baldwin, T. O., Chen, L. H., Chlumsky, L. J., Devine, J. H., and Ziegler, M. M. (1989) Site-directed Mutagenesis of Bacterial Luciferase: Analysis of the 'Essential' Thiol, *J. Biolumin., Chemilumin. 4*, 40-48.

46. Xin, X., Xi, L., and Tu, S-C. (1991) Functional Consequences of Site-Directed Mutagenesis of Conserved Histidyl Residues of the Bacterial Luciferase α Subunit, *Biochemistry 30*, 11255-11262.

47. Abu-Soud, H., Mullins, L. S., Baldwin, T. O., and Raushel, F. M. (1992) Stopped-Flow Kinetic Analysis of the Bacterial Luciferase Reaction, *Biochemistry 31*, 3807-3813.

48. Abu-Soud, H. M., Clark, A. C., Francisco, W. A., Baldwin, T. O., and Raushel, F. M. (1993) Kinetic Destabilization of the Hydroperoxy Flavin Intermediate by Site-directed Modification of the Reactive Thiol in Bacterial Luciferase, *J. Biol. Chem. 268*, 7699-7706.

49. Francisco, W. A., Abu-Soud, H. M, Topgi, R., Baldwin, T. O., and Raushel, F. M. (1996) Interaction of Bacterial Luciferase with 8-Substituted Flavin Mononucleotide Derivatives, *J. Biol. Chem. 271*, 104-110.

50. Entsch, B., Palfey, P. A., Ballou, D. P., and Massey, V. (1991) Catalytic Function of Tyrosine Residues in *para*-Hydroxybenzoate Hydroxylase as Determined by the Study of Site-directed Mutants, *J. Biol. Chem. 266*, 17341-17349.

51. Palfey B. A., Entsch B., Ballou D. P., and Massey V. (1994) Changes in the catalytic properties of *p*-hydroxybenzoate hydroxylase caused by the mutation Asn300Asp, *Biochemistry 33*, 1545-1554.

52. Ryerson, C. C., Ballou, D. P., and Walsh, C. T. (1982) Mechanistic Studies on Cyclohexanone Oxygenase, *Biochemistry 21*, 2644-2655.

53. Schwab, J. M., Li, W. B., and Thomas, L. P. (1983) Cyclohexanone Oxygenase: Stereochemistry, enantioselectivity, and regioselectivity of an enzyme-catalyzed Baeyer-Villiger reaction, *J. Am. Chem. Soc. 105*, 4800-4808.

54. Hastings, J. W., Balny, C., Christian Le. P., and Pierre, D. (1973) Spectral properties of an oxygenated luciferase-flavin intermediate isolated by low-temperature chromatography, *Proc. Natl. Acad. Sci. 70*, 3468-72.

55. Baldwin, T. O. and Ziegler, M. M. (1992) in Chemistry and biochemistry of Flavoenzymes (Müller, F., ed) vol. III, pp. 467-530, CRC Press, Boca Raton, FL.

56. Kertesz, M.A. (1999) Riding the sulfur cycle – metabolism of sulfonates and sulfate esters in Gram-negative bacteria, *FEMS Microbiol. Rev. 24*, 135-175.

57. Eichhorn, E., Van der Ploeg, J. R., and Leisinger, T. (1999) Characterization of a two-component alkanesulfonate monooxygenase from *Escherichia coli*, *J. Biol. Chem. 274*, 26639-26646.

58. Huang, S. and Tu, S-C. (1997) Identification and characterization of a catalytic base in bacterial luciferase by chemical rescue of a dark mutant, *Biochemistry 36*, 14609-14615.

59. Rieder, S.V. and Rose, I.A. (1959) The mechanism of the triosephosphate isomerase reaction, *J. Biol. Chem. 234*, 1007-1010.

60. Eichhorn, E., Davey, C. A., Sargent, D. F., Leisinger, T., and Richmond, T. J. (2002) Crystal structure of *Escherichia coli* alkanesulfonate monooxygenase SsuD, *J. Mol. Biol. 324*, 457-468.

61. Fisher, A. J., Thompson, T. B., Thoden, J. B., Baldwin, T. O., and Rayment, I. (1996) The 1.5-Å resolution crystal structure of bacterial luciferase in low salt conditions, *J. Biol. Chem. 271*, 21956-21968.

62. Shima, S., Warkentin, E., Grabarse, W., Sordel, M., Wicke, M., Thauer, R. K., and Ermler, U. (2000) Structure of coenzyme F(420) dependent methylenetetrahydromethanopterin reductase from two methanogenic archaea, *J. Mol. Biol. 300*, 935-950.

63. Aufhammer, S. W., Warkentin, E., Berk, H., Shima, S., Thauer, R. K., and Ermler, U. (2004) Coenzyme binding in F_{420}-dependent secondary alcohol dehydrogenase, a member of the bacterial luciferase family, *Structure 12*, 361-370.

64. Farber, G. K. and Petsko, G. A. (1990) The evolution of α/β barrel enzymes. *Trends Biochem. Sci.* 15, 228-234.

65. Lin L. Y., Sulea, T., Szittner, R., and Vassilyev, V., Purisima, E. O., and Meighen, E. A. (2001) Modeling of the bacterial luciferase-flavin mononucleotide complex combining flexible docking with structure-activity data, *Protein Sci. 10*, 1563-71.

66. Baldwin, T. O., Ziegler, M. M., and Powers, D. A. (1979) Covalent structure of subunits of bacterial luciferase: NH_2-terminal sequence demonstrates subunit homology, *Proc. Natl. Acad. Sci. 76*, 4887-4889.

67. Paquatte, O. and Tu, S-C. (1989) Chemical modification and characterization of the alpha cysteine 106 at the *Vibrio harveyi* luciferase active center, *Photochem. Photobiol. 50, 817-825.*

68. Li, L., Liu, X., Yang, W., Feng, X., Wang, W., Feng, L., Bartlam, M., Wang, L., and Rao, Z. (2008) Crystal structure of long-chain alkane monooxygenase (LadA) in complex with coenzyme FMN: Unveiling the long-chain alkane hydroxylase, *J. Mol. Biol. 376*, 453-465.

69. Aparicio, R., Ferreira, S. T., and Polikarpov, I. (2003) Closed conformation of the active site loop of rabbit muscle triosephosphate isomerase in the absence of substrate: Evidence of conformational heterogeneity, *J. Mol. Biol. 334*, 1023-1041.

70. Brzović, P. S., Hyde, C. C., Miles, E. W., and Dunn, M. F. (1993) Characterization of the functional role of a flexible loop in the α-subunit of tryptophan synthase

from *Salmonella typhimurium* by rapid-scanning, stopped-flow spectroscopy and site-directed mutagenesis, *Biochemistry 32*, 10404-10413.

71. McMillan, F. M., Cahoon, M., White, A., Hedstrom, L., Petsko, G. A., and Ringe, D. (2000) Crystal structure at 2.4 Å resolution of *Borrelia burgdorferi* inosine 5′-monophosphate dehydrogenase: Evidence of a substrate-induced hinged-lid motion by loop 6, *Biochemistry 39*, 4533-4542.

72. Lolis, E., Alber, T. C., Davenport, R. C., Rose, D., Hartman, F. C., and Petsko, G. A. (1990) Structure of yeast triosephosphate isomerase at 1.9-Å resolution, *Biochemistry 29*, 6609-6618.

73. Lolis, E. and Petsko, G.A. (1990) Crystallographic analysis of the complex between triosephosphate isomerase and 2-phosphoglycolate at 2.5-Å resolution: Implications for catalysis, *Biochemistry 29*, 6619-6625.

74. Pompliano, D. L., Peyman, A., and Knowles, J. R. (1990) Stabilization of a reaction intermediate as a catalytic device: definition of the functional role of the flexible loop in triosephosphate isomerase, *Biochemistry 29*, 3186-3194.

75. Baldwin T. O., Hastings J. W., and Riley P. L. (1978) Proteolytic inactivation of the luciferase from the luminous marine bacterium *Beneckea harveyi*, *J. Biol. Chem. 253*, 5551-5554.

76. Njus D., Baldwin, T. O., and Hastings, J. W. (1974) A sensitive assay for proteolytic enzymes using bacterial luciferase as a substrate, *Anal. Biochem. 61*, 280-287.

77. Holzman, T. F., Riley, P. L., and Baldwin, T. O. (1980) Inactivation of luciferase from the luminous marine bacterium *Beneckea harveyi* by proteases: evidence for a protease labile region and properties of the protein following inactivation, *Arch. Biochem. Biophys. 205*, 554-563.

78. Low, J.C. and Tu, S-C. (2002) Functional roles of conserved residues in the unstructured loop of *Vibrio harveyi* bacterial luciferase, *Biochemistry 41*, 1724-1731.

79. Sparks, J.M. and Baldwin, T.O. (2001) Functional implications of the unstructured loop in the $(\beta/\alpha)_8$ barrel structure of the bacterial luciferase α subunit, *Biochemistry 40*, 15436-15443.

80. Nicoli, M. Z., Meighen, E. A., and Hastings, J. W. (1974) Bacterial luciferase. Chemistry of the reactive sulfhydryl, *J. Biol. Chem. 249*, 2385-2392.

81. Nicoli, M. Z. and Hastings, J. W. (1974) Bacterial luciferase. The hydrophobic environment of the reactive sulfhydryl, *J. Biol. Chem*. *249*, 2393-2396.

82. Gao, B. and Ellis, H. R. (2005) Altered mechanism of the alkanesulfonate FMN reductase with the monooxygenase enzyme, *Biochem. Biophys, Res. Comm. 331*, 1137-1145.

83. Riddles, P. W., Blakeley, R. L., and Zerner, B. (1979) Ellman's reagent: 5,5′-dithiobis(2-nitrobenzoic acid)—a reexamination, *Anal. Biochem. 94*, 75-81.

84. Jocelyn, P. C. (1987) Spectrophotometric assay of thiols, *Methods Enzymol. 143*, 44-67.

85. Francisco, W. A., Abu-Soud, H. M., DelMonte, A. J., Singleton, D. A., Baldwin, T. O., and Raushel, F. M. (1998) Deuterium kinetic isotope effects and the mechanism of the bacterial luciferase reaction, *Biochemistry 37*, 2596-2606.

86. Valton, J., Mathevon, C., Fontecave, M., Nivière, V., and Ballou, D. P. (2008) Mechanism and regulation of the two-component FMN-dependent monooxygenase ActVA-ActVB from *Streptomyces coelicolor*. *J. Biol. Chem.* 283, 10287-10296.

87. Yeh, E., Cole, L. J., Barr, E. W., Bollinger, J. M., Ballou, D. P., and Walsh, C. T. (2006) Flavin redox chemistry precedes substrate chlorination during the reaction of the flavin-dependent halogenase RebH, *Biochemistry 45*, 7904-12.

88. Gao, B. and Ellis, H. R. (2007) Mechanism of flavin reduction in the alkanesulfonate monooxygenase system, *Biochim. Biophys. Acta. 3*, 359-367.

89. Abdurachim, K. and Ellis, H. R. (2006) Detection of protein-protein interactions in the alkanesulfonate monooxygenase system from *Escherichia coli*, *J. Bacteriol.* 23, 8153-8159.

90. Sreerama, M. and Woody, R.W. (2000). Estimation of protein secondary structure from circular dichroism spectra: Comparison of CONTIN, SELCON, and CDSSTR methods with an expanded reference set, *Anal. Biochem. 287*, 252–260.